

# **Initial Assessment of Uncertainties Associated with BADGER Methodology**

Manuscript Completed: September 2012

Date Published: September 2012

Prepared by

J. A. Chapman and J. M. Scaglione

Oak Ridge National Laboratory

Managed by UT-Battelle, LLC

Oak Ridge, TN37831-6170

A. Pulvirenti, NRC Project Manager

M. Aissa, NRC Technical Monitor

**Prepared for**

**Division of Engineering**

**Office of Nuclear Regulatory Research**

**U. S. Nuclear Regulatory Commission**

**Washington, DC20555-0001**

**NRC Job Code V6243**



## FOREWORD

The degradation of neutron absorbing materials in spent fuel pools has prompted the staff to undertake a review of the tools and methods used by the industry to ascertain the condition of panels. Boraflex and Carborundum have degraded severely through chemically-induced changes and dissolution. Boral<sup>®</sup> has degraded by corrosion and deformation. Consequently, the subcriticality margins that existed when neutron absorbers were first installed have decreased. As margins decrease, one must have confidence in the neutron absorber data used in criticality analyses to demonstrate compliance with the subcriticality requirements specified by Title 10 of the Code of Federal Regulations Section 50.68 (10 CFR 50.68) or General Design Criteria (GDC) 62. Therefore, when using surveillance methods to determine the areal density of neutron absorbers in spent fuel pools, it is necessary that associated uncertainties be catalogued in a systematic manner.

The staff has focused on the surveillance methods for neutron absorber panels. Specifically, the staff has undertaken a review of the Boraflex rack life extension computer code (RACKLIFE) and the Boron Areal Density Gauge for Evaluating Racks (BADGER) in-situ measurement technique. The primary focus of this report is the uncertainty associated with the BADGER in-situ instrument. The uncertainty associated with RACKLIFE is discussed in the companion report: RACKLIFE, and BADGER: Description and Uncertainties (T. C. Haley).

The BADGER system was originally designed, assembled, and tested in the early-to-mid 1990s by Northeast Technologies Company (NETCO, now a subsidiary of Curtiss-Wright), as a nondestructive scoping tool to evaluate neutron absorbers placed in spent fuel racks. While BADGER is employed primarily to measure the degradation of Boraflex neutron absorbing material, it is theoretically applicable to any neutron absorber and has, in fact, been used for the phenolic matrix absorber Carborundum.

The analysis and assessment of the BADGER instrument and the associated measurement methodology yielded three principal findings. First, detailed documentation is required in order to conduct a rigorous quantitative uncertainty analysis. This includes technical specifications and/or quality control test reports. For BADGER, such documentation is not publicly available nor was it available to the authors of this report. Therefore, a Type B analysis, as defined by National Institute for Standards and Testing for use in cases where supporting measurement data is not available, was conducted. Estimates of uncertainty that appear in this report are a combination of data, analytical estimates and expert opinions.

Secondly, although the Type B analysis did not provide quantitative estimates for each contributor to overall uncertainty, several contributors to uncertainty were identified that can potentially invalidate measurement results. Examples of such errors are use of the instrument in a very high gamma field, the improper adjustment of low-level pulse discrimination, inconsistency in operator interpretation of data, and material mismatch between calibration and test panel. Flux-trap racks, a configuration where two neutron absorber panels are interposed between spent fuel assemblies, are especially susceptible to high error because neutrons must travel through two panels to the detector.

Lastly, head misalignment could contribute an estimated uncertainty of  $\pm 40$  percent to the overall BADGER results. The uncertainty resulting when the source and detector head are not properly aligned was estimated using the MAVRIC neutron radiation transport sequence in the SCALE criticality package. This 40 percent error may be significantly higher if the rack cell walls are warped or deformed.

Uncertainties associated with over 40 different factors affecting the measurement accuracy of the BADGER system were assessed, but documented information was available for less than five. In addition to discussing contributors to uncertainty, this report provides examples of the types of data and information necessary for a more rigorous calculation of uncertainty. The report illustrates the need to

more closely scrutinize actual information and data associated with BADGER campaigns, and quantify uncertainties that propagate in criticality calculations.

## EXECUTIVE SUMMARY

This report documents the review of the design, use, and implementation of BADGER,<sup>\*</sup> the Boron-10 Areal Density Gauge for Evaluating Racks. The review was specifically intended to understand the magnitude of the uncertainties involved in the application of the methodology for evaluating spent-fuel-pool neutron absorber panels. BADGER is a nondestructive test (NDT) instrument that measures *neutron transmission* through interposing panels of light water reactor (LWR) spent fuel racks between a <sup>252</sup>Cf neutron source and four boron trifluoride (BF<sub>3</sub>) neutron detectors. The neutron transmission measurement is used to characterize the physical properties of the neutron absorber panels. While originally designed for the measurement of Boraflex, BADGER has also been used in conjunction with other neutron-absorbing materials. Measurement results are used by licensees to demonstrate, in part, compliance with Title 10 CFR 50.68, Criticality Accident Requirements.

BADGER uses BF<sub>3</sub> gas-filled detectors. Gas-filled detectors were among the first devices used for radiation detection. While BF<sub>3</sub> tubes have been used in many neutron detection applications, their use for measuring areal density of <sup>10</sup>B in situ in spent fuel pool neutron absorber panels can be challenging. BF<sub>3</sub> detectors tend to be reliable and offer good neutron/gamma-ray discrimination at a reasonable efficiency. The interaction probability for gamma-rays is relatively low (typically orders of magnitude lower than thermal neutron interaction probabilities) when the device is used in acceptable gamma environments, and when the detector and electronics have been selected properly to accommodate the upper range of gamma-ray dose rates to be encountered. For measurements in a spent fuel pool, where high gamma-ray fluxes (~1000 R/hr) may be encountered, the gamma-ray sensitivity of the detector may dominate all other considerations.

In the course of conducting the uncertainty assessment, it was found that no information was available regarding specific performance testing of the device to identify and evaluate sources of error. It was also found that BADGER testing has been conducted in a heuristic manner (example inferences provided in Section 2) since its inception as measurement campaigns encountered different spent fuel pool rack designs and introduced new information that needed to be accounted for in the overall test protocol. However, the original demonstration measurement results<sup>†</sup> do not account for many of the engineering deployment uncertainties that arise in practice for in situ measurements. As a result, a Type B uncertainty analysis was conducted in accordance with NIST Technical Note 1297,<sup>‡</sup> such that estimates of uncertainty are provided on the basis of many years of experience conducting neutron measurements, and writing American National Standards Institute (ANSI), American Society for Testing and Materials (ASTM), International Standards Organization (ISO), and International Electrotechnical Commission (IEC) standards on the conduct of radiation measurements for nondestructive assay (NDA) and NDT systems.

A summary listing of parameters that can impact the measurement performance of BADGER was documented in this report and is presented in Section 6. Each of the individual parameters was grouped into categories reflecting different aspects of the BADGER system and how the results are used. Because

---

<sup>\*</sup>BADGER: Boron-10 Areal Density Gauge for Evaluating Racks, developed by Northeast Technology Corporation for the Electric Power Research Institute (EPRI).

<sup>†</sup>Electric Power Research Institute (EPRI), "BADGER, A Probe for Nondestructive Testing of Residual Boron-10 Absorber Density in Spent Fuel Storage Racks: Development and Demonstration," TR-107335, EPRI, Palo Alto, CA, October 1997.

<sup>‡</sup>National Institute of Standards and Technology, "Guidelines for Evaluating and Expressing the Uncertainty of NIST Measurement Results," *United States Department of Commerce, Technology Administration, National Institute of Standards and Technology (NIST), Technical Note 1297, 1994.*

of limitations and constraints affiliated with obtaining test reports, procurement specifications, technical specifications, and operating procedures (including those for quality control), uncertainties of individual components cannot be quantified nor combined in any scientifically defensible manner, with the information available to the authors. As such, no justification can be made for an estimate of total measurement uncertainty for the BADGER system. Monte Carlo radiation transport calculations documented in Appendix A show that the influence of individual parameters could be in excess of  $\pm 40$  percent each on reported average areal densities. Thus, the total uncertainty stemming from all the different sources examined in this report could be much greater.

# CONTENTS

	<u>Page</u>
FOREWORD .....	i
EXECUTIVE SUMMARY .....	iii
LIST OF FIGURES .....	ix
LIST OF TABLES .....	xi
ACKNOWLEDGMENTS .....	xiii
LIST OF ACRONYMS AND UNITS .....	xv
1 INTRODUCTION .....	1
2 BACKGROUND .....	3
3 METHOD OF REVIEW .....	10
4 BADGER SYSTEM DESCRIPTION .....	12
4.1 SOURCE/DETECTOR MODULES .....	13
4.2 DRIVE SYSTEM .....	14
4.3 NUCLEAR ELECTRONICS.....	14
4.4 DATA ACQUISITION AND CONTROL COMPUTER.....	14
5 BADGER SYSTEM DISCUSSION AND RELEVANT OBSERVATIONS ON UNCERTAINTY... 15	
5.1 NEUTRON SOURCE.....	16
5.1.1 Count Rate.....	16
5.1.2 Source Strength and Decay .....	17
5.1.3 Neutron Moderation by Covers on Heads .....	17
5.2 DETECTOR CHARACTERISTICS .....	17
5.2.1 Size .....	18
5.2.2 Efficiency .....	18
5.2.3 Fill Gas Pressure.....	18
5.2.4 <sup>10</sup> B Enrichment of the Gas.....	19
5.2.5 Aging of BF <sub>3</sub> Detectors .....	19
5.2.6 Detector Wall Material .....	19
5.3 INTERFERENCE .....	20
5.3.1 Background Neutron Flux from Surrounding Assemblies .....	20
5.3.2 Gamma Interference .....	20
5.4 ELECTRONICS .....	21
5.4.1 EMI Susceptibility.....	22

## CONTENTS (continued)

	<u>Page</u>
5.4.2 RF Pickup .....	22
5.4.3 Amplifiers, Discriminators, Power Supply, Acquisition Board .....	22
5.4.4 Signal Processors .....	22
5.4.5 Discriminators for Pileup Rejection, Wall Effect .....	23
5.4.6 Dead Time .....	23
5.5 APPARATUS GEOMETRY .....	23
5.5.1 Head Misalignment .....	24
5.5.2 Rack Cell Fit .....	26
5.5.3 Compression Springs, Shims, Vertical Offsets .....	26
5.5.4 Effect of Rack Cell Deformation: Panel Cladding Bulges, Collisions with Assemblies ...	26
5.5.5 Determination of Detector Coverage of Panel Area .....	26
5.6 CALIBRATION .....	27
5.6.1 Number, Range, and Precision of <sup>10</sup> B Areal Density of Standard Panels .....	27
5.6.2 Standard Panel Degradation .....	28
5.6.3 Adjustment of Calibration Procedure for Specific Pool Characteristics .....	28
5.6.4 Relevance of Standard Panel Material to Rack Panel Material .....	29
5.6.5 Location and Acclimatization of Calibration Cell in Pool .....	30
5.6.6 Choice of “Zero-Loss” Panel and Uncertainty of Actual <sup>10</sup> B Areal Density .....	30
5.6.7 Nonlinearity of Calibration Curve, Especially as Applied to Flux-Trap Racks .....	32
5.6.8 Uncertainties in Calibration Slope, Especially as Applied to Flux-Trap Racks .....	32
5.6.9 Frequency of Calibration during a BADGER Campaign .....	34
5.6.10 Confirmatory Analysis with Destructive Examination .....	34
5.6.11 Panel-Specific Use and Interpretation of Unattenuated Region Data .....	35
5.6.12 Algorithms to Convert BADGER Trace Data into Input for Calibration Curve .....	36
5.7 DATA PROCESSING .....	37
5.7.1 Reliance on Operator Experience to Detect and Characterize Heterogeneous Degradation .....	37
5.7.2 Applicability of Boraflex-Based Algorithms to Non-Boraflex Material Such as Boral <sup>®</sup> or Metamic .....	39
5.7.3 Feedback Procedure .....	39
5.8 STATISTICAL EXTRAPOLATION AND SURVEILLANCE FREQUENCY .....	40
5.8.1 Choice of Test Panels to Survey .....	40

## CONTENTS (continued)

	<u>Page</u>
5.8.2 Lack of Duplicate Scans of the Same Test Panel .....	40
5.8.3 Application of Results of Selected Panels to Entire Pool.....	41
5.8.4 Frequency of BADGER Campaigns, Especially for Panel Materials Where Intermediate Computational Methods Such As RACKLIFE Are Unavailable.....	42
5.8.5 Application of Final Output to Criticality Analyses of Record.....	42
5.8.6 Use of Final Output in Abnormal or Accident Sequence Criticality Analyses .....	43
6 SUMMARY.....	45
7 CONCLUSION.....	58
8 REFERENCES .....	60
APPENDIX A.....	A-1
APPENDIX B .....	B-1
APPENDIX C .....	C-1

This Page Intentionally Left Blank

# LIST OF FIGURES

		<u>Page</u>
Figure 2.1.	Typical spent fuel pool for U.S. nuclear power plant.....	4
Figure 2.2.	Typical Region I spent fuel pool rack configuration.....	5
Figure 2.3.	Typical Region II spent fuel pool rack configuration.....	5
Figure 2.4.	Degraded Boraflex.....	6
Figure 4.1.	Axial cross-section depiction of BADGER in operation in a spent fuel pool.....	12
Figure 4.2.	Figure showing close proximity of source to absorber material and neutron detectors (BWR BADGER system). .....	13
Figure 5.1.	BF <sub>3</sub> circuit diagram.....	21
Figure 5.2.	Detector probe orientation.....	25
Figure 5.3.	Representative calibration curve. ....	34
Figure 5.4.	Representative Region II spent fuel pool storage cell.....	35
Figure 5.5.	BADGER detector traces.....	38
Figure A.1.	Cutaway view of representative Region II BWR storage rack model.....	A-3
Figure A.2.	Areal density calibration curve for optimum source and detector head orientation positioning.....	A-4
Figure A.3.	Source and detector head positioning with 3° twist misalignment for detector head.....	A-5
Figure A.4.	Source and detector head positioning with a 0.66-cm probe center-to-center offset misalignment. ....	A-5
Figure A.5.	Change in recorded areal density due to twist misalignment. ....	A-6
Figure A.6.	Change in recorded areal density due to offset misalignment.....	A-7

This Page Intentionally Left Blank

# LIST OF TABLES

	<u>Page</u>
Table 5-1. Example calibration cell data .....	33
Table 6-1. Summary table of measurement system sources of uncertainty .....	47
Table A-1. Relative change in areal density due to twist misalignment.....	A-6
Table A-2. Relative change in areal density due to offset misalignment .....	A-7
Table B-1. MAVRIC-generated optimum orientation configuration results.....	B-2
Table B-2. MAVRIC-generated twist misalignment configuration results.....	B-3
Table B-3. MAVRIC generated offset misalignment configuration results.....	B-4

This Page Intentionally Left Blank

## **ACKNOWLEDGMENTS**

This work was performed under contract with the U.S. Nuclear Regulatory Commission (NRC) Office of Nuclear Regulatory Research. The authors thank A. Pulvirenti and J. Barr, the NRC Project Managers; M. Aissa, M. Gavrilas, and C. Harris of the Office of Nuclear Regulatory Research (RES); E. Wong and K. Wood of the Office of Nuclear Reactor Regulation (NRR); and Dr. Thomas Haley (consultant) for their support and guidance. Many valuable review comments were received from NRC staff members. The authors also wish to thank D. E. Mueller and B. J. Marshall for their reviews and D. J. Weaver and D. P. Stevens for assistance in formatting and preparation of the final document.

This Page Intentionally Left Blank

## LIST OF ACRONYMS AND UNITS

ANSI	American National Standards Institute
ASTM	American Society for Testing and Materials
BADGER	<u>B</u> oron-10 <u>A</u> real <u>D</u> ensity <u>G</u> auge for <u>E</u> valuation of <u>R</u> acks
Boraflex	a silicon-based composite of the neutron absorber, boron-10
$^{10}\text{B}$ areal density	density thickness ( $\text{g}\cdot\text{cm}^{-2}$ ) of boron-10 in neutron absorbers
BWR	boiling water reactor
CE	CE certification refers to products eligibility to be sold in European Union
CFR	<i>Code of Federal Regulations</i>
EMI	electromagnetic interference
EPRI	Electric Power Research Institute
GDC	general design criterion
GUM	guide to the expression of uncertainty in measurement
IEC	International Electrotechnical Commission
IEEE	Institute of Electrical and Electronics Engineers
IN	information notice
ISO	International Standards Organization
LLD	lower level discriminator
LWR	light water reactor
MSE	mean square error
NDA	nondestructive assay
NDT	nondestructive testing
NETCO	Northeast Technology Corporation
NIM	nuclear instrumentation module
NIST	National Institute of Standards and Technology
NRC	Nuclear Regulatory Commission
PWR	pressurized water reactor
QC	quality control
RACKLIFE	Boraflex <u>R</u> ack <u>L</u> ife Extension Computer Code
RF	radio frequency
SCA	single channel analyzer
TC	Tennelec Corporation
TMU	total measurement uncertainty
TTL	transistor-transistor logic
UL	Underwriters Laboratories
ULD	upper level discriminator

This Page Intentionally Left Blank

# 1 INTRODUCTION

Criticality safety analyses are performed to demonstrate that a proposed fuel storage configuration meets the applicable requirements of Title 10 of the *Code of Federal Regulations* (CFR) Part 50.68, “Criticality accident requirements,” (Reference 1) and Part 50 Appendix A General Design Criterion (GDC) 62, “Prevention of criticality in fuel storage and handling” (Reference 2). Several options for criticality control are available to licensees including use of a geometrically safe configuration, soluble boron, and interstitial neutron absorber panels. As spent fuel pool strategies shift to maximizing storage density, reliance on neutron absorber panel reactivity control has increased. Utilities have typically used neutron absorbers such as Boraflex, Boral<sup>®</sup>, Metamic<sup>™</sup>, and Carborundum in spent-fuel storage racks to control reactivity where boron-10 (<sup>10</sup>B) is the principal neutron-absorbing material contained in the plate. Neutron-absorbing materials used in spent fuel pools and credited to demonstrate compliance with NRC regulations are exhibiting degradation, as documented in Information Notices (INs) 87-43, 93-70, 95-38, and 2009-26 and Generic Letter (GL) 96-04 (References 3, 4, 5, 6, and 7). As discussed in Reference 6, a position has been taken that the degradation mechanisms and deformation rates of any of the neutron-absorbing materials in the spent fuel pool are not well understood. Therefore, licensees that credit the use of a neutron-absorbing material to maintain subcriticality in their spent fuel pool must monitor it for any indications that degradation of the material may be occurring that can result in noncompliance with criticality requirements for spent fuel pools.

A nondestructive measurement system was developed by Northeast Technology Corp. for the Electric Power Research Institute (EPRI), named *BADGER* (Boron-10 Areal Density Gage for Evaluating Racks) (Reference 8). The *BADGER* system is being used by utilities to monitor and estimate the extent of degradation of the neutron absorber panels to determine whether sufficient absorber remains to meet subcriticality margin requirements. *BADGER* is used to measure neutron transmission in 2-inch increments up the vertical length of a rack cell wall in a spent fuel pool. Through calibration and the use of various algorithms, the neutron transmission measurement is converted to a <sup>10</sup>B areal density estimate.

The purpose of this report is to provide a technical assessment of the *BADGER* system surveillance tool, for both pressurized water reactor (PWR) and boiling water reactor (BWR) rack designs, in an effort to understand the magnitude of the uncertainties as well as any limitations in its methodology and application. In particular, this report reviews the implementation of the *BADGER* system in measuring neutron transmission, correlating neutron count rates to absorber areal density, and determining how this information is applied to criticality evaluations of spent fuel pools, and identifies parameters that contribute most to uncertainty. Uncertainties considered include the use of the instrument in a very high gamma field, the improper adjustment of low-level pulse discrimination, inconsistency in operator interpretation of data, and material mismatch between calibration and test panel. The terms “error” and “uncertainty” are used throughout this document. The statistical definitions and usage of these two terms may have different interpretations. However, the major point of this document is to identify issues which may cause measurement deviation from a true value, whether or not the issues are termed errors or uncertainties.

Though most of the test data information reviewed and examples provided are from Boraflex evaluations, the overall assessment is being conducted in terms of general applicability independent of the specific neutron absorber material used in the spent fuel pool rack.

This Page Intentionally Left Blank

## 2 BACKGROUND

Neutron absorbers for spent fuel pool racks are typically composed of a neutron absorber nuclide within a matrix that maintains the distribution of the absorber material. Both metal matrix and non-metal-matrix neutron absorber materials have been produced and are currently being used for spent fuel pool applications. The *Handbook of Neutron Absorber Materials for Spent Nuclear Fuel Transportation and Storage Applications* (Reference 9) provides a listing of data and product information for a number of metal matrix neutron absorbers that are commercially available and have had the most widespread use in spent fuel storage and transportation applications, as well as information on non-metal-matrix absorbers, newly proposed aluminum matrix composites, and emerging materials. The primary function of the neutron absorber is to provide sufficient thermal neutron removal along the active fuel region between adjacent fuel assemblies.

Spent fuel pools that employ absorber panels may consist of one of two types of rack systems (or a combination of the two)—(1) flux trap or *Region I* systems, which contain two absorber panels separated by a water gap between panels, and (2) higher-density, *egg-crate* or *Region II* systems, where only a single absorber panel is interstitial to the spent fuel assemblies. A photograph of a typical spent fuel pool with racks is shown in Figure 2.1, and example *Region I* and *Region II* rack configurations taken from Reference 9 are illustrated in Figure 2.2 and Figure 2.3, respectively. The focus of this evaluation is based on the application of BADGER to *Region I* and *Region II* spent fuel pool rack configurations. The different rack configurations are designed to account for different levels of fuel assembly reactivity and for more effective space utilization. Some variability exists within the rack designs themselves, including fabrication and material specifications in addition to design and dimensional differences. Materials susceptible to expansion or blistering, such as Carborundum or Boral<sup>®</sup>, can prevent fuel assemblies from being inserted or removed, as well as change the criticality control conditions.

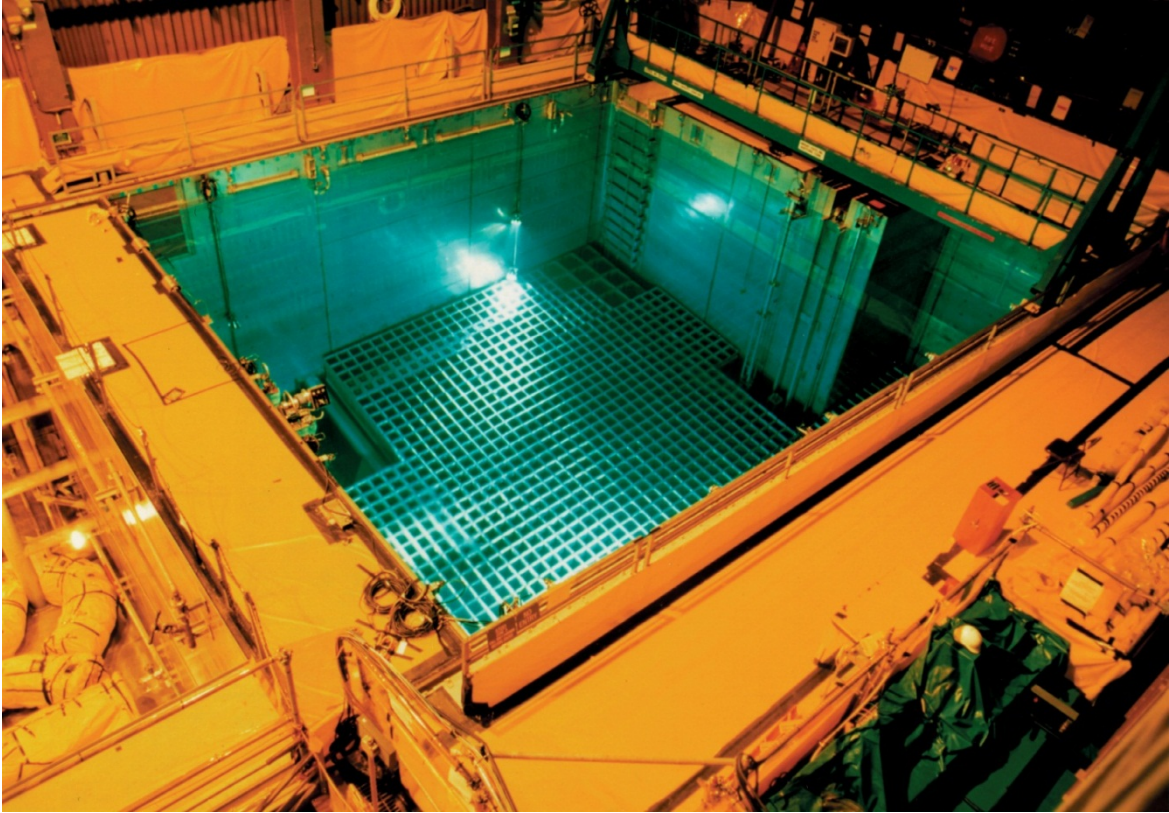


**Figure 2.1. Typical spent fuel pool for U.S. nuclear power plant (NRC file photo).**

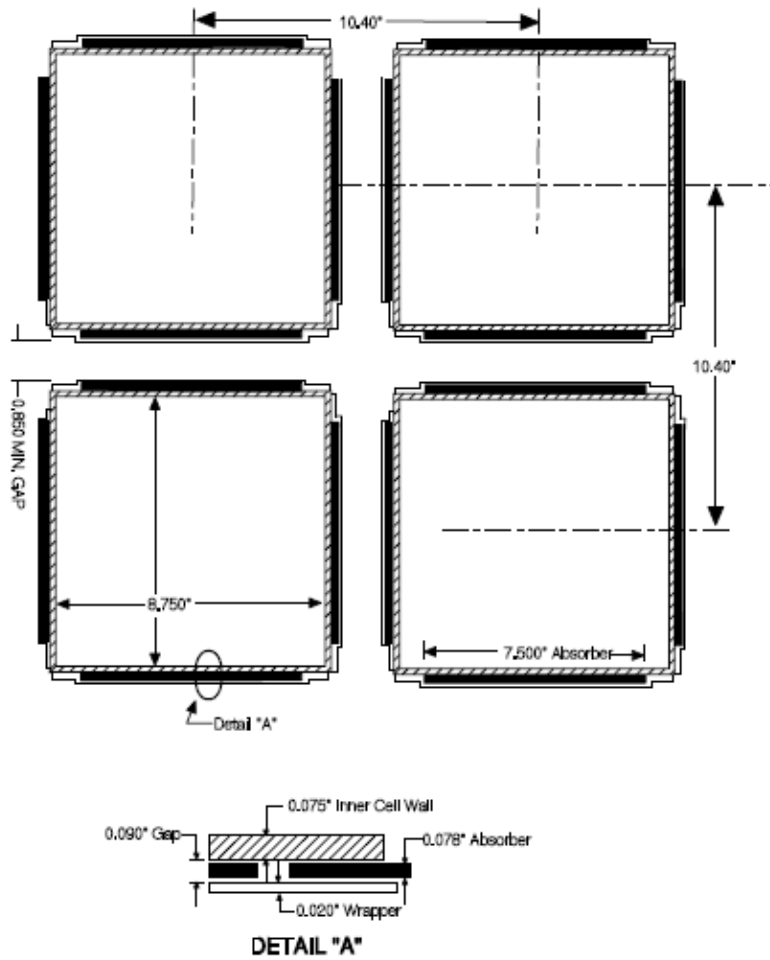


Figure 2.2. Typical Region I spent fuel pool rack configuration.  
(Adapted from Reference 9 with permission of EPRI.)

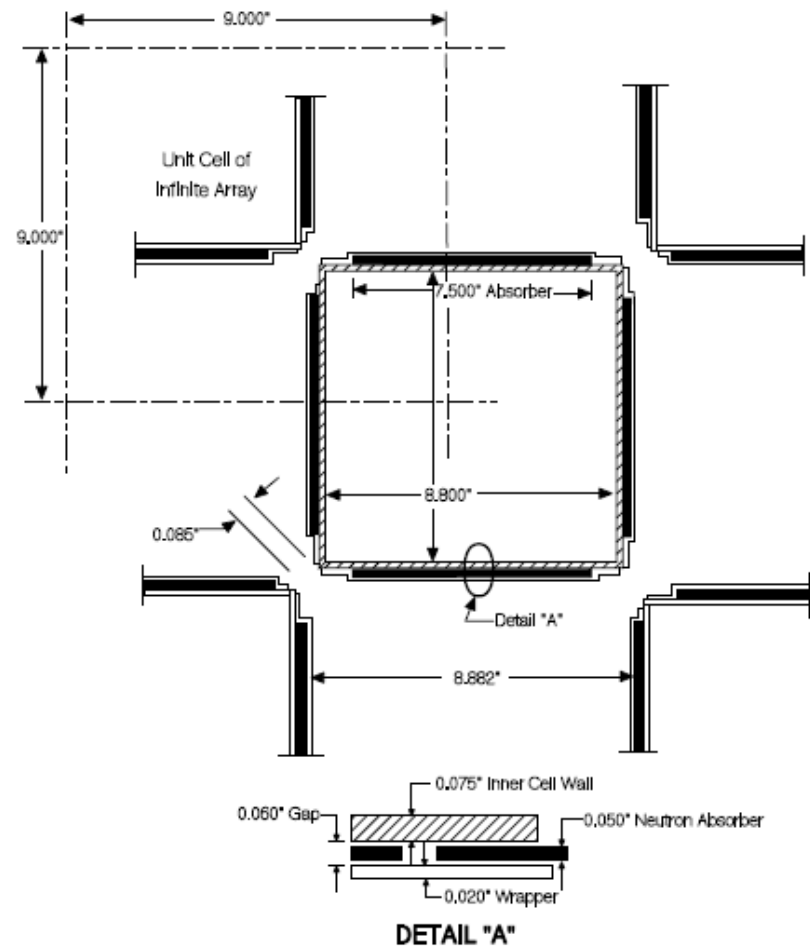
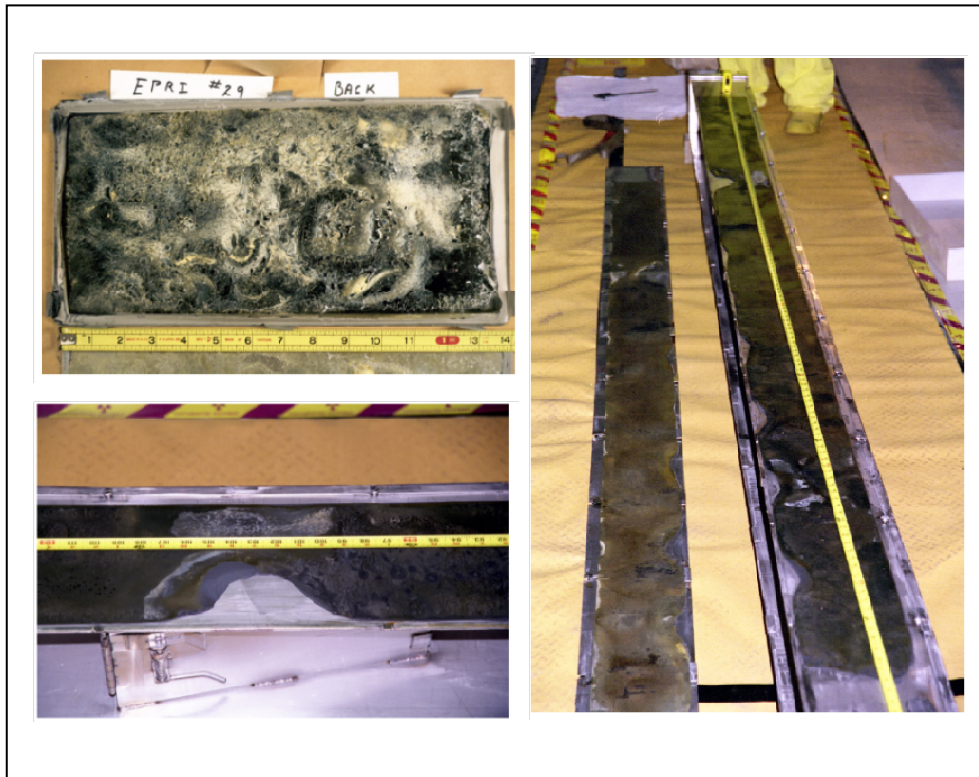


Figure 2.3. Typical Region II spent fuel pool rack configuration  
(Adapted from Reference 9 with permission of EPRI.)

As an outcome of the observed in-service deterioration of Boraflex, the BADGER system was developed as a nondestructive in situ means to estimate the  $^{10}\text{B}$  areal density remaining in neutron absorber materials installed in spent fuel racks for the purpose of reactivity control. Examples of the material degradation experienced with Boraflex are illustrated in Figure 2.4 below, which indicate the potential for dimensional changes and compositional changes. The BADGER system would need to be able to detect these types of changes. A thorough discussion of the chemical and physical processes that result in Boraflex degradation is provided in Reference 10.



**Figure 2.4. Degraded Boraflex (from Reference 11 with permission of EPRI).**

BADGER employs a well-understood physics method of measuring the attenuation of thermal neutrons through an absorber panel between the neutron source and the detectors. American Society of Testing and Materials (ASTM) C1671 (Reference 12) discusses neutron attenuation, converting measured count rates to areal density through the use of calibration standards, and provides the following definition:

*neutron attenuation* – for neutron absorber materials, a process in which a material is placed in a thermal neutron beam, and the number of neutrons transmitted through the material in a specified period of time is counted. The neutron count can be converted to areal density by performing the same test on a series of appropriate calibration standards and comparing the results.

Although ASTM C1671 is specific to boron-based metallic absorbers for use in dry cask storage and transportation systems, it provides a discussion on the conduct of neutron attenuation testing for determining the  $^{10}\text{B}$  content of a neutron absorber material, which is similar in principle to what BADGER has been designed for and how it is being implemented.

The BADGER nondestructive test (NDT) device was developed in the mid 1990s and first reported in EPRI Topical Report TR-107335 (Reference 8). The system was designed to conduct scoping studies to evaluate the degradation (or loss) of  $^{10}\text{B}$  areal density in Boraflex in conjunction with the RACKLIFE (Reference 13) computational package. The RACKLIFE computer program was developed to assess in-service performance of Boraflex (Reference 14) and provide a predictive capability. Hence, it would not be considered applicable for use with other neutron absorber materials. The BADGER scan results have been used to establish estimates of neutron absorber panel  $^{10}\text{B}$  areal densities as well as to characterize dissolution and anomalies such as gaps and cracks.

Several reports infer that BADGER testing has been conducted in a heuristic manner since its inception. These reports discuss how process and design modifications have been implemented as operational experience has grown, challenges to system performance are encountered, and the range of applicability of the system is expanded. Some reports indicate that system refinements have been implemented including use of stronger sources, refinements to measurement processing software, and incorporation of computer models to help account for calibration cell and rack cell differences. Specific examples of inferences from Reference 8 include statements such as: (1) "...the experience at PB2 [Peach Bottom Unit 2] served to identify some changes to the test procedures and detector block which will improve the precision of the areal density measurements"; and (2) "Larger detectors have been added to the BWR BADGER systems based on the experience at MNS2 [McGuire Nuclear Station Unit 2]". Other references such as Reference 15 (Part 3: NET-279-01) also support the conclusion regarding heuristic deployment, "Since different reference unirradiated panels from the previous test campaigns in 2000 and 2004 were selected for the current campaign, an attempt was made to determine a conservative "correction factor" that can be applied to the relative % deviation (non-gap) to allow a comparison to previous campaign results."

Neutron detectors, signal-chain processing electronics, and data acquisition systems for conducting in situ measurements have advanced substantially since BADGER was first designed. Most of the advancements came after 2001, when an international effort began to test, evaluate, and ultimately improve the reliability and performance of radiation measurement systems. One of the more relevant advancements that is being used as a basis of the current state of the art regarding conduct of nondestructive assay (NDA) in this review was the development of ASTM Standard C1592M-09, "Standard Guide for Making Quality Nondestructive Assay Measurements" (Reference 16), which was first issued in 2004.

The benefit of the last 15 years or so, with the increased requirements to implement performance testing radiation measurement systems for signal-to-noise effects, electromagnetic interference (EMI) susceptibility, radio frequency (RF) interference, and neutron/gamma ( $n/\gamma$ ) discrimination, is that radiation measurement systems are more reliable than before. Radiation measurement systems not only require an extensive set of laboratory testing but also in situ test results to identify all sources of uncertainty, to take measures to identify all sources of bias and reduce these sources, and to ensure variance reduction techniques are employed to improve precision. A description of the BADGER system is provided in Reference 8, which was published in 1997. No other information was available for review describing the current status of the BADGER system or improvements that have been incorporated post 2001 to indicate that the more recent advancements in technology and practice to improve nuclear measurement reliability and quality control (QC) have been incorporated.

To facilitate a common terminology in the subsequent discussions in this report describing the materials used for calibration and test, the following additional definitions are provided.

**Calibration cell:** portable arrangement of walls that contain neutron absorbers of known size and a certified/traceable  $^{10}\text{B}$  areal density. The calibration cell is used to calibrate BADGER over the range of

anticipated  $^{10}\text{B}$  areal density in the test panels. BADGER calibration is the process of fitting an exponential function of neutron transmission (ratio of the neutron count rates, attenuated to unattenuated region of calibration cell). The calibration cell configuration(s) are similar (but not identical) to BWR and PWR spent fuel pool rack cells. The calibration cell is transported between measurement sites.

**Standard panel:** a neutron absorber panel in the calibration cell of known size and certified/traceable  $^{10}\text{B}$  areal density.

**Reference cell:** an existing spent fuel pool rack cell that has a record maintained by the licensee of receiving no substantial gamma radiation dose, above which could alter the properties of the neutron absorber material. It is assumed that the neutron absorber panels associated with the reference cell are un-degraded and unchanged from the as-built condition. The reference cell has also been referred to as the zero-dose panel or zero-dose cell. The purpose of the reference cell is to account for local, site-specific measurement variability in the design and manufacture of specific racks deployed in the spent fuel pool that are not accounted for in the calibration cell.

**Reference panel:** a neutron absorber panel from the reference cell that is considered to be un-degraded, and from which all test-panel-measured neutron transmission measurement data is indexed against or referenced to.

**Test panel:** a spent fuel pool storage rack panel within a rack cell that has been exposed to conditions that may degrade the  $^{10}\text{B}$  areal density. BADGER conducts neutron transmission measurements on a subset of test panels within the spent fuel pool storage racks, at nominally 72 vertical positions.

This Page Intentionally Left Blank

### 3 METHOD OF REVIEW

Conducting a laboratory measurement of  $^{10}\text{B}$  areal density in a planar media can be quite easily accomplished with excellent repeatability (precision) and accuracy, with total measurement uncertainty (TMU) well below a few percent for a single-sided 95 percent confidence interval. However, challenges are encountered in the performance of these measurements within spent fuel pool storage racks e.g., operating under more than 6.5 meters (20 ft) of water, differences in rack designs, environmental instabilities affecting constant source-to-detector orientation, source/detector module wear over time, or background radiation. As a result, considerable uncertainties can be introduced when performing measurements under in-situ conditions. To implement the method effectively and to reduce uncertainty, controls need to be in place to ensure that proper engineering and/or administrative measures are taken.

All measurements contain uncertainty. The magnitude of the uncertainty must be established to understand if the results are adequate for their intended purpose. According to the National Institute of Standards and Technology (NIST) Technical Note 1297, “Guidelines for Evaluating and Expressing the Uncertainty of NIST Measurement Results” (Reference 17), also known as the International Standards Organization (ISO) Guide to the Expression of Uncertainty in Measurement (GUM), components of uncertainty can be classified into different categories based on the method of evaluation: Type A and Type B.

Type A uncertainty evaluation:

An uncertainty evaluation based on any valid statistical method for treating data (e.g., calculating the standard deviation of the mean of a series of independent observations or using the method of least squares to fit a curve to data to estimate the parameters of the curve and their standard deviations).

Type B uncertainty evaluation:

An uncertainty evaluation based on scientific judgment using all relevant information available (e.g., previous measurement data, experience with or general knowledge of the behavior of similar measurements, manufacturer’s specifications).

While a Type A uncertainty analysis is the principal objective of most uncertainty analyses, and preferred over a Type B analysis, there were no publicly available test records or peer-reviewed publications for BADGER showing how the BADGER system technical specifications have been satisfied. A Type A evaluation is “based on valid statistical methods for treating calibration and performance test data.” American Society of Testing and Materials (ASTM) test standards require a complete description of the test instrument, proper use of the instrument, interferences, sources of error, calibration, procedures and use, algorithms, precision and bias, and precautions.

A variety of reports primarily from EPRI and Northeast Technology Corporation (NETCO) were reviewed for this assessment. In general, most of the NETCO documents for BADGER test campaigns were similar in format and provided post-processed results and limited numeric data that was insufficient to facilitate a detailed quantitative (Type A) uncertainty analysis. Recognition of this limitation is also reflected in Reference 10 (p. 5-24), where it is stated that “there is insufficient data to make confident calculations of uncertainties due to the calibration cell, but the following is observed....” Hence, only a Type B uncertainty analysis can be conducted on BADGER at this time.

This Page Intentionally Left Blank

## 4 BADGER SYSTEM DESCRIPTION

Two BADGER systems have been fabricated, one for PWR spent fuel racks and one for BWR spent fuel racks. Initial design and fabrication testing was conducted in a clean pool at Pennsylvania State University, with spent fuel pool demonstration projects conducted at Peach Bottom Unit 2 and McGuire Unit 2, for the BWR and PWR systems, respectively (Reference 8).

BADGER consists of four subassemblies: (1) a source and detector module, which is inserted into the spent fuel pool, with the neutron absorber test panel interposed between each module; (2) an electromechanical drive system to lower and raise the source/detector module; (3) nuclear electronics modules for each neutron detector; and (4) a data acquisition computer. An axial cross-section depiction of the BADGER systems is provided in Figure 4.1.

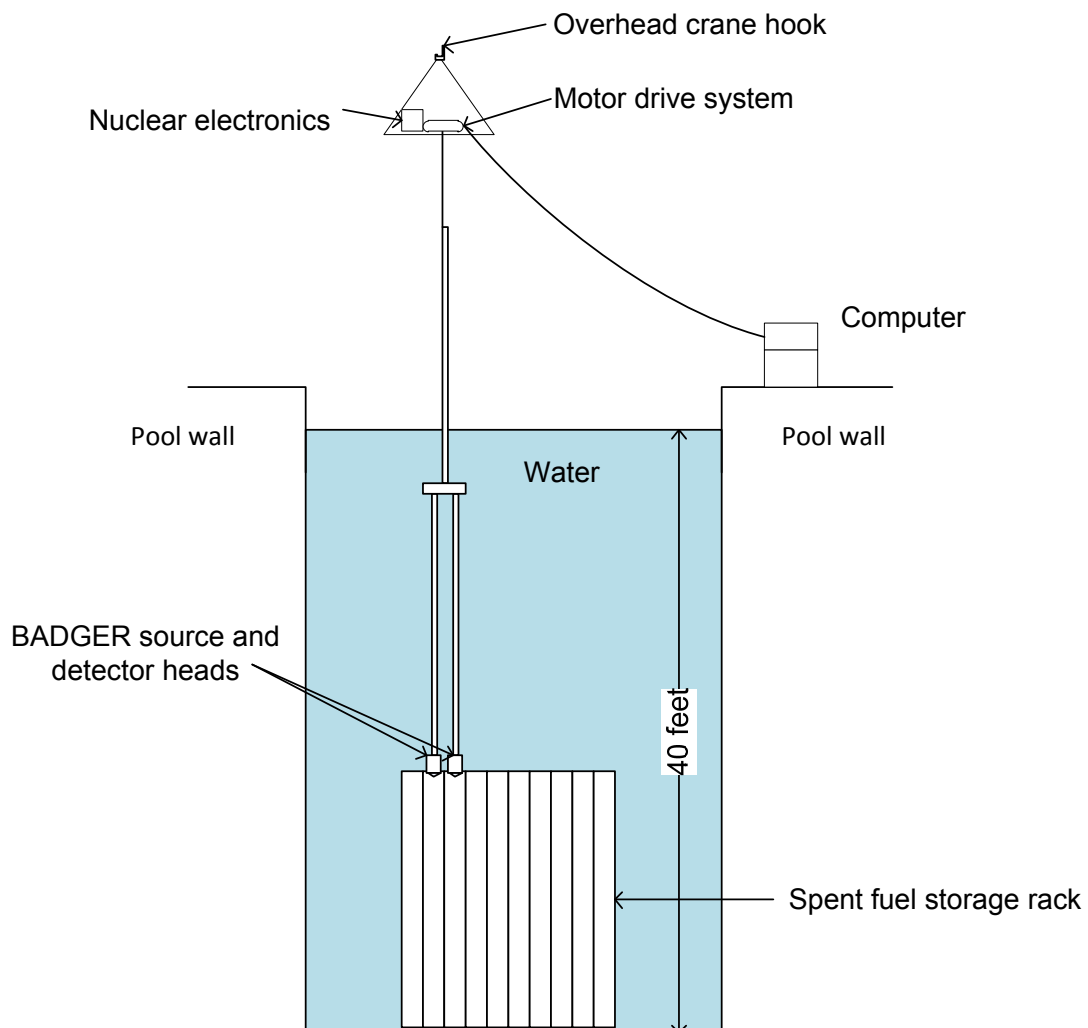


Illustration recreated from Reference 8.

**Figure 4.1. Axial cross-section depiction of BADGER in operation in a spent fuel pool. (Adapted from Reference 8 with permission of EPRI.)**

## 4.1 SOURCE/DETECTOR MODULES

For the BWR system, the heads consist of water-filled aluminum boxes, 5.75 in. (14.6 cm) per side with tapered lead-ins on the bottom surface, connected to aluminum suspension poles. The source head contains a watertight aluminum tube, which houses the  $^{252}\text{Cf}$  spontaneously fissioning neutron source when the equipment is in use. The detector head contains an aluminum block mounted on one inside face of the head, which houses four micro boron trifluoride ( $\text{BF}_3$ ) detectors. The detectors are encapsulated in watertight enclosures, which are sealed to the waterproof detector cables (Reference 8, p. 17).

For the PWR system, the heads are similar, with major differences being in materials of construction and dimensions of various components owing to the larger rack cells for PWR assemblies (e.g., 8 in. (20.3 cm) per side with 6 in. (15.2 cm) height and tapered lead-ins). In the PWR system, steel suspension poles are used instead of aluminum, and the PWR source head is filled with high-density polyethylene, which contains a watertight aluminum source tube (Reference 8, p. 17).

A cross-sectional view of the BWR BADGER system in optimum orientation within a representative spent fuel rack is presented in Figure 4.2. This simple illustration shows the neutron absorber between the adjacent cells, the neutron source head, and the four-detector assembly.

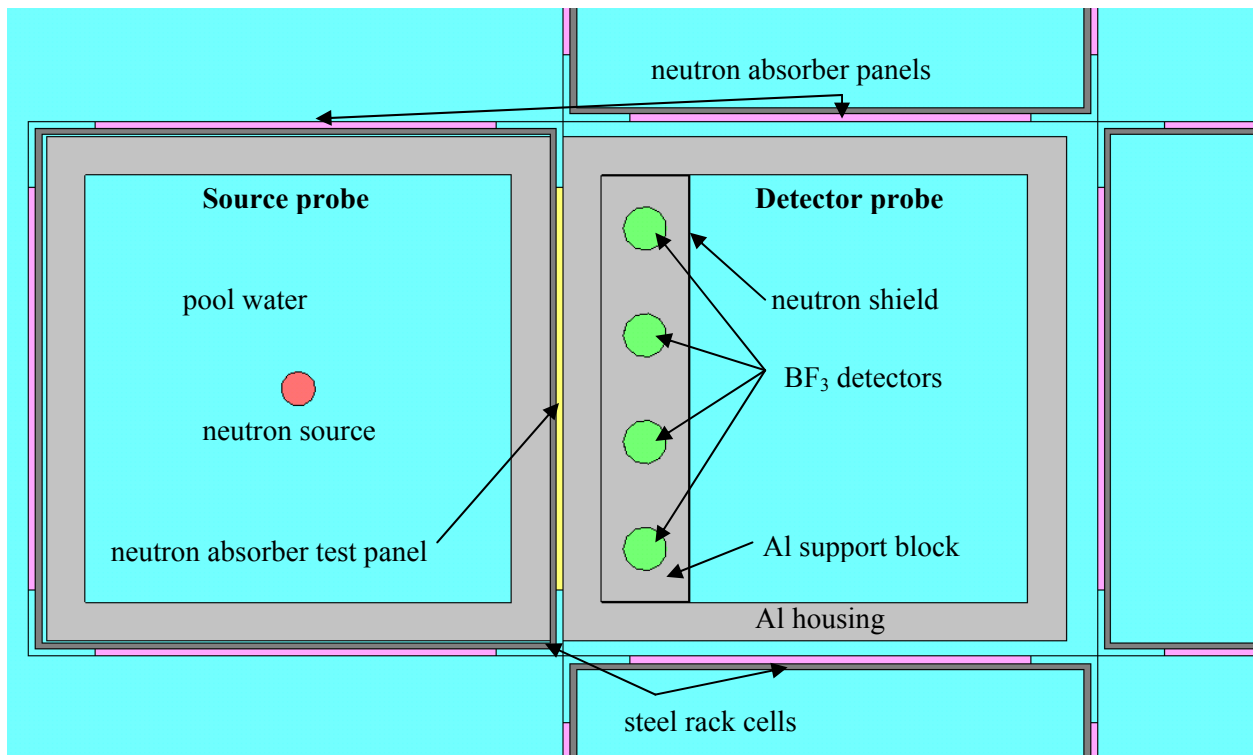


Figure 4.2. Figure showing close proximity of source to absorber material and neutron detectors (BWR BADGER system).

## **4.2 DRIVE SYSTEM**

An electromechanical drive system allows the source/detector heads to be lowered into the cells adjacent to the test panel of interest, and then moves the source and detectors axially up the test panel in 2-in. (5 cm) increments. The drive system consists of a stepper motor, gearbox, and winch assembly. A shaft encoder provides a precise measure of the vertical positioning of the source/detector module within the cell. A load sensor trips the drive motor if the source/detector head becomes stuck or lodged (Reference 18).

## **4.3 NUCLEAR ELECTRONICS**

Each of four neutron detectors is configured with independent signal chains. According to NETCO Drawing No. 092-01 (Reference 8, Figure 2-9), each detector is connected to a Tennelec Corporation (TC)-174 pre-amplifier. The coaxial cable length from the detector to the TC-174 is 40 ft (RG 59 or RG 62). The charge pulse from the TC-174 is fed to a TC-146 linear amplifier single-channel analyzer (SCA). A transistor-transistor logic (TTL) pulse out from the TC-246 amplifier is fed to a PC-based scaler board, the CTM-10 offered by Keithley Instruments. A mini nuclear instrumentation module (NIM) bin provides  $\pm 24 \text{ V} \pm 12 \text{ V}$  power to the neutron detector high-voltage bias supplies (a TC-948) (Reference 8, NETCO Drawing 092-01, 8/14/1997).

## **4.4 DATA ACQUISITION AND CONTROL COMPUTER**

The Keithley CTM-10 counter board/scaler is interfaced in the computer docking station to the analog data bus for controlling the source/detector head position. The computer interfaces via RS-232/485 serial communications with the stepper motor, shaft encoder, and load cell, all of which are used to position and control the source/detector heads.

## 5 BADGER SYSTEM DISCUSSION AND RELEVANT OBSERVATIONS ON UNCERTAINTY

This section provides a description of factors that affect the measurement precision and accuracy of BADGER as implemented by the BADGER operator and data analyst. A Type B uncertainty analysis (Reference 17) of the BADGER system was performed with the recognition and understanding that available information for review was limited. An evaluation of the magnitude of uncertainties is presented, but it is incomplete from a quantitative standpoint because of a lack of published performance data on the calibration functions, background subtraction methods, establishment of the unattenuated zero intercept, data reduction methods, and conduct of Analysis Of Variance (ANOVA) tests on the influence factors affecting system precision and accuracy. The semi-quantitative estimate of uncertainties is developed based on best practices in the science of radiation-measurement-based nondestructive testing (NDT), national consensus standards, and an analysis of published BADGER results.

The output of BADGER is the measured thermal neutron response from four separate BF<sub>3</sub> detectors. From the neutron count rate, neutron attenuation ratios are developed from which absorber panel characteristics are derived such as absorber areal density, absorber gap locations, and distribution of gaps. Measured values may vary randomly from measurement to measurement as the result of several factors, including environmental fluctuations, operator inconsistencies, and inaccuracies in the vertical indexer. Some of these factors are intrinsic to the selected components and are correlated, while others are independent. A proper understanding of the measurement equipment, the principles of the test, and the influence of the environment is necessary to appropriately combine the individual component uncertainties into a TMU. Hence, combining the error terms in a meaningfully scientific fashion as in a complete Type A analysis is not possible.

Customarily, in NDA/NDT systems if the device is to be used *qualitatively* (or for “indication only”), then a complete system design, reliability, and test package may not be required, depending on the application. However, as discussed in Reference 19, quantitative radiation measurement devices are typically designed with a clear set of specifications, operating conditions for deployment, interference factors that are understood and controlled in the implementation, administrative control points, and ultimately, acceptable tolerances/uncertainties over the range of performance. When the systematic uncertainties have been developed, boundary conditions can be set on the performance of each parameter with a corresponding “uncertainty budget” (Reference 17).

A large majority of the measurement influence parameters that were evaluated as part of this study would have ordinarily been examined during a product design, development, and quality certification process. In this process, system technical specifications are written and qualified. BADGER product development, technical specifications, and experimental test reports were not available for review, therefore limiting the depth of this evaluation. Engineering design is typically used to improve the overall performance of a system in an effort to satisfy specifications that are established by the user of the measurement results. Engineering controls are developed to reduce measurement bias. Administrative controls are developed to reduce error—both systematic and random—during implementation on-site. In this context, quality control is a process used to ensure that measurement systems are performing to the requisite specifications within established and accepted component uncertainty ranges, and to identify when the process is out of statistical control and action is required to correct the problem. This is not to be confused with procedural protocols designed to reduce measurement uncertainty.

The following good practices for performing measurements are described in ASTM Standard C1592M-09 (Reference 16).

1. Identify all contributors to systematic error (bias) in the measurement.
2. Eliminate all systematic error introduced in the acquisition of raw data.
3. Evaluate remaining bias factors and either develop software algorithm correction factors to compensate for these factors, or propagate the effects of these factors into the overall uncertainty model equations through ANOVA or other suitable tests.
4. Develop procedures that include steps to ensure that all engineering design features are implemented in the course of a measurement campaign. These engineering controls are necessary to ensure that the assumptions used in the uncertainty analysis are in fact valid.
5. Calculate total propagated uncertainty in the calibration function that relates neutron transmission to  $^{10}\text{B}$  areal density and gap detection (width and length of gap).
6. Develop administrative procedures to conduct QC tests of the instrument hardware to ensure hardware and data acquisition modules are within statistical control.

When achieved, the TMU is estimated according to a mathematical construct like that offered by Reference 20: “A system bias represents a systematic error introduced into all measurements. If, during TMU development it is determined that a system bias is present, it is expected that a correction factor will be added to the software to remove the bias. In the absence of a system bias, the square of the Relative Standard Deviation (RSD)-measured, is equal to the sum in quadrature of the RSDs of item specific error, calibration error, and random error:

$$\text{RSD}_{(\text{Measured})}^2 = \text{RSD}_{(\text{item bias})}^2 + \text{RSD}_{(\text{calibration})}^2 + \text{RSD}_{(\text{random})}^2$$

## 5.1 NEUTRON SOURCE

### 5.1.1 Count Rate

In neutron attenuation testing, the random, Poisson-distributed statistical relative error in neutron counting is equal to the square root of the number of counts divided by the number of counts (Reference 12), assuming there is zero neutron background and no interference terms from neutron scatter. Neutron source intensity, measurement count time, and neutron detector efficiency are interrelated system design components to be optimized for performance, reliability, precision, and accuracy. For example, to achieve Poisson counting statistics of 1 percent, the total number of neutron counts per measurement point would be at least 10,000 per detector. With a reported 1,000 counts per detector, the relative theoretical Poisson counting error is 3.2 percent. Several plots show BADGER count rates in the absorber region less than 20 cps (e.g., Reference 8, Figures 3-16 and 4-10). Over a 10-second count time, this would result in a counting uncertainty no better than 7–8 percent. A low Poisson count rate and low detector efficiency may synergistically magnify the contribution to uncertainty from other factors, for example, not adjusting the discriminator to account for pulse pileup from high gamma-ray dose rates; differential loss (or gain) in neutron count rate from absorption, reflection, and moderation between source and detector; energy-dependent neutron flux down scattered below effective irradiation of the panel; and inadequate correction for  $^{252}\text{Cf}$  source decay. To reduce uncertainty, all detection

specifications should be proven sufficient to meet technical basis design objectives for a given source strength. No experimental data was provided to estimate the impact of “net neutron count rate from direct neutron absorption” on implementation of BADGER.

### 5.1.2 Source Strength and Decay

Short count time is a desired performance characteristic of the BADGER system for each axial elevation scan. A larger  $^{252}\text{Cf}$  neutron source strength may result in shorter counting times to produce a given and constant statistical error. To reduce the Poisson count error, count time may be extended or a higher intensity  $^{252}\text{Cf}$  source may be selected (Reference 21). With a yield of  $2.34 \times 10^6$  neutrons/second per microgram, safe handling limits of special-form  $^{252}\text{Cf}$  sources normally limit the useful mass to less than a milligram, or roughly a half a curie (1 Ci = 1.86 mg  $^{252}\text{Cf}$ ). The 49 CFR §173.435 (Reference 22) A1 quantity for  $^{252}\text{Cf}$  (domestic use) is 2.7 Ci or about 5 mg. This would be the upper limit for use by the system. It is important to decay-correct the source, given the relatively short half-life of 2.65 years (Reference 23), for all QC checks. If an aged source is used, then it is important to decay-correct using a method similar to that described by Reference 21. Typically, for measurement systems that use radioactive sources, as the selected source decays the minimum source intensity for ensuring that adequate counting statistics are acquired in the measurement time interval of interest can be identified in the system QC charts.

The  $^{252}\text{Cf}$  source intensity can change by approximately 0.7 percent per 10 days of BADGER testing, resulting in a gradually increasing error on the measured count rate during a single BADGER measurement campaign. No experimental data was provided to estimate impact of source strength and decay on implementation of BADGER.

### 5.1.3 Neutron Moderation by Covers on Heads

An important physical effect associated with the selection and use of the  $^{252}\text{Cf}$  transmission source is related to the design of the source head assembly. Specifically, the neutron spectrum hardness (and intensity) should be matched for the local measurement conditions to reduce uncertainty considering (1) distance from the source to the neutron-absorber test panel wall, (2) design of neutron howitzer/collimator to obtain uniform neutron flux at the panel and of the optimum hardness, (3) local  $^{10}\text{B}$  density-thickness range of the neutron absorber, and (4) neutron moderator thickness for the detector head assembly. If the neutron transmission spectrum is too soft for the  $^{10}\text{B}$  density thickness of interest, the differential count rate per unit loss of absorber will be too small to be effective. These effects can lead to relatively large uncertainties in the calibration model selected for the test panels between the various measurement geometries for BWRs and PWRs, but most notably for the Region I flux trap design, where the transmission neutrons must travel multiple mean free paths before contacting the face of the test panel under inspection.

No information was available for review on how these effects and issues are accounted for with the BADGER system to develop an uncertainty estimate. If not well evaluated and accounted for, the exponential slowing down of neutrons and absorption loss in any material other than the absorber under evaluation can lead to significant biases.

## 5.2 DETECTOR CHARACTERISTICS

No information was available on the make and model of the  $\text{BF}_3$  detector tubes used by the BADGER system. Parameters specific to the  $\text{BF}_3$  detectors, such as size, intrinsic efficiency, fill pressure,  $^{10}\text{B}$  enrichment, and materials of construction (i.e., wall materials and anode size and materials) all affect

detector performance. The uncertainties associated with these parameters are not independent and can vary depending upon external environmental effects (i.e., temperature). Trade-offs between these parameters are used within the design selection process to ensure that the target performance requirements are achieved. No information was available regarding performance requirements for the detectors used by BADGER. An example performance requirement is “the usable thermal neutron sensitivity in a gamma field of  $10^3$  R/hr shall be equal to or greater than 5 counts per (second·nv) with the system adjusted to permit no more than 1 count per second background caused by gamma-induced pulse pileup” (Reference 24) (nv is the product of neutron density, n, in neutrons per cubic centimeter, and velocity, v, in centimeters per second). Another characteristic of importance, particularly for multi-detector systems, is detector-to-detector manufacturing tolerance. For multiple BF<sub>3</sub> tubes operated with one high voltage power supply, gain-matching of the tubes must be accounted for in not only evaluating efficiency changes (between detectors), but also for adjusting the lower-level discriminator (LLD) when gamma-ray interference becomes an issue. The performance characteristics are certified by the manufacturer and provide well-established uncertainty ranges associated with the design for a given operating environment range. In systems such as BADGER, these performance metrics are evaluated and controlled in accordance with QC charts to ensure that the desired level of performance is maintained within the known uncertainty range, or budget. As indicated in Reference 25, selecting a proper neutron detector for a specific application requires a combined engineering evaluation for establishing trade-offs in the interdependent design parameters, as described below.

### 5.2.1 Size

The BF<sub>3</sub> detectors used by BADGER are either 1/2 in. (1.3 cm) or 5/8 in. (1.6 cm) in diameter for the BWR and PWR systems, respectively, and have a 2 in. (5 cm) active length (Refs. 8 and 18). Typically, during measurement system design such as the BADGER system, the designer evaluates trade-offs between uncertainties and optimizing detector operational aspects when developing the engineering specifications. Examples of trade-offs include using a longer or larger diameter tube, the effect of n/γ discrimination, or broader spatial resolution. This specific technical information is either proprietary or not available. The effects of detector tube diameter are discussed further in Section 5.4.5.

### 5.2.2 Efficiency

Because the neutrons are in a scattering medium, taking the area of the detectors subtending the solid angle at a distance,  $r$ , from the source ( $A/(4\pi r^2)$ ) is not applicable for characterizing detector efficiency. Detection efficiency is integrated over the energy-dependent macroscopic absorption cross section for the BF<sub>3</sub> gas in the detector. Variation or bulk differences in the materials, material thicknesses, and moderator atom density between the source and detector significantly affect the integrated count of the detector. To quantify the uncertainty in efficiency, the efficiency can be tested empirically over the range of measurement geometries: Region I, Region II, or any BWR- or PWR-specific rack design, adequately accounting for the various magnitudes of the moderating region between the source and the detectors. This specific technical information is either proprietary or not available. A specification sheet for the neutron detector operating characteristics was not provided.

### 5.2.3 Fill Gas Pressure

The gas pressure can impact the magnitude of the individual pulses related to gamma-ray interactions in the counter walls and gas. Reference 26 indicates that BF<sub>3</sub> is particularly sensitive to contamination in the fill gas, especially at high pressures. This is reaffirmed in Reference 27, where it is stated that the performance of BF<sub>3</sub> as a proportional gas is poor when operated at high pressures, so typical tubes limit

the pressure to about 0.5 to 1.0 atm. No experimental data was provided to estimate the impact of fill gas pressure on BADGER system performance.

#### **5.2.4 $^{10}\text{B}$ Enrichment of the Gas**

Neutrons are detected in the boron trifluoride ( $\text{BF}_3$ ) gas based on the  $^{10}\text{B}(n, \alpha)^7\text{Li}$  reaction. To improve detection efficiency, the  $\text{BF}_3$  is typically enriched in  $^{10}\text{B}$ . Reference 27 indicates that commercial  $\text{BF}_3$  detectors are highly enriched in  $^{10}\text{B}$ , resulting in an efficiency of approximately five times greater than if the gas contained naturally occurring boron with a  $^{10}\text{B}$  to  $^{11}\text{B}$  natural abundance of 20 weight percent and 80 weight percent, respectively. No information was available for review regarding the  $^{10}\text{B}$  enrichment in the  $\text{BF}_3$  tubes used by BADGER. However, most practical  $\text{BF}_3$  counters are filled with boron trifluoride enriched to approximately 96 percent  $^{10}\text{B}$  (Reference 27). The determination of  $^{10}\text{B}$  enrichment is made during the design specification test stage of the project and is not known.

#### **5.2.5 Aging of $\text{BF}_3$ Detectors**

All instrumentation ages from a variety of environmental factors. The  $\text{BF}_3$  tubes used by BADGER are sealed counters, which can eventually develop leaks and gradual contamination of the fill gas. Quality control charts are typically established to detect out-of-tolerance detector and electronics performance. Reference 8 (Section 4.2.1) indicates that the detector becomes inoperable if water leaks into it. In the case of aging detectors, a QC chart maintained with a neutron check source will reveal when breakdown in the detector has occurred, or when detector degradation is sufficient to require replacement. An example QC check requirement could be that the count rate be maintained within  $\pm 5$  percent of expected, per 100 hours of testing (Reference 24). Quality control procedures, methods, and QC results are not available for BADGER in order to make a determination on uncertainty contribution.

#### **5.2.6 Detector Wall Material**

Wall materials selected for the neutron detector can influence detector performance due to the interaction of gamma-rays in the detector wall. The physical process in selecting the wall material that contributes to uncertainties is  $n/\gamma$  discrimination (Reference 28, Section 13.3). This dependence is primarily based on the gamma-ray induced Compton electron production in the wall, which in turn produces a column of ionization as it traverses the detector. Pileup pulses caused from the ion pairs created in the detector from secondary gamma interaction becomes problematic in small  $\text{BF}_3$  detectors and needs to be properly engineered and tested in gamma-ray fields greater than several hundred rads per hour for use in spent fuel pools. Materials typically used for  $\text{BF}_3$  tubes consist of aluminum, copper, and steel, with aluminum having the lowest thermal neutron absorption cross section of the three materials. A detector model was not provided, and a specification for wall material was not available; therefore, no estimate of uncertainty can be provided on this important neutron detector property and operating characteristic.

An additional uncertainty associated with the wall material that can affect the counting data can result from the  $\text{BF}_3$  detector tube manufacturing process. A study conducted in Reference 26 indicates that in low-neutron-density counting configurations, background count rates could be of the same order of magnitude as the expected neutron event counting rate. Background counts can be generated as a result of alpha surface contamination of the wall material. Results of the study found that background counts could vary considerably among the different counters tested, but counts were also found to be correlated with inside surface area when the counters were from the same manufacturer. Background count rate variability ranged from 0.005 to 0.05 counts per minute per square inch of inner surface. As discussed in Section 5.6, there is no information available regarding how the background count evaluation is performed.

## 5.3 INTERFERENCE

### 5.3.1 Background Neutron Flux from Surrounding Assemblies

The BADGER operator's preference for a panel scan, provided the spent fuel pool has the flexibility for fuel movements, is to remove all neutron sources, e.g., spent fuel assemblies, from the cells surrounding the test panel. In order to minimize neutron streaming into the detectors from neutron sources other than the  $^{252}\text{Cf}$ -attenuated neutron beam, a minimum of at least two, and preferably three, cells surrounding the test panel should be clear of spent fuel assemblies.\* The detector block is also equipped with a neutron shield on the back and sides as a mitigation measure against neutrons streaming into the detectors from other sources. However, because the number of cleared cells proximate to the test panel is unknown, and appears to vary during actual deployment of BADGER, there is a possibility of fast neutrons streaming through the adjacent cells without being absorbed and reaching the detector in the epithermal range sufficient to lead to a small number of counts.

No experimental data is available on the design of the detector cavity to shield the sides, top, bottom, and back from in-scattered neutrons (neutrons other than from direct transmission); however, there was some discussion of scatter effects based on MCNP modeling of the system in Reference 29. Uncertainties due to background flux could be reduced if the neutron shield was selected and designed for maximum effectiveness, and confirmed by laboratory experiments. In-scattered flux can be determined by removing neutron absorber panels from around the detector head, one at a time, and measuring the total neutron flux. For each panel removed—top, bottom, rear—the count rate in the detectors should increase from the in-scattered flux. From the reports publicly available, there is no scientific means to estimate, as implemented, the degree of bias from neutron in-scatter, reflection, and absorption from adjacent materials in the rack.

### 5.3.2 Gamma Interference

Gamma-ray interaction probabilities in the wall and in the gas of the detector tube are relatively small, but when gamma-rays interact in the wall or  $\text{BF}_3$  gas, secondary electrons are created, which, in a proportional counter are swept to the anode, creating small-amplitude pulses – “noise.” A more detailed description of how gas-filled detectors detect radiation is available in Reference 30. As the gamma-ray flux increases, an electron shower is created in the detector tube. The small pulses from the electron shower are integrated over the time constant of the tube, creating a charge pulse that is proportional to the total charge collected. In a  $\text{BF}_3$  proportional counter, the neutron reaction products from the  $^{10}\text{B}$  reactions produce much larger pulses than the electrons produced by the photons. However, as the gamma-ray flux increases the pulse amplitude from the gamma-induced electron shower increases, to an extent that the pulse height may be equal to or greater than the amplitude affiliated with the collection of charge from neutron interactions. Above this energy-dependent gamma-ray dose-rate threshold, a pulse from gamma-ray interactions cannot be discriminated from a neutron detection event. Different wall materials and thicknesses will result in different reaction rates. By using a discriminator, i.e., the SCA, as discussed in more detail in Section 5.4.5, the counter can be set to read only the larger pulses.

If the design of the detectors and electronics has not been selected and evaluated properly, neutron count results will be erratic and unreliable. Because of the high radiation environment near spent fuel activated hardware in the spent fuel pool and the small detector tube diameters, gamma-ray interference is an important aspect that needs to be controlled. Without proper n/ $\gamma$  discrimination the detector will count

---

\*. Personal communication with Thomas C. Haley, 2012.

gamma-rays as neutrons, and in a high gamma field above the detector design limit, the detector may saturate and essentially fail, e.g., register very high number of counts. An example of process controls outside the operation limits is provided in Reference 15 (Part 3: NET-229-01), where during the testing process, one of the BF<sub>3</sub> detectors was identified as becoming sporadically operative due to suspected gamma radiation damage from a spent burnable poison assembly in a cell adjacent to cells being tested. The uncontrolled environment was due to operator error and using the system outside its range of applicability. If the detectors are used outside the range of applicability, the measured result can be significantly in error. In this example, the detector actually failed, and the results from it were no longer used. However, all detector results from that test campaign could be significantly in error if they were operated outside the rated detector specification limits.

During design, the instrument specifications for n/γ discrimination are determined based on the anticipated neutron count rates and photon exposure rates to be encountered (this is further discussed in Section 5.4.5). Hence, the detector uncertainty should essentially be low (<2 percent on count rate) or within manufacturer specifications when operated in accordance with the design limits. If operated outside the design limits, then the counting results are unreliable. This parameter must be thoroughly evaluated in the design-specification period of system development. Failure to discriminate gamma-induced signals could be the most significant contributor to uncertainty, if uncorrected. Provided the neutron detector and electronics are specified and tested properly (to account for the high radiation dose), then a QC program can be put in place to manage detector uncertainty due to gamma interference. If the gamma-ray flux is too high, then a different detector with a higher Q-value, such as a fission chamber, could be employed.

## 5.4 ELECTRONICS

The nuclear electronics used by the BADGER system include a preamplifier, amplifier, discriminator/single-channel analyzer (SCA), high-voltage power supply, and data acquisition board/scaler. A basic circuit diagram for a BF<sub>3</sub> counter is illustrated in Figure 5.1.

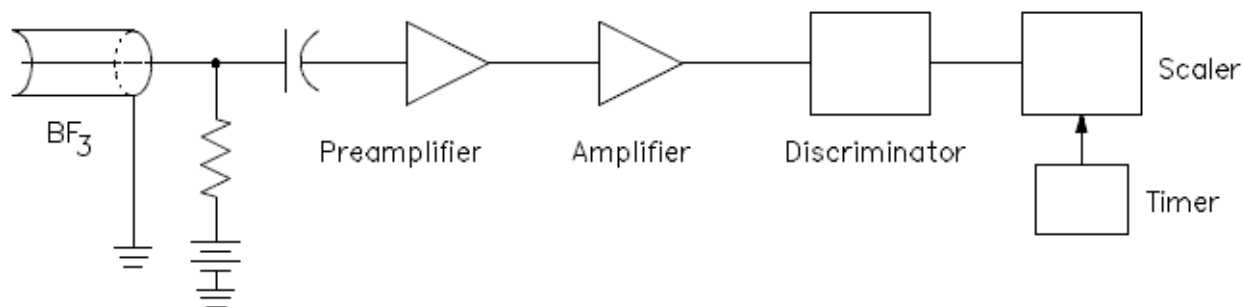


Figure 5.1. BF<sub>3</sub> circuit diagram. (*Source:* Reference 30.)

Similar to the design selection of the detectors, the uncertainties associated with selection of the electronics components are not independent and can vary depending upon external environmental effects (e.g., high gamma-ray field). During the design process, trade-offs among these parameters are evaluated in order to select a design which ensures that the target performance requirements are achieved. The performance characteristics of the electronics modules must be certified for use with established uncertainty ranges. These components are controlled in accordance with QC charts to ensure that the desired level of performance is maintained within the known uncertainty range. No specific performance

requirements were available for the parameters described in the following subsections to support an estimate of associated uncertainty contribution. Typically, with regard to nuclear electronics, it is not an uncertainty but an erroneous result that occurs when the components are not selected properly.

### **5.4.1 EMI Susceptibility**

Electromagnetic interference (EMI) can be a significant problem in nuclear detectors and electronics. Interference manifests itself as spurious counts in the signal train. All nuclear measurement instruments need to be tested to ensure that the interferences from EMI are corrected for, or minimized, in the design phase of the project. The test requirements for this parameter are provided in International Electrotechnical Commission (IEC) Standard 61000-4-3, “Electromagnetic compatibility (EMC) – Part 4-3: Testing and measurement techniques–Radiated, radio-frequency, electromagnetic field immunity test” (Reference 31). Additional guidance and explanation of the physical problem is provided in NUREG/CR-5609, “Electromagnetic Compatibility Testing for Conducted Susceptibility Along Interconnecting Signal Lines” (Reference 32).

It is not known whether BADGER is Underwriters Laboratories (UL) listed or CE marked. It is also not known what degree or level of environmental testing was performed on the system to meet the intention of the IEC standards.

### **5.4.2 RF Pickup**

The degree to which RF interference and susceptibility affect the BADGER system could be quantified according to the IEC standards presented above in Section 5.4.1.

### **5.4.3 Amplifiers, Discriminators, Power Supply, Acquisition Board**

Field problems such as spiking in neutron count rate, noise in signal processing chain from RF pickup, or EMI susceptibility have been reported (Reference 10), suggesting that instrument error and uncertainty can be significantly greater than anticipated, especially when quantitative results are desired. A large majority of this error may simply be due to using 15-year-old NIM bins and analog nuclear electronics, which age with time. Additionally, the BADGER electronics diagram (Ref. 8, Figure 2-9) indicates that the preamplifier is located about 40 ft from the detector tube. Typically, the preamplifier is located as close to the detector as possible to minimize noise or signal degradation from the length of the cable. Uncertainties may be reduced if signal chain processing is improved, particularly given the recent improvements in both analog and digital electronics for counting neutrons.

### **5.4.4 Signal Processors**

The signal processing electronics such as preamplifier, amplifier, scaler, and acquisition board need to be selected based on environmental specifications required of the measurement. If the signal processing has not been proven to be reliable (i.e., with regard to noise; RF pickup; EMI susceptibility; cabling connection issues; impedance-matched cables, preamp, amp; etc.), then the system is not reliable. Applicable Institute of Electrical and Electronics Engineers (IEEE), ASTM, IEC, ISO, and American National Standards Institute (ANSI) standards are available to assist in the overall design and procurement effort for system components.

### 5.4.5 Discriminators for Pileup Rejection, Wall Effect

Neutrons are detected in  $\text{BF}_3$  proportional detectors via the  $^{10}\text{B}(n,\alpha)^7\text{Li}$  reaction. The  $^{10}\text{B}$  neutron absorption reaction results in the production of an alpha particle and a  $^7\text{Li}$  recoil nucleus that travel in opposite directions. When the kinetic energy from these particles is completely deposited in the detector fill gas, a large pulse is recorded with a typical reaction energy (Q-value) of 2.31 MeV (94%) or 2.79 MeV (6%) (Reference 27). Because the tube diameter is small relative to the range of both the alpha particle and the  $^7\text{Li}$  ion, a significant fraction of neutron-induced charge pulses, the alpha particle and recoil lithium ion nucleus, strike the wall before depositing all of their energy in the fill gas resulting in a significant fraction of charge pulses of smaller amplitude than a “full energy” event, ranging from  $\sim 0.84$  MeV and higher. The cumulative effect of the particle interactions with the wall is known as the “wall effect” in gas chambers and results in incomplete charge collection at the anode. The wall effect is not significant in neutron counting when gamma-ray fluence rates are small, for example, less than 10 mR/h. With higher gamma-ray fluxes, the wall effect combined with the gamma-ray interference becomes a significant issue: gamma-ray interactions are counted as neutrons, as described further below. To offset the gamma-ray interference effect, the lower-level discriminator is set to reject gamma-induced pulses. The wall effect becomes more pronounced as the detector tube diameter is decreased. A small fraction of neutron interactions, depending on angle of incidence and location of interaction within the tube can result in both recoil nuclei striking the wall. This is seen as a slightly lower-energy tail to the left of the 0.84 MeV pulse.

As the gamma-radiation field intensity increases, the number of photon interactions in the gas and detector wall increases. In other words, a high number of gamma rays produce a high number of secondary electrons that can add up to a high enough amount of energy to register as a false neutron count. All pulses above the LLD and below the upper-level discriminator (ULD) are recorded as neutron count events, which represents the detector system count window that would be set on a SCA. If the LLD is set too low for the environment being measured, then gamma-ray induced pulses would be counted as neutrons. The LLD must be set to a higher energy than these pileup pulses to avoid spurious counts in the neutron pulse window. However, as the LLD setting is increased to reduce the impact of pileup pulses, the counts per unit neutron flux are decreased. A smaller fraction of the true neutron signal is integrated over the pulse height distribution. Hence, neutron detection efficiency is reduced. The effect on efficiency for a given count window size can be accounted for during calibration, but the effect on the neutron count rate above the LLD from gamma-rays is highly-variable and not something that can be estimated through calibration.

### 5.4.6 Dead Time

The BADGER system operates in “pulse mode,” where the signal from each interaction is processed individually. One of the main problems with detection systems that operate in pulse mode is that two interactions must be separated by a finite amount of time if they are to produce distinct signals. This time interval is referred to as the dead time of the system. Interactions that occur during the dead time are not counted resulting in lower count rates. Dead time losses can become problematic when high counting rates are encountered. No technical information was provided to evaluate the effect of dead time.

## 5.5 APPARATUS GEOMETRY

A number of design and fabrication parameters are reflected in the conduct of making an accurate neutron transmission measurement. It is much simpler to control the measurement when performed on coupon samples removed from the spent fuel pool. In coupon interrogation, the measurement geometry—between the source-coupon detectors—can be very accurately controlled using precision counting jigs and

counting assemblies. ASTM C1671-07 describes the qualification and acceptance process for neutron absorbers, including a goodness-of-fit test for determining a confidence interval based on coupon sampling. In addition, a new ASTM standard committee has been formed to write a standard for laboratory-grade coupon neutron transmission measurements. As a general rule, the accuracy and precision of any NDA/NDT device employed in situ is typically two to three times worse than for laboratory sample/coupon analysis. That is to say, suppose a laboratory measurement can be made with a TMU of  $\pm 5$  percent; designers of a comparable in situ method will be challenged by in situ geometries and environmental conditions such that making a measurement with a TMU of “just”  $\pm 10$  percent to  $\pm 15$  percent becomes a substantial design goal. For the overall BADGER instrument, it should be stressed that the apparatus geometry for neutron transmission measurements in situ is the most substantial contributor to error (assuming a good calibration and that  $n/\gamma$  discrimination is acceptable), and in this case specifically because the  $^{252}\text{Cf}$  source irradiation is a broad, conical beam across the face of a panel, and the measurement geometry is a near-field measurement such that any variation in the source-to-panel and panel-to-detector geometry will cause a significant change in neutron count rate.

In the case of BADGER, which is an in situ NDT method, it is exceedingly difficult to design, fabricate, and thereby control the important measurement parameters governing neutron moderation, reflection, and absorption consistently within a panel, and between panels. A broad beam, conical neutron transmission measurement across a surface, in situ, is by nature difficult to perform with any type of laboratory-grade precision and accuracy. Many factors come into play because of the neutron slowing-down process and ultimately the reliable and consistent detection of neutrons in a confined and less than ideally characterized measurement geometry. This was discussed in the MCNP modeling effort (Reference 29). Specific parameters of influence that can affect measurement performance associated with the apparatus geometry are (1) head misalignment, (2) rack cell fit, (3) use of mechanical controls, (4) rack cell variations and deformations, and (5) use of detector data to represent panel coverage.

### **5.5.1 Head Misalignment**

Source and detector head misalignment can have a significant impact on measurement results. The term "misalignment" refers to any orientation where the source and detector heads are not flush with the cell wall between them. The relative error is magnified at close measurement geometries (e.g., a few inches) among the source to absorber panel, and absorber panel to detector probes, such that any distortion in counting geometry will affect the neutron flux in the detectors, considerably. The optimum counting geometry and three misalignment variations possible in counting geometry – tilt, twist, and offset – were adapted from Reference 8 and are shown in Figure 5.2. The effect of geometric measurement error is exponential: the neutron count rate in any given neutron detector varies exponentially with placement.

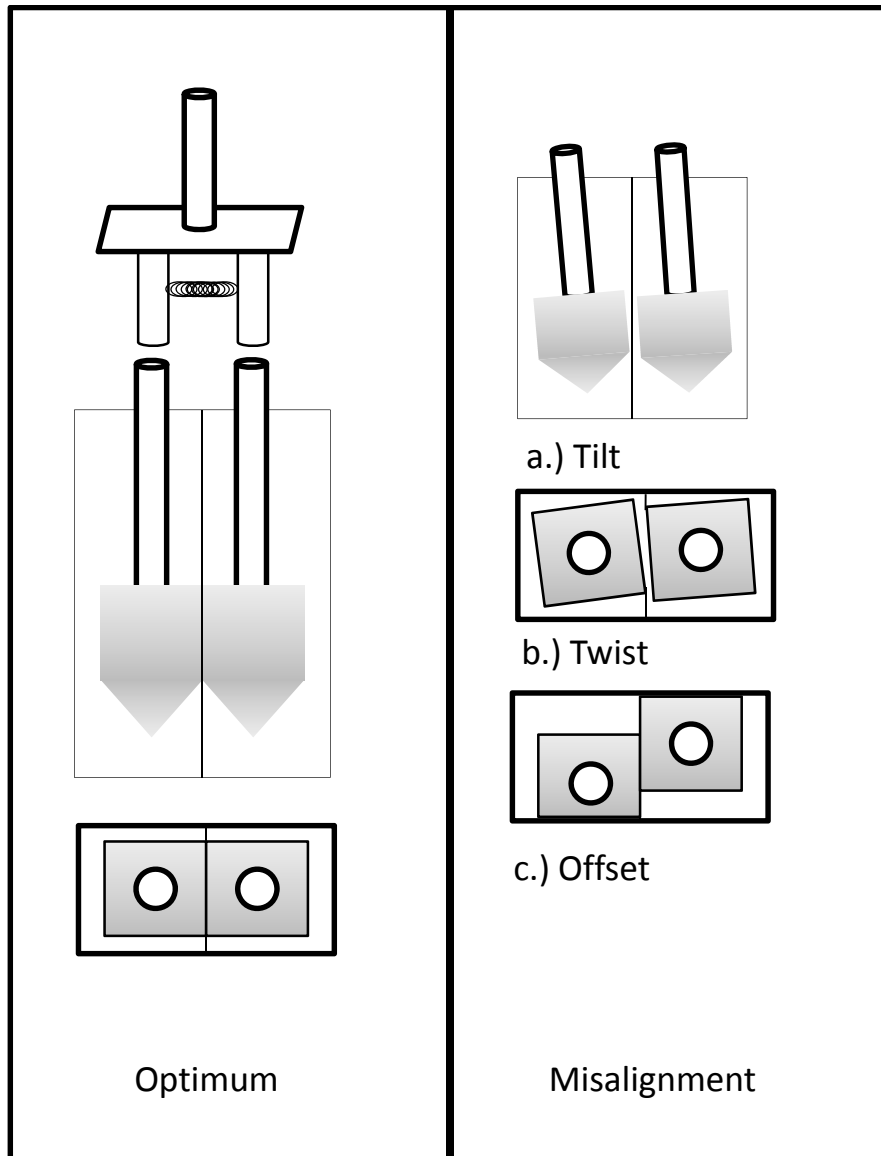


**Figure 5.2. Detector probe orientation. (Adapted from Reference 8 with permission of EPRI.)**

At such close range, a minor  $\frac{1}{4}$ -in. (0.6 cm) shift in the neutron detector *away from* the source can result in a count rate change of approximately 10 percent. The bias on areal density is approximately the product of the bias in count rate and the slope of the calibration curve, resulting in a  $^{10}\text{B}$  areal density change by at least 20 percent. While the front-to-back geometric variation is the most extreme case, side-to-side geometric variation and detector-source twisting can also introduce large uncertainties. Relative average areal density uncertainties of 15 percent to 43 percent were observed in the SCALE models represented in Appendix A. In addition to the geometry change, misalignment uncertainties are also dependent upon the panel areal density being scanned. These results are illustrative uncertainties based on a BWR Region II rack module design. The relative uncertainty is expected to be similar in magnitude for other unbored Region II rack modules but would be expected to be higher for bored moderator systems and flux trap rack designs as a result of the overall reduction in thermal neutron count rates. Uncertainties in BADGER as deployed may be more accurate if they are evaluated by direct performance testing of the device, for example by destructive examination of test panels, rather than by estimating with Monte Carlo neutron transport calculations, as performed in this report and as discussed in Reference 29.

## 5.5.2 Rack Cell Fit

Uncertainty associated with the rack cell fit can result in head misalignment as discussed in Section 5.5.1. Section 5.5.3 discusses the use of mechanical controls to reduce the potential for misalignment. Any other uncertainty introduced from rack cell fit issues will be site and/or rack module specific and will vary from pool to pool. Therefore, no general estimate of uncertainty can be provided at this time.

## 5.5.3 Compression Springs, Shims, Vertical Offsets

As discussed in Section 5.5.1, tilt, twist, and offset geometry variations can have a significant impact on the reported areal densities as determined with the BADGER system. Even though two BADGER designs have been constructed, one for PWR assembly racks and one for BWR assembly racks, to account for the rack cell size difference, variability still exists among rack designs. When the clearance between the rack cell walls and the detector heads is large, shims are used to mechanically reduce the range of lateral movements. In addition, a compression spring has been mounted above the heads to keep each module butted flush against the rack cell wall under investigation, and to ensure that the source-panel-detector assemblies are held firm against each other, and constant along the length of a test panel to the fullest extent practicable. The desired level of compression by the spring being applied unevenly, or shim wear, could introduce a bias due to head misalignment.

Vertical offset is a difficult geometric effect to control. With a 2-inch (5 cm)  $\text{BF}_3$  detector, any small change (e.g., fraction of an inch) in the vertical offset will create a relatively significant change in neutron count rate similar to that discussed in Section 5.5.1. To maintain low uncertainty due to head offsets, routine checks and inspections can be conducted to ensure that mechanical controls are performing as desired.

## 5.5.4 Effect of Rack Cell Deformation: Panel Cladding Bulges, Collisions with Assemblies

References 9 and 33 identify some physical characteristics that are expected to be encountered during BADGER measurement campaigns: Boraflex shrinks, cracks, and develops gaps; Boral<sup>®</sup> blisters and bulges; Carborundum warps, stretches, and shrinks; and spent fuel racks can warp over time. As a result, maintaining well-characterized counting geometry can be challenging, depending on the magnitude of these physical deformities in the panels. The contribution to measurement uncertainty from physical effects in the deformation of the test rack cell may be mitigated if the calibration cell incorporates a set of calibration plates exhibiting similar effects. The bias in this term must be evaluated since the relative change in the counting geometry is significant due to (1) broad beam irradiation of point  $^{252}\text{Cf}$  source across panel surface  $\sim 3\text{--}4$  in. (7.6 – 10.2 cm) from source; (2) detectors  $\sim 0.5$  in. (1.3 cm) from panel; and (3) bulges reported with dimensions of  $\frac{1}{4}$  in. (0.6 cm) or more. Neutron transmission measurements are very sensitive to these changes in measurement geometry. Uncertainty in areal density values would be similar to or greater than that described in Section 5.5.1 across an axial segment where deformation exists.

## 5.5.5 Determination of Detector Coverage of Panel Area

A broad-beam point source projection across a panel surface several inches from the source is subject to specific measurement controls that need to be in place to ensure the uniformity of the irradiation. Uncertainty can be quite high, as opposed to a uniform, "pencil-beam" irradiating flux used in a laboratory-grade coupon-sample analysis (ex situ). According to Reference 8, the number of detectors selected (four) was based on the appearance of gaps of a specific size in the early 1990s, based in part on

coupon samples that had been analyzed as well as other in situ blackness testing measurements. It is difficult to read the raw trace data from the BADGER reports to determine whether detector coverage is complete or not; however, there are some adjustments that can be used in the data reduction algorithm to look at the effective growth of a gap along the horizontal plane.

Provisions do not exist in the data reduction software to correlate the count rate in the two outer detectors relative to the two inner detectors. This is left up to the operator (or analyst) to examine this ratio and to identify nonuniformity of  $^{10}\text{B}$  areal density across the panel width laterally. This is a subjective evaluation, and not always performed, that in turn is used to reexamine or reestimate the integrity of the neutron absorber at the edge (edge dissolution). A description of how the BADGER scan data is interpreted is provided in Section 5.2 of Reference 10. Each of the four neutron detectors has its own specific calibration curve, and averages between the inner and outer detectors can be compared for consistency across an axial segment of the panel.

## 5.6 CALIBRATION

Although not described in any of the BADGER reports, prior to the conduct of a measurement inspection, most measurement systems are tested to ensure that the electronics are performing within specification according to control charts that are kept for each system. Electronic adjustments may be made to ensure that the lower-level discriminator on the amplifier is set properly (for n/ $\gamma$  discrimination), that the high-voltage plateau is established on each of the four neutron detectors, and that the source-decay-corrected neutron rate in the detectors measured from the  $^{252}\text{Cf}$  is within nominal statistical expectation. In addition to the electronic tests of the nuclear instrumentation, the neutron background in the vicinity of the calibration panel and the test panels needs to be evaluated. There was no evidence in the open literature on how the background evaluation is performed. Good practices for calibration, as discussed in ASTM C1592M-09 (Reference 16), can lower uncertainty. Once the system is proved to be within statistical control, accurate calibration cell scans can be conducted.

Calibration is the engineering process of relating the measurement system response (measurand) to the derived parameter of interest. A calibration curve relates the measured neutron count rate to  $^{10}\text{B}$  areal density and to percent degradation from the reference panel. The calibrations performed on-site are described to some degree in Reference 34, but several of the specific calibration and data reduction steps necessary to construct the mean square error (MSE) terms in the calibration matrix are not publicly available. Therefore, all calculations performed in this section use data for illustrative purposes only. This is a significant limitation of attempting to estimate uncertainty in the calibration functions alone.

### 5.6.1 Number, Range, and Precision of $^{10}\text{B}$ Areal Density of Standard Panels

A calibration mathematical relationship (or function) is developed from a calibration cell consisting of a range of absorber plates with known  $^{10}\text{B}$  areal densities. Reference 10 indicates that the calibration cell contains Boraflex panels of various known  $^{10}\text{B}$  areal densities with well-characterized gaps. The  $^{10}\text{B}$  areal densities of the calibration panels were reported as known from material certification sheets and verified by chemical assay and neutron attenuation testing.

Based on the information reviewed, it appears that the calibration cell has changed over time. A single rack cell configuration from 1998 is described in Reference 29 as being composed of a rack cell with a single region for absorber panel placement representative of a Region II rack on one side and a Region I rack on the other. Although not explicitly stated, it is assumed that absorber panels of different areal densities are placed axially in order to develop the calibration curve. A more recent description (i.e., 2010 report) discusses a 3 $\times$ 3 calibration cell, illustrated in Reference 35 (Figure 2-4), that contains 21

different standards including four Boral<sup>®</sup> standards (Reference 35, Table 2-1), and a specific reference panel that is representative of panels in the Turkey Point 4 Region 2 racks. Consistent with the information presented in Reference 10, processes described in Reference 12, and assuming that the development of the calibration cells and panel certification process would have been controlled under an NQA-1 quality assurance program (Reference 36), there would be objective evidence which demonstrates that potential uncertainties in the calibration due to <sup>10</sup>B areal density uncertainty in the calibration standards are negligible. However, this type of information was unavailable for review; therefore, no estimate on uncertainty can be made.

When fitting exponentially distributed measurement data, in particular, it is important to select the range of calibration plates over the range of use of the device, to determine and optimize the number of calibration plates around the test panel <sup>10</sup>B areal density. Regarding the number of calibration standards, Reference 37 (Section 2.3.6.2) indicates that a minimum of five discrete known calibration plates of specified <sup>10</sup>B areal density are required for a linear calibration curve, and that 10 plates should be adequate for more complicated models. It is noted in Reference 16 that the amount of effort expended on calibration should be commensurate with the quality objectives of the measurement results. Calibration standard and curve data were unavailable for review, so no estimate on uncertainty can be provided.

### **5.6.2 Standard Panel Degradation**

A standard panel in this subsection is in reference to the different calibration standard panels that make up the calibration cell. As implied in Reference 8 and Reference 35, a calibration cell is brought from site to site and lowered into the pool at the beginning of the BADGER measurement campaign. After it is used to develop a calibration function, it could be removed immediately, or after the measurement campaign is completed. Either way, the time in pool, and therefore its exposure to gamma radiation, will be minimal, so the expectation is that there should be negligible degradation of the calibration standard panels. This can be confirmed with a proper QC program and establishment of an inspection process. Uncertainty associated with degradation of the calibration standards should be negligible in comparison to the other factors that can influence measurement error.

However, if a calibration standard panel(s) suffers degradation, this will result in increased spread of transmission ratios about a given standard areal density and should be reflected as additional uncertainty associated with the calibration curve fit to the data points. Because the calibration cell is only used for determining the slope, this uncertainty would propagate forward as a slope uncertainty when the test panel areal densities are being calculated. The uncertainty in <sup>10</sup>B areal density measurement of the test panels will be directly proportional to the increased uncertainty associated with the calibration standard panel degradation.

### **5.6.3 Adjustment of Calibration Procedure for Specific Pool Characteristics**

BADGER conducts a relative, not an absolute, measurement. When the physical properties of the inspected panel and the calibration panel are identical, accurate relative measurements can be made. Ideally, the materials and the geometry of the rack would be identical to those of the calibration cell. Unfortunately, this is not the case because of differences in rack modules between various spent fuel pools. Some physio-geometric differences between calibration cells and rack cells may impact measurement uncertainty commensurate with the degree of difference, but may also invalidate the calibration function for the rack cells. Pool-specific characteristics contribute to uncertainty associated with the calibration process. Therefore, adjusting the calibration procedure to account for rack- and spent-fuel-pool-specific characteristics reduces uncertainty. For example, a difference in flux trap spacing (for different spent fuel pool racks) can cause a shift in the neutron energy spectrum from what

was used for establishing the slope in the calibration function. Additionally, adjustments to account for significant differences between rack cell configurations and the calibration cell configuration may be necessary.

Some test reports such as Reference 18 list NETCO-developed pool specific procedures in the reference sections; however, the information was unavailable for review.

#### **5.6.4 Relevance of Standard Panel Material to Rack Panel Material**

The effects of self-shielding, streaming, and channeling of neutrons between absorber particles can vary significantly for different materials. Neutron channeling and streaming occur when the distribution of boron in the absorber panel matrix is heterogeneously distributed such that a path between boron particles exists that allows neutrons to penetrate the absorber sheet without attenuation. Self-shielding is in reference to the neutron absorber particles at the surface absorbing neutrons before they can penetrate deeper into the absorber material. The materials' heterogeneity parameters (e.g., particle composition, size, dispersion) of the calibration cell and test panels must be similar for accurate calibration. The effect of heterogeneity of composition is more pronounced in soluble boron environments. For example, consider a PWR spent fuel pool that contains soluble boron in the moderator and test panels with different levels of degradation. The test panels that have exhibited degradation may have void regions within the panels with different porosity levels. In addition to water moderator, these pores could also contain soluble boron that would not be captured in scans of the calibration standards or the reference panel but will affect the thermal neutron attenuation rates. The impact of this difference in heterogeneous properties depends upon the amount of degradation, the areal density of the test panel, and the amount of soluble boron present in the pores. In addition, neutron in-scatter will be dependent on local measurement perturbations from scallops, warp, and geometric effects.

To account for differences between the standard panel material and the rack panel material, including but not limited to: inhomogeneities, composition changes, material losses, and dimensional changes, appropriate adjustments or correction factors would be needed to ensure that the physical measurement distortions, compositional changes, and all other relevant differences are accounted for when developing calibration model uncertainties. Alternatively, if like-for-like characteristics are not available, computational assessments and bounding system performance studies could possibly be conducted to estimate TMU introduced by the physical differences between the calibration panel, reference panel, and actual panel under test. These assessments and studies would need to account for physical differences between the standard panels and the rack panels.

As discussed in Reference 38, experimental and calculational results have indicated that neutron channeling effects diminish as the thickness of the neutron absorber increases, given a constant volumetric density. Hence, for high areal densities or thicknesses, when the neutron transmission is small, the impact of different materials should be small. However, the rate of change in areal density as a function of neutron transmission will be different for different materials (Reference 39), resulting in a calibration curve that is not representative of the material of interest. Accuracy of neutron transmission measurements is very susceptible to the physical properties of the calibration cell standards matching the test panels. Based on the limited documentation reviewed, the estimated relative uncertainty associated with using different calibration standard materials from the rack cell materials (provided  $^{10}\text{B}$  is the primary neutron absorber isotope) is estimated to be  $\pm 30$  percent which takes into consideration existing guidance for spent fuel storage and transportation applications regarding credited neutron absorber (Reference 40). If a different absorber (e.g., gadolinium) is used, no estimate can be made without detailed experimental data.

For on-site calibration, a standard calibration panel that is identical in all physical properties and characteristics as the test panel(s) (i.e., rack designs with corresponding matching “representative” calibration panels) is likely to generate the lowest uncertainty. In situ neutron transmission measurements are very sensitive to variation in measurement geometry. If “representative” calibration panels for reference panels are not available, then uncertainties might possibly be addressed, at a minimum, by developing a technical basis document which includes radiation transport-based calculations which can be used to supplement the detector response functions to get a better estimate of the bounds.

### **5.6.5 Location and Acclimatization of Calibration Cell in Pool**

The information reviewed indicates that the calibration cell is either placed on top of empty rack modules (Reference 41, p. 4-10), or next to the rack modules (Reference 35) in the vicinity of the cells being tested. This non-standard placement of the calibration cell introduces uncertainties due to background radiation and specific environmental effects manifested in the response of the neutron detector. For example, an important aspect may be the temperature dependence of the neutron detector efficiency when the detector is placed in the pool and then equilibrates in the thermal regions near adjacent spent fuel assemblies. Reference 24 provides example detector specification data and states that “at ambient temperatures ranging from room temperature to 300°F (149 °C) the thermal neutron sensitivity... shall be within ±20 percent of the room temperature value.” Local pool temperatures can vary across different regions of the pool. This can result in different levels of mixing from thermal gradients (i.e., local soluble boron concentration distribution/stratification) and possible differences between the calibration cell, the reference cell, and the test cell environmental conditions. Hence, the uncertainty in the overall response functions will change because of environmental influences specific to the pool region in which that test is being conducted, and such effects could be minimized by allowing the system to acclimate to the conditions representative of the panels to be scanned, so that all measurements are performed under similar environmental influence conditions.

### **5.6.6 Choice of “Zero-Loss” Panel and Uncertainty of Actual <sup>10</sup>B Areal Density**

As defined in Section 2, the zero-loss, or zero-dose, panel is the *reference panel* to which all test panels are indexed. The reference panel allows the transformation of the measurement into a percent loss. Because the <sup>10</sup>B areal density of the reference panel is a key term in the calculation equation (see Reference 10) of the <sup>10</sup>B areal density of the test panel, uncertainty in the reference panel will affect the uncertainty of the overall BADGER output. To mitigate this major source of uncertainty, strict adherence to administrative controls must be enforced on the reference panel to ensure that degradation in the <sup>10</sup>B areal density is zero. The level of administrative controls required for this assurance was not available; however, according to the calibration formulations provided in the literature, the neutron transmission relationship is deliberately indexed back to the reference panel, linearly. Some of the test campaign reports had originally identified no dose panels as being in use but were later determined to have received dose; in other instances, reference panels that should not have any losses were observed to have losses. Although dose is considered a contributor to absorber loss, especially for Boraflex, there are other spent fuel pool environment conditions that can also lead to absorber degradation, such as heat and pool chemistry. Hence, all panels will potentially be subject to degradation once inserted into the spent fuel pool. Reference 12 indicates that the transmission ratio comparison should be compared against the calibration standards directly.

The principal contributors to uncertainty in actual  $^{10}\text{B}$  areal density of the reference panels are a lack of detailed records for specific panels, the use of batch processing, manufacturing variability within a given batch, and erroneous identification of panel dose. Rack cell panel variations of  $\pm 10$  percent from nominal are typical (Reference 18).

The reference panel provides the set of BADGER measurements from which a percent degradation value, percent  $D$ , is calculated according to Reference 34 (Equation 3.3.1):

$$\%D = \left( \frac{\rho - \rho_r}{\rho_r} \right) 100\%$$

where  $\rho$  is the  $^{10}\text{B}$  areal density measured in the test panel and  $\rho_r$  is the  $^{10}\text{B}$  areal density measured in the reference panel. An underestimation of the  $\rho_r$  in the reference panel will result in an overestimate of the percent degradation. Consider the following simple example:

The reference panel is assumed to have a  $\rho_r$  of  $0.06 \text{ g/cm}^2$ . Suppose a test panel areal density,  $\rho$ , is measured to be  $0.05 \text{ g/cm}^2$  based on the calibration curve. The percent degradation is thus calculated to be  $-16.7$  percent. Later, it is realized that the reference panel had been degraded because it had been exposed to some external gamma-ray flux and was thus not a true zero-dose panel. If the  $^{10}\text{B}$  areal density of the true zero-loss panel were actually a  $\rho_r$  of  $0.065 \text{ g/cm}^2$ , then the percent degradation of the test panel would be recalculated to be  $-23.1$  percent. The error in the reference panel assumption would have yielded a nonconservative result: the percent degradation of  $-16.7$  percent was smaller than the true degradation of  $-23.1$  percent.

Based on this example, it is shown that identifying the reference panel areal density correctly and to ensure adequate controls are in place to ensure that the reference panel suffers no neutron absorber loss is paramount to limiting uncertainty. An  $8.3\%$  ( $(0.065-0.06)/0.06$ ) degradation or change in areal density in the reference panel which is not detected or known results in a bias of  $38\%$  ( $8.3\%/23.1\%$ ) in the percent degradation value when uncorrected for.

If the reference panel  $^{10}\text{B}$  areal density value is biased (that is, the assumed  $^{10}\text{B}$  areal density differs by an unknown amount), all examined test panel biases will be of the same sign and magnitude. Additionally, the density of the test panel  $\rho$  initially increases as the panel undergoes radiation-induced shrinkage and subsequently decreases as the panel undergoes dissolution. Therefore, comparing the as-is density  $\rho$  of the test panel to the density of a zero-loss reference panel density  $\rho_r$  to determine if or how much degradation has occurred is problematic and potentially a source of uncertainty.

### 5.6.7 Nonlinearity of Calibration Curve, Especially as Applied to Flux-Trap Racks

The calibration curve for implementation of BADGER is established by performing a nonlinear regression model of neutron transmission on  $^{10}\text{B}$  areal density. The ratio of the neutron intensity (count rate) in the attenuated region to unattenuated region ( $I/I_0$ ) is equal to an exponential function in the parameter  $\rho x$ ,  $^{10}\text{B}$  areal density ( $\text{g}/\text{cm}^2$ ):  $I/I_0 = \exp(-\Sigma_a/\rho] \cdot \rho x)$ , where  $\Sigma_a$  is the integral macroscopic absorption cross section integrated over neutron energies impinging upon the absorber panel,  $\rho$  is the volumetric density ( $\text{g}/\text{cm}^3$ ), and  $x$  is the thickness of the absorber panel (cm). Given calibration plates of areal density,  $\rho_i$ , for  $i = 1$  to 5, the ratio of count rates in a given detector is regressed on the  $\rho x_i$  values. Estimation of the least-squares fit parameters and associated MSE terms must be evaluated and propagated through calibration.

The flux-trap Region I design is subject to an additional uncertainty in the fit parameters given that  $^{252}\text{Cf}$  source neutrons must penetrate two panels before reaching the neutron detector. The hardness of the spectrum needs to be evaluated to ensure that the second panel is not near “infinitely thick” to the thermalized neutron spectrum.

### 5.6.8 Uncertainties in Calibration Slope, Especially as Applied to Flux-Trap Racks

Spectral effects from differing geometry between the actual rack cell and the calibration cell may produce a different detector response to changes as a function of areal density. There is some question regarding the consistency of the energy distribution of the neutron interrogating flux between the calibration cell, the reference panel, and the panels under investigation. It is noted that the slope of the calibration cell curve for a flux trap can be extremely steep as a result of the blackness of the neutron absorber, especially at higher  $^{10}\text{B}$  areal densities. Small changes in the neutron transmission ratio can result in a relatively large change in the reported areal density. Therefore, slope errors have a large influence on measured areal density. Use of a two-point calibration (min, max) as described in early BADGER test reports (Reference 8) assumes that the instrument is linear over the interval of interest. This will increase uncertainty for an exponential/logarithmic functional fit because there are insufficient degrees of freedom to estimate the MSE in the fit parameters. The calibration functions require further evaluation to ultimately determine the various sources of uncertainty in the function. However, the Watt-fission spectrum of neutrons emitted from the  $^{252}\text{Cf}$  source are down-scattered by the time they reach the first panel in a flux-trap design. Neutrons that penetrate the first panel of a flux trap (closest to the source head), with sufficient energy to do so, are subsequently down-scattered prior to reaching the face of the second panel of the flux trap (closest to the detector head). The down-scattered flux is of such low energy that the second panel is under-sampled and thereby overmoderated. Without knowing the degradation in the first panel (closest to the source head), there is no way to estimate degradation (or areal density) in the second panel (closest to the detector head) of the flux-trap because BADGER takes an integrated combined measurement of the entire flux trap.

Consider the following hypothetical calibration cell consisting of panels A, B, C, and D with known areal densities of 0.0212, 0.0148, 0.0085, and 0.0042 g <sup>10</sup>B/cm<sup>2</sup>, respectively. A subset of simulated count rate data was taken from Appendix A, which is representative of the BADGER system for this example and is illustrated in Table 5-1.

**Table 5-1. Example calibration cell data**

Panel	Areal density (g <sup>10</sup> B cm <sup>-2</sup> )	Counts (attenuated)	Counts (unattenuated)	T (attenuated/ unattenuated)
A	0.0212	88	386	0.2280
B	0.0148	99	386	0.2562
C	0.0085	125	386	0.3239
D	0.0042	180	386	0.4662

To illustrate the impact of a two-point calibration, consider panels A and D. Because there are two points, the slope is  $\Delta y/\Delta x = m = -0.0237$  (note y is areal density and x is  $\ln[T]$ ). Using the areal density function relationship described in Reference 10(Eq. 5-1),

$$\rho_{A,ij} = \rho_{A,0} + m \cdot \ln(T_{ij}) \quad (5-1)$$

where

$\rho_{A,ij}$  = <sup>10</sup>B areal density of a test panel,

$\rho_{A,0}$  = <sup>10</sup>B areal density of the reference panel,

m = slope determined from a separate calibration function,

$T_{ij}$  = the transmission ratio, which is the count rate ratio of the test panel to the reference panel,

and a reference cell panel areal density,  $\rho_{A,0}$ , equal to panel A, the test panel scan data with transmission ratios corresponding to the B and C areal densities will be in error by 24 percent and 52 percent, respectively. As discussed in Reference 10, it appears that over time the use of the calibration cell has changed to include more than a two-point calibration. However, the details of how the calibration function is determined and ultimately used were unavailable for review.

An additional uncertainty can be introduced into the calibration function from the count rate data, and the uncertainty is more prevalent when the thermal neutron transmission ratio is lower, such as in a flux trap design. Considering the discussion on count rate in Section 5.1.1, assume that the calibration is conducted with longer count times, and thus higher counts, such that 1 percent Poisson counting error is achieved. The test cell scans are conducted quickly, resulting in higher counting error (e.g., 7 percent). Neutron transmission is a ratio, so combining the test cell uncertainty results in a combined uncertainty of ~10 percent approximated by the following relationship:

$$\sigma = T \sqrt{\left(\frac{\sigma_x}{x}\right)^2 + \left(\frac{\sigma_y}{y}\right)^2} \cong 10\% \text{ (} x \text{ and } y \text{ are count rates making up } T, 200 \text{ for this example).}$$

This represents the combined uncertainty on T, the ratio of x:y. Using the fitted equation in Figure 5.3, for a transmission ratio,  $\ln(T)$ , of -0.83, corresponding to an areal density of 0.0092, the areal density range is 0.005 g <sup>10</sup>B/cm<sup>2</sup>, which equates to an uncertainty range of +19 percent to -26 percent. This uncertainty would need to be combined with any uncertainty introduced from the slope and can quickly escalate.

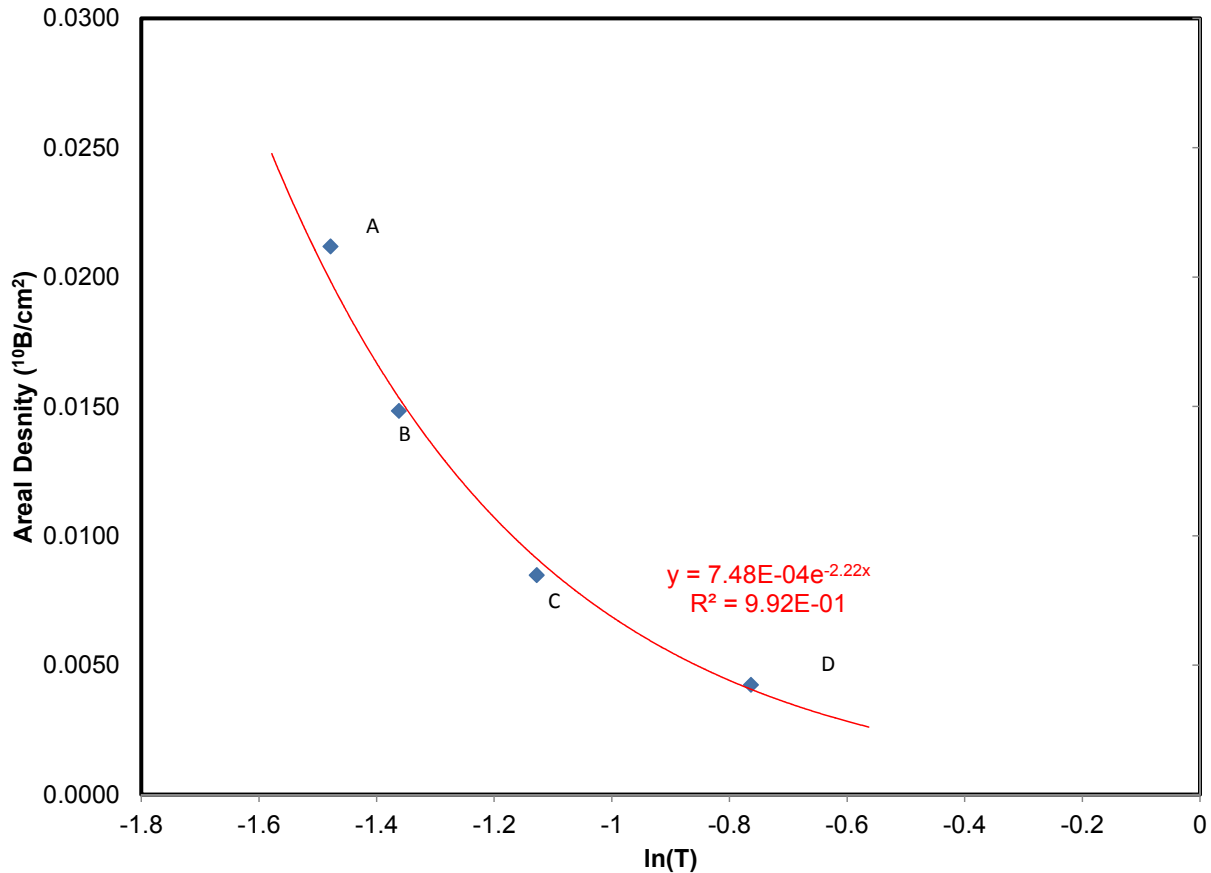


Figure 5.3. Representative calibration curve.

### 5.6.9 Frequency of Calibration during a BADGER Campaign

Specific calibration frequencies during a BADGER campaign were not available. Reference 37 indicates that calibration control measurements should be taken at the start of each day or as often as experience dictates. The time between checks can be lengthened if the instrument continues to stay in control. From Reference 10, it appears that the latter is currently being implemented because the calibration frequency during a BADGER campaign is low (i.e., once or twice during a campaign). The low calibration frequency is in part due to the experience base developed with the BADGER system for Boraflex racks. In lieu of calibration, confirmatory checks are made by comparing the unattenuated region scans of each  $i$ th panel, and then correcting for measurement “drift” (Reference 10). If the BADGER method is applied to neutron absorbers other than Boraflex, that experience is lost, and the uncertainty of infrequent calibrations returns. Conducting BADGER calibrations at higher frequencies until equivalent experience with the material is gained will reduce uncertainty associated with the calibration frequency. The QC and recalibration plan used for ensuring measurement quality is unknown, so no estimate of uncertainty can be made.

### 5.6.10 Confirmatory Analysis with Destructive Examination

The purpose of the BADGER system is to perform nondestructive examination of a panel to evaluate whether it can still be relied upon for suppressing reactivity. Hence, confirmatory analyses with destructive examination are really only available during the design and test phase of the system to assess

the performance, and build confidence in the analysis capability. Removal of panels for destructive examination for comparison purposes after each BADGER test may actually introduce more uncertainty into the overall results because of the handling operations.

Reference 41 (Section 3.2) describes special test cells from which destructive examinations were performed to evaluate the condition of the Boraflex. It was not indicated that BADGER scans were conducted prior to the examinations. No estimate on uncertainty can be provided at this time based on available destructive analysis results.

### 5.6.11 Panel-Specific Use and Interpretation of Unattenuated Region Data

In the MCNP validation report (Reference 29), a long count (i.e., minutes) is described as being taken in the unattenuated region from which to estimate the “drift” variation in the normalization of the neutron intensities between the  $i$ th panel measurement to the reference panel. As shown in Figure 5.4 below, the unattenuated region at the top of each panel is a several inch region where the neutron absorber is not present, but the distance between the BADGER neutron source head and detector head can be held constant. In other words, the rack cell wall and wrapper are still interposed between the source and detector head but the neutron absorber material is not present. An intercomparison between the detector count rate in the unattenuated region of the  $i$ th panel to the unattenuated region of the reference panel is used to correct for localized drift (Reference 10). No specific information or data has been provided to estimate the magnitude of the correction and its associated error.

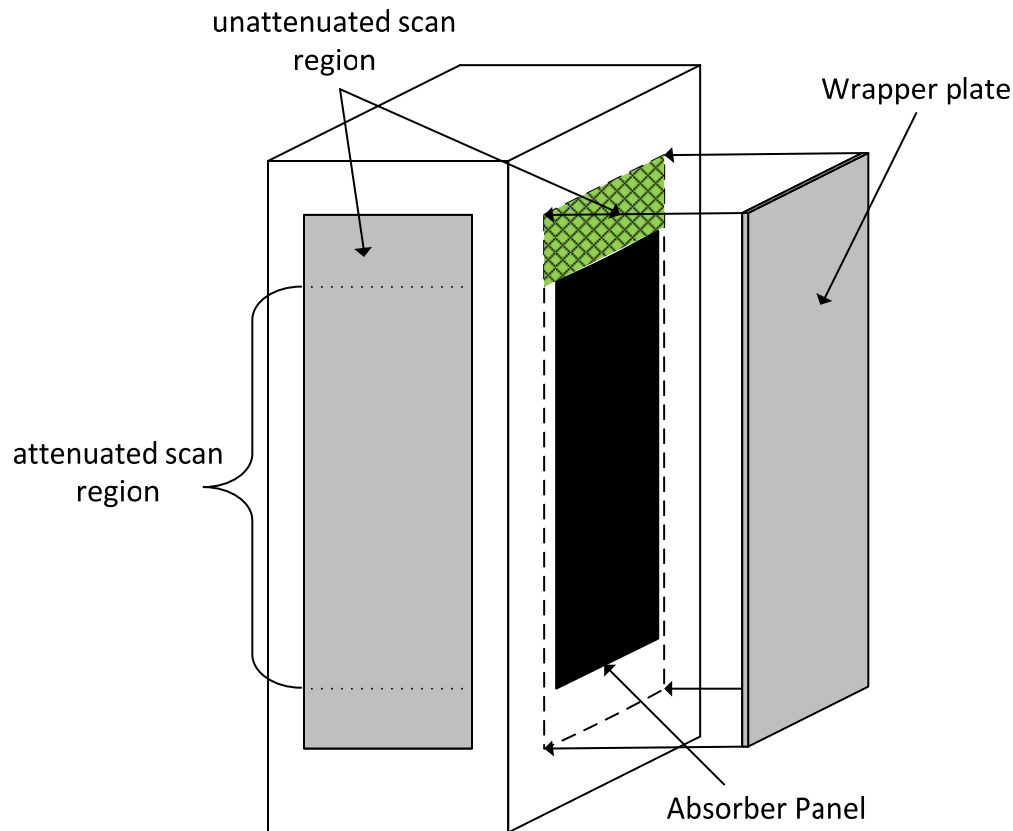


Figure 5.4. Representative Region II spent fuel pool storage cell (Reference 34).

## 5.6.12 Algorithms to Convert BADGER Trace Data into Input for Calibration Curve

The MSE from the nonlinear or linearized least-squares calibration curve should be used to propagate the uncertainty in the areal-density standards, the Poisson error in the count rate of the detector, and any other terms that influence the calibration. Areal density is inversely proportional to neutron count rate, by a  $1/e$  function as derived.

$$T = \frac{I}{I_0} = e^{-\Sigma_a t} \quad (5-2)$$

where

- $I$  = neutron counts registered in presence of absorber,
- $I_0$  = neutron counts registered in absence of absorber,
- $\Sigma_a$  = macroscopic absorption cross section of absorber,  $\text{cm}^{-1}$ ,
- $t$  = thickness of absorber, cm.

Neutron transmission,  $T$ , is the ratio of  $I/I_0$  (the ratio of counts in the attenuated region to the unattenuated region). The  $^{10}\text{B}$  areal density ( $\text{g}/\text{cm}^2$ ), the derived parameter of interest, is the product of the  $^{10}\text{B}$  density,  $\rho$  ( $\text{g}/\text{cm}^3$ ), and the thickness of the absorber material,  $t$ , in centimeters. This nonlinear relationship is linearized in  $\ln(T)$  and estimated from a linear least-squares regression. Based on a measurement of  $T$ ,  $^{10}\text{B}$  areal density,  $\rho t$  ( $\text{g}/\text{cm}^2$ ), is predicted from the calibration function. As long as all measurement conditions are held “constant” between measurements of neutron intensity, a linear least-squares fit of neutron transmission versus  $^{10}\text{B}$  areal density will result in a calibration function that theoretically could be as precise as a few percent.

Areal densities are derived from the basic detector count rate data by developing a semi-log least-squares fit of the natural logarithm of measured neutron transmission,  $T$ , against the calibration standard panel and reference panel  $^{10}\text{B}$  areal densities. When applied to the panel measurement investigation, the areal density is calculated from the following function (Reference 8, p. 4-30):

$$^{10}\text{B Areal Density} = m \cdot \ln(T) + b \quad (5-3)$$

where

- $T$  = neutron transmission ratio,
- $m$  = slope of the calibration curve,
- $b$  = intercept with the ordinate (the reference panel).

The neutron transmission ratio,  $T$ , is defined as the average count rate through the absorber region (away from gaps) divided by the detector count rate above the absorber region with only stainless steel and water separating the detectors from the source. As described in Reference 8 (p. 4-30), the slope,  $m$ , is determined by measuring  $T$  in the calibration cell at two areal densities that bound the tested areal densities. The constant  $b$  is determined by measuring  $T$  in an actual rack cell that has not sustained absorber loss (reference panel). A derivation of this basic equation that relates the test panel directly to the reference panel was provided in Reference 10 (Eq. 5-1), and is also described in Section 5.6.8.

To minimize uncertainty when developing the calibration curve, the measurement conditions that need to be met include (1) neutron background is proven small and/or accounted for; (2) neutron in-scatter into the detector assembly is evaluated and corrected for; (3) the total count (number of neutron events recorded) is statistically reliable, that is, greater than 5,000 counts per detector per measurement step; (4) repeat measurements are conducted during calibration to estimate MSE (Reference 17 recommends at

least four repeat measurements); (5) the calibration function has calibration points spanning the range of areal density of anticipated test panels; (6) the calibration panels are manufactured to within a tolerance of less than a few percent; (7) the calibration equation offset (or  $y$ -intercept) is forced to 1 (i.e.,  $I/I_0$  is equal to 1 when the  $^{10}\text{B}$  areal density is zero; and (8) an analysis of variance is conducted to estimate the error terms in the calibration function, and whether a weighted least-squares analysis is a better approach to reducing the MSE.

A technical basis document typically contains a systematic parametric evaluation of the calibration function describing the mathematical relationship between measured neutron transmission of a test panel and the  $^{10}\text{B}$  areal density.

**Boraflex Panel Gap size.** A separate calibration function, and least-squares analysis, of gap size versus count rate has not been provided but is referenced in Reference 18 (NET-287-01, p. 18): “Gap size is determined by utilizing a transmission ratio fit derived from calibration cell data ... and ... in addition to gaps and cracks, other anomalies were observed.” Reference 8 indicates that the measurement uncertainty for gap size is +0.5/-0.0 in. (1.3 cm) for gaps smaller than 2.0 in. (5.1 cm) and +1.0/-0.0 in. (2.5 cm) for gaps larger than 2.0 in. (5.1 cm) Uncertainty in gap elevation was reported as  $\pm 1.0$  in. (2.5 cm). Reference 18 and several others indicate that BADGER's ability to detect gaps is limited to +1/3 in. (0.85 cm) based on experimental evaluations. Cracks were defined as lateral anomalies that are smaller than 1/3 in. (0.85 cm) axially, but because cracks are below BADGER's resolution, it is possible that they could be regions of local dissolution that do not fully penetrate the thickness of the absorber panel. It is at the discretion of the test engineer to distinguish between gaps and cracks when interpreting the test data. Boraflex is known to undergo radiation-induced shrinkage, asymptotically approaching 4.1 percent, resulting in densification and gap formation (Reference 10). No information was available for review describing how the uncertainties between gap sizes and panel densification are accounted for in the algorithms for calculating areal density. A description of how the BADGER scan data is interpreted is provided in Reference 10(Section 5.2) where it is stated that features such as gaps, local dissolution, scallops, etc. are often difficult to characterize in practice.

Details of the calibration curves used and how the contributing parameter uncertainties are propagated forward were not available for review, so no estimate on uncertainty can be made at this time.

## 5.7 DATA PROCESSING

### 5.7.1 Reliance on Operator Experience to Detect and Characterize Heterogeneous Degradation

Each of the four detector responses is treated independently, with each of the four detector traces (neutron count rate or normalized count rate) displayed by the software, such as the trace shown in Figure 5.5, which was taken from Reference 35. A plot of normalized count rate for each detector, one through four, shows that a gap was detected at 30 in. (76 cm) and 125 in. (317.5 cm), and that once the source/detector heads are located at the top of the panel in the unattenuated region ~145 in. (368 cm) to 155 in. (394 cm)), the count rate ratio steps up in magnitude by a factor between ~50 and ~130. BADGER relies on a skilled technician and engineering operator for implementation, use, and data interpretation so that conclusions about the scans can be made. There is also a strong reliance built upon RACKLIFE predictions to aid the operator in identifying when the scans are incorrect (Reference 10, Section 4.3.4). It is at the operator's discretion on how to ensure “quality data” is acquired, determine the measurement repeat frequency, evaluate whether electronics failed during a measurement, establish mechanical offsets in the adjustment of the source and detector heads, and so forth. A discussion on how trace data is analyzed is provided in Reference 10(Section 5.2).

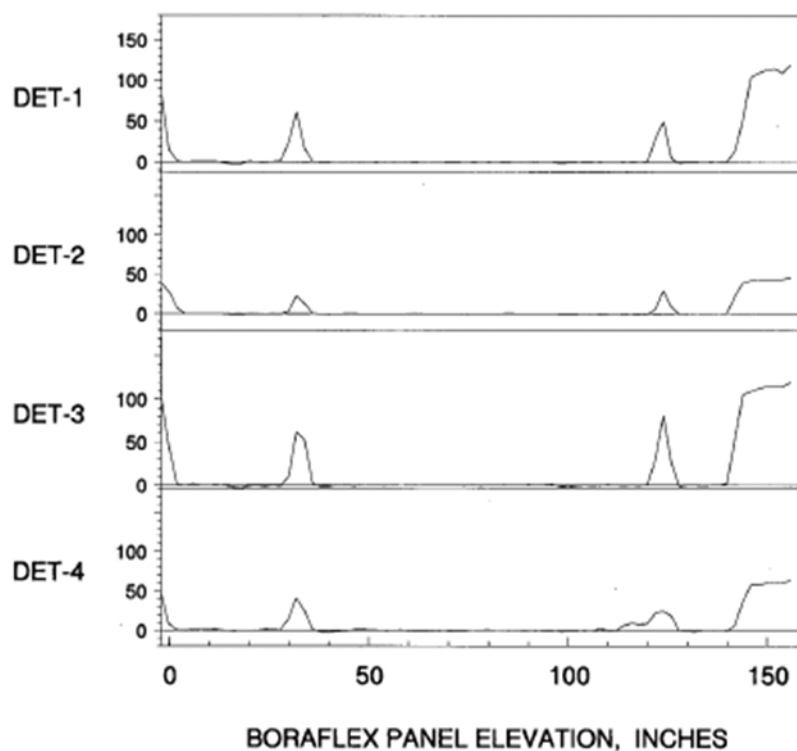


**Figure 5.5. BADGER detector traces (Reference 35).**

High uncertainty can be introduced in the results as a result of operator interpretation, especially regarding decisions on censoring data. Some examples identified in BADGER test reports indicated that due to system noise, results from certain detectors were considered unreliable, but the scans from the other detectors were still used. The data trace plots showed a clear offset from the rack cell descriptions and significant variability in length. To minimize the uncertainty of operator interpretation, standardized decision processes could be developed for incorporating feedback (Section 5.7.3) when a change in condition is observed.

Reference 10 indicates that the experience of the operator and the analyst is a strong determinant in reducing uncertainty and discusses how they need to attune themselves to be able to characterize BADGER scan results. There was no information available regarding the training and qualification requirements for the operators or analysts; therefore, it is not clear how this uncertainty is controlled. Reference 42 indicates that to make quality NDA measurements, training of measurement personnel is required, and that the level of training needed is dependent upon the complexity of the measurement technique and the responsibilities of the personnel. An example good practice guide for training and qualification of NDA personnel is available in ASTM C1490-04, *Standard Guide for the Selection, Training and Qualification of Nondestructive Assay (NDA) Personnel* (Reference 42) that may be beneficial to reducing uncertainties associated with interpreting BADGER scan data.

Mathematical data reduction for the averaging of all raw data would need to be presented in order to propagate uncertainties to a total measurement uncertainty. For example, Reference 8 (Section 3.2.2) states the following: “In regions containing a gap, all counts in excess of 3 sigma of the mean count rate in the region without gaps are not considered in determining the panel areal density.” The basis of this statistical approach for characterizing a given panel was unavailable to be examined. Additionally, it was

not clear that the methodology includes rejecting count rates that fall below three sigma of the mean count rate when determining the panel areal density. To produce low uncertainty results, the data reduction algorithm needs to incorporate consideration of the following mathematical constructs: (1) how each detector,  $i = 1$  to 4, is evaluated individually, and then summed or averaged for purposes of gap detection; (2) how mean and standard deviation are calculated for each detector, for each panel-segment response, and for each panel; (3) how the background is measured and interpreted for determining the mean transmission and associated standard deviation, at which the 3-sigma decision is made; and (4) how repeat measurement results replace or add to the “bulk” statistical quantities, i.e., sampling with or without replacement. Detector spatial resolution evaluations would be needed to examine what gap detection width is allowable and whether the four-detector assembly is sufficiently sensitive to this width, at the 3-sigma decision point, or the equivalent/improved statistical method for detecting and reporting gaps.

The following information would be needed for review to quantify the uncertainty associated with the use of reduced statistical data on an individual, *measured* panel (number of gaps, gap width, and average  $^{10}\text{B}$  areal density) to infer or predict the performance of BADGER for a whole panel: (1) the statistical selection methodology for which  $n$  of  $N$  panels are measured; (2) a description of the propagated measurement uncertainty in each panel measurement; (3) a description of the algorithm used to calculate average panel  $^{10}\text{B}$  areal density from local data points, given heterogeneous degradation; and (4) a statistical methodology for combining sampling error and measurement error.

### **5.7.2 Applicability of Boraflex-Based Algorithms to Non-Boraflex Material Such as Boral<sup>®</sup> or Metamic**

No information was available regarding algorithms except the basic derivations from the attenuation relationship. However, the application of BADGER scan data and the panel selection process is highly focused to support use of RACKLIFE, which is Boraflex specific and not applicable to other materials. The formation of anomalies in non-Boraflex materials and impacts to the localized geometry of the measurement will significantly impact the count rate of neutrons transmitted through the neutron absorber and will need development of material-specific algorithms for proper characterization and identification.

### **5.7.3 Feedback Procedure**

For the operations and use procedure, clear specifications for registering information and data on any physical conditions of a given segment measurement that could cause a “change of condition” allows identification of when the results may no longer be valid or an adjustment needs to be made. A “change of condition” such as a spent fuel pool region with a better or worse mixing region which could affect soluble boron concentration, significant panel batch differences, test panel areal density outside range of calibration, or other changes, could mean that the calibration curve, or assumptions used in the development of it, is invalid. Some feedback into or correction of the data set would need to be developed to ensure that the number of repeat measurements is minimized and that data censoring is appropriate. Several reports indicate that there are sizeable operator issues with the conduct of the measurements.

To minimize uncertainty and promote repeatability in future BADGER scans, operator experience and system adjustments should be captured for future use. For example, operator responses to key measurement parameters can be written into the measurement logbook and evaluated to determine conditions that would invalidate the calibration and test assumptions. Another effective method for ensuring that measurement results are repeatable and stable is to select a subset of measurements and conduct a repeat measurement. This approach is commonly utilized in other NDT applications. The sample repeats may be selected in regions of the test where difficulties may have been encountered or

there is some question in the examiner's mind that the measurement may have been compromised or in error. Sample repeats may also be selected at random to test and ensure system performance. A combination of resampling approaches may be developed.

## **5.8 STATISTICAL EXTRAPOLATION AND SURVEILLANCE FREQUENCY**

### **5.8.1 Choice of Test Panels to Survey**

The information reviewed, which is primarily based on Boraflex degradation, indicates that the panel selection process has been biased toward supporting RACKLIFE. The actual panel selection process to survey with BADGER was unavailable for review, but based on the information available in the test reports, the distribution of the selected sample set typically attempts to include a range of panel exposures, including what is considered to be the most severe exposure history based on dose and time in service as well as a number of panels that are not expected to show degradation. Note that RACKLIFE estimates degradation based on several factors in addition to dose and time in service (e.g., silica content in solution), which is further explained in Reference 10. This panel selection process is consistent with the objectives for assessing overall spent fuel pool absorber conditions but is not conducive to assessing panel characteristics for criticality safety analyses because the distributions are convoluted with low degradation and high degradation information. Because RACKLIFE was developed specifically for Boraflex, it may introduce additional uncertainties if it is used for panel selection for other neutron absorber materials (e.g., Boral<sup>®</sup>). No uncertainty estimate can be made as this is site specific and contingent upon how the BADGER data is collected and applied.

### **5.8.2 Lack of Duplicate Scans of the Same Test Panel**

Duplicate BADGER scans can be used within a single measurement campaign or in subsequent campaigns to determine in situ measurement reproducibility and to spot trends in the overall performance of the device.

A very limited number of panels are scanned in subsequent campaigns, which would be beneficial for evaluating trends. Because of system modifications and large uncertainties in earlier campaigns, the limited repeat panel data is unreliable for trending analyses. This is due to the selection of too few panel samples, improper calibration, and system modifications between campaigns. For example, if the reference panel <sup>10</sup>B areal density, i.e. the y-intercept *b* of Equation 5.3, was inaccurate, then all of the test panel areal densities would be biased, causing the average across one campaign to be different from the next in unexpected ways. If, instead, the slopes based on the calibration cell were inaccurate, then local degradation could be accentuated with large calibration slopes. That is, one campaign could observe local dissolution due to large slopes yielding variations in count rate that lead to large computed variations in areal density, while another campaign would observe more uniform dissolution due to small slopes yielding variations in count rate that lead to small computed variations in areal density. This indicates that the calibration is perhaps the most important aspect for BADGER operation.

An example of how process uncertainty is associated with the gap identification protocol is provided in Reference 15 (Part 2: NET-229-01). Panel rescans of the same panel from opposite directions were conducted in an attempt to increase the precision of the results for the rescanned panels. It was indicated that most of the rescans showed good correlation between the two scans. However, one pair, U11 East/V11 West, showed variability in the interpretation of local anomalies. One scan showed six gaps with a maximum size of 1.96 in. (4.96 cm), while the other showed five gaps with a maximum size of 5.16 in. (4.98 cm). This indicates an uncertainty range of 24 percent to 32 percent in gap size

identification if two 1.96 in. (4.98 cm) gaps were combined in the second scan compared to the 5.16 in. (13.1 cm) gap. The difference in these results is likely due to a slight neutron spectral shift through the steel cell wall before traversing through the neutron absorber material and into the detector tubes compared to the scan in the other direction. This method is not consistent with Reference 12, which indicates that neutron attenuation measurements shall use the same test equipment and configuration. Reversing the orientation of the probes changes the configuration and effectively invalidates the original calibration function.

### **5.8.3 Application of Results of Selected Panels to Entire Pool**

The number of cells in a spent fuel pool may number in the thousands. Thus, not all panels are measured. Rather, a small subset of panels is selected for NDT, based on in-service knowledge about the panels—for example, from the total integrated gamma-ray dose to the panel and an estimate of  $^{10}\text{B}$  loss based on in-service history from the RACKLIFE software for Boraflex.

The actual panel selection process to survey with BADGER was unavailable for this review, but based on the information provided in various test reports, the distribution of the selected sample set typically attempts to include a range of panel exposures, including what is considered to be the most severe exposure history based on dose and time in service as well as a number of panels that are not expected to show degradation. The majority of the test panel data reflects a selection process designed to provide confirmation of the RACKLIFE code predictions and for developing future projections as illustrated in Reference 10 (Figures 4-9 and 4-10), which is consistent with the initial development objectives established in the mid-1990s. The panel results are then used to update the RACKLIFE predictions for characterizing the other panels in the rest of the spent fuel pool. RACKLIFE  $^{10}\text{B}$  areal density loss algorithms are only applicable to Boraflex degradation as described in Reference 10 and are not applicable for other types of neutron absorber materials.

To date, in a number of test campaigns, the number of panels preselected for testing was reduced in number during the testing because of time constraints. For example, Reference 18 had preselected 45 panels for evaluation but actually scanned only 32. Other test campaigns show panel measurement data being rejected with no explanation. It is not clear how these changes in the test sample population are being conducted while preserving an adequate sample population that is representative of the panels in the pool.

Without knowing local conditions of neutron absorber degradation in a spent fuel pool, a specific statistical sampling method cannot be prescribed. There are several common methods to select from, in order to minimize the sample size,  $N$ , yet keeping the MSE reasonably small to meet performance objectives for evaluating overall pool performance. Biased or random sampling can be used depending on project objectives. Several statistical sampling and test methods have been used for the analysis of sampled data in nuclear operations: (1) lot tolerance percent defective, (2) complete block design, (3) randomized complete block design, and (4) stratified random sampling, to name a few. Controls can be used to ensure that the sample design and outcome of the measurement results satisfy the selected method assumptions and constraints before statistical results can be reported for the projected performance of the entire pool, (e.g., number of gaps per panel, gap size per panel, and minimum  $^{10}\text{B}$  areal density).

#### **5.8.4 Frequency of BADGER Campaigns, Especially for Panel Materials Where Intermediate Computational Methods Such As RACKLIFE Are Unavailable**

For neutron absorber materials where methods to predict panel degradation between BADGER measurement campaigns is not available, the frequency of campaigns should be determined on the basis of the known or projected degradation rate, and the margin between the minimum projected  $^{10}\text{B}$  areal density and the value used in the criticality analysis. A graded approach to measurement frequency could be used. Historically with BADGER, estimated degradation rates were generated using the RACKLIFE software. In many applications where Boraflex is not the neutron absorber being evaluated, RACKLIFE is not applicable, and therefore other means would need to be developed in conjunction with estimating poison panel degradation in order to more accurately determine the optimum frequency for the use of BADGER.

#### **5.8.5 Application of Final Output to Criticality Analyses of Record**

NETCO has developed a method for incorporating the BADGER scan results into an assessment of the reactivity effects of local panel degradation utilizing Monte Carlo sampling techniques (Reference 18, p. 40). Details of the method were unavailable for review, but partial descriptions are provided in Reference 43 (Section 4.0 in NET-173-01) and Reference 44. Note that Reference 43 was developed in 2001, and subtle differences were observed in the description of implementation provided in Reference 44, which was written in 2010. Therefore, it is not clear if there are multiple methods or the method as described has changed, and hence, no definitive conclusions could be made regarding application of the BADGER scan data to the criticality safety evaluations of record.

In general, from the partial descriptions reviewed, the method(s) can be summarized as random sampling of panel local degradation features from BADGER scan data that are used to simulate rack panel conditions in a representative reactivity equivalence model. Because criticality is a local phenomenon, care must be taken with how the localized conditions associated with panel degradation, gaps, cracks, and anomalies as well as associated uncertainties are incorporated into the representative reactivity equivalence model. Therefore, the following observations are provided for consideration regarding application of BADGER scan data to criticality safety evaluations.

1. The description provided indicates that each panel is being treated independently for simulation in the reactivity equivalence model. It is not clear that correlations between highly degraded panels or large gaps collocated in the same rack cell region are being accounted for in the Monte Carlo sampling process. For example, a panel that experienced high dose at some point in time was in a cell that had other panels that would have also been susceptible to receiving high dose at that time. Therefore, a correlation would exist for high loss panels on a per rack cell basis. Observations of the panel trace data in the reviewed BADGER test reports showed several instances where gaps are present at nearly the same axial elevation for multiple panels within the same rack cell (e.g., rack cell AA27 of Reference 18 and C6 of Reference 35). Typically, all four panels of a cell are not tested, but because the panel scan data is being treated independently in the reactivity equivalence model, correlations do not appear to be accounted for in this method.
2. The description of the method provided in Reference 43 indicates that the reactivity equivalence model is simulated multiple times to establish a distribution of  $k_{eff}$  calculations from which an estimated bounding value at a 95 percent probability for a 95 percent confidence interval is selected. Details of how this is being performed were not available for review, but depending

upon how biases are incorporated into the sampled panel degradation distributions, the use of the maximum  $k_{eff}$  plus two-sigma may be more appropriate.

3. Panel absorbed dose and B<sub>4</sub>C loss predicted by RACKLIFE algorithms specific to Boraflex degradation are used as input parameters for panel selection and distribution within the reactivity equivalence model. Hence, the current panel selection process and methodology would not be appropriate for application to other neutron absorber materials (i.e., materials other than Boraflex).
4. The calculations of the panel areal density accounts for two major sources of uncertainty in the testing process, namely, measurement uncertainty and statistical uncertainty (Reference 35, Appendix C). An analysis of the uncertainty associated with the distribution fit function(s) also should be included.
5. An additional uncertainty component which is especially important in applications where RACKLIFE is not applicable, is to ensure that panel selection is based on a statistically valid sampling plan that accounts for both sampling and measurement error and includes consideration of potential correlations in sample results.
6. An additional uncertainty which can be introduced into application of the BADGER scan data is process implementation variability. For example, Reference 43 (Section 4.0 in NET-173-01) indicates that the base case represents the Boraflex panel at its minimum certified areal density and thickness, whereas in Reference 16 (Section 4.0) it was indicated that the base case is based on the nominal areal density and thickness. The latter results in an additional bias that needs to be accounted for in the criticality safety evaluation.

### **5.8.6 Use of Final Output in Abnormal or Accident Sequence Criticality Analyses**

Consistent with the requirements of 10 CFR 50 Appendix A GDC 62, “Prevention of Criticality in Fuel Storage and Handling” (Reference 2), the spent fuel pool must remain subcritical at all times. Hence, the 0.95  $k_{eff}$  subcritical limit (10 CFR 50.68) must also be maintained for abnormal or accident scenarios. A potential outcome of a seismic event, dropped fuel assembly, or other load on a rack module containing degraded absorbers is the movement of the remaining Boraflex or other neutron-absorbing material. Such movement can potentially resulting in alignment and/or enlargement of gaps within a rack cell or groups of cells leading to an increase neutron transparency. No information was available for review about how this is addressed in the criticality analyses.

This Page Intentionally Left Blank

## 6 SUMMARY

A Type B uncertainty analysis (Reference 17, NIST Technical Note 1297) was conducted on BADGER, a NDT instrument that measures neutron attenuation in spent fuel panels in situ. The uncertainty analysis methodology used has become known as GUM, the ISO “Guide to the Expression of Uncertainty in Measurement.” A Type B analysis is based on scientific judgment using all relevant information available, with the recognition and understanding that available information may be, and probably is, limited. There are no BADGER-specific consensus standards in existence that describe the calibration protocols and functions, the determination of the calibration offset, i.e., the zero intercept, for the reference panel, or the recommended QC tests specifically required.

The accuracy of the BADGER neutron absorber measurement system is primarily a function of

- the equipment’s ability to discriminate between the radiation of interest and the background radiation field,
- the quality of the equipment calibration and subsequent equipment operation,
- the consistent and reliable positioning of the neutron absorber between the source head and detector head, and
- the ability of the operator to properly use the equipment and interpret the data.

Standards are available that describe in concise ways how nuclear instrumentation should be functionally checked: for example, IEEE N323A-1997, “Radiation Protection Instrumentation Test and Calibration, Portable Survey Instruments” (Reference 45).

This section provides a summary table of parameters that can impact the measurement performance of BADGER. Each of the individual parameters was grouped into categories reflecting different aspects of the BADGER system and how the results are used. Details of each parameter are presented in Table 6-1, but the reader is cautioned that it may not be possible to combine reported uncertainties in a meaningful and useful way.

Table 6.1 consolidates the measurement parameters that give rise to uncertainties in the use and application of BADGER. The parameters are grouped into eight categories corresponding to the Section 5 discussion. The headings of the table columns are defined here, and some notations are explained.

**Section:** Section of the report where the measurement category was discussed in detail.

**Measurement category/subsection:** Category of the measurement system and subsection discussed.

**Physical influence parameter:** Physical parameters or characteristics for each measurement element. These parameters are the specific detailed influence factors that affect measurement bias and uncertainty. An example is neutron count rate in a detector. As the count rate increases, measurement uncertainty improves.

**Information used to support discussion:** Primary source(s) of information used to support estimate of uncertainty described as follows:

- **Expert Judgment** – Much of the BADGER system design and test information is company proprietary or undocumented. The value reported for uncertainty, consistent

with a Type B uncertainty analysis, is based on expert elicitation and professional judgment by experienced subject matter experts in NDT using in situ neutron transmission and attenuation (i.e., the authors of this report). Note that any information provided based on expert judgment has an inherent assumption that the BADGER system, implementation, and use are consistent with applicable industry codes and standards and proper QA/QC principles have been applied.

- **Proprietary Information** – This notation is used to identify proprietary data that is available to the NRC, but not available to the public.
- **Publicly Available** – This notation is used to identify data and reports that are publicly available.
- **First-Principle Computation** – The authors have calculated from Monte Carlo analysis or first principles the magnitude of a reported error term. First-principle computations are used to estimate the relative level of uncertainty in a given parameter.
- **No Information Available** – No reports or data are available with expressly written statements on a parameter-by-parameter evaluation of bias or uncertainty terms.

**Comments regarding relative uncertainty:** Summary discussion about the measurement parameter of influence and reflection about the vetted relative uncertainty value for each measurement element (or group).

**Primary reference source:** Citations from which the relative uncertainty value was obtained or derived.

**Uncertainty range:** Uncertainties are binned into three categories:

1. For individual parameters supported by first-principle calculations or test data, quantitative relative uncertainty values are presented.
2. For parameters where expert judgment was used as in a Type B analysis, uncertainties were given a designation of “low” or “high.”
  - a. Values identified as “low” are considered to be small in comparison to the other overall contributors to uncertainty and considered to have ~2 percent uncertainty or less.
  - b. Parameters with values identified as “high” can contribute an uncertainty so high as to potentially invalidate results alone, even if all other parameters were of low uncertainty.
3. The designation *INQ* indicates that insufficient data was available for review to support quantifying an uncertainty range for a given parameter.

Examples of the types of data which, if provided, may yield enough information to produce an uncertainty, or calculate a more precise uncertainty, are listed in brackets.

**Table 6-1. Summary table of measurement system sources of uncertainty**

Section	Report subsection	Physical influence parameter	Information used to support discussion	Comments regarding relative uncertainty	Primary reference source	Uncertainty range
<b>5.1</b>	<b>Neutron Source</b>					
	5.1.1	Count rate	Publicly available	No experimental data provided to estimate impact of parameter on overall uncertainty on implementation of BADGER. With reported count times per axial measurement of 10 seconds, the net count rate of 1,000 net counts per count interval gives a relative error of roughly 3 to 4%, neglecting contribution from background. Relative error of Poisson counting statistics given by the relative error in subtracting background count rate from gross count rate, adjusted for any effect associated with pulse pile-up, or variability in the in-scatter from neutrons not originating from the <sup>252</sup> Cf source and transmitted directly through the Boraflex. From looking at traces of count rate data published in Reference 8, count rates appeared to be ~200 neutron counts per 10-sec interval (sometimes less), in which case the Poisson error is on the order of 7–8% and will increase based on other neutron count rate effects mentioned above. These effects require additional evaluation.	Reference 8 (Figures 3-16 and 4-10)	≥8% on count rate [Neutron count rate uncertainty should be documented in system test and all panel measurement results.]
	5.1.2	Source strength and decay	No information available	No information available on source strength. The half-life of <sup>252</sup> Cf = 2.65 years, which yields ~0.7% change per 10 days. Corrections and adjustments for source decay should be accounted for in the calibration and on-site QC measurements with normalization correction made accordingly	Reference 23	INQ [Decay-corrected source strength should be presented on calibration and measurement data records]
	5.1.3	Neutron moderation by covers on heads	No information available	No experimental data provided to estimate impact of parameter on overall uncertainty on implementation of BADGER. This is likely to be a large contribution to uncertainty to invalidate results for Region I racks, in particular, where the system is overmoderated and the irradiating neutron flux on the second panel of two is thermalized to such an extent that the <sup>10</sup> B areal density is infinitely thick to the flux.	N/A	INQ [Neutron moderation and down-scatter effects and the influence on system accuracy and precision should be documented in the system test plan.]

Section	Report subsection	Physical influence parameter	Information used to support discussion	Comments regarding relative uncertainty	Primary reference source	Uncertainty range
<b>5.2</b>	<b>Detector characteristics</b>					
	5.2.1	Size	No information available	Performance Specification reflected in count rate (Section 5.1.1) and panel coverage (Section 5.5.5)	N/A	INQ [Neutron detector specifications should be provided in technical design basis document of the system, which captures the trade-offs on count time, count rate, spatial resolution, wall effects, and any other specific measurement parameter that impacts data quality objectives.]
	5.2.2	Efficiency	No information available	Performance Specification reflected in count rate (Section 5.1.1)	N/A	INQ [Same as previous]
	5.2.3	Fill gas pressure	No information available	Performance Specification reflected in count rate (Section 5.1.1)	N/A	INQ [Same as previous]
	5.2.4	<sup>10</sup> B enrichment of the gas	No information available	Performance Specification reflected in count rate (Section 5.1.1)	N/A	INQ [Same as previous]
	5.2.5	Aging	Expert judgment	QC to maintain within design limits. If unaccounted for, results are unreliable.	Reference 8 and Reference 24	INQ [Neutron detector aging is accounted for by a QC measurement program to ensure that the detector produces a consistent and reliable performance with time. When out of control, the detector is repaired or replaced (but normally replaced)].

Section	Report subsection	Physical influence parameter	Information used to support discussion	Comments regarding relative uncertainty	Primary reference source	Uncertainty range
	5.2.6	Wall material	No information available	Different wall materials will result in different scattering and absorption rates, and can also contribute to background counts.	N/A	INQ [Neutron detector specifications should be provided in technical design basis document of system, which captures the trade-offs on count time, count rate, spatial resolution, wall effects, and any other specific measurement parameter that impacts data quality objectives.]
<b>5.3 Interference</b>						
	5.3.1	Background neutron flux from surrounding assemblies	No information available	There is no evidence that either engineering controls and/or administrative controls are used to understand, measure, and evaluate background neutron count rates. Background in this case refers to neutrons entering the detector(s) from other adjacent spent fuel assemblies and not to "background" neutrons reflected or in-scattered from the <sup>252</sup> Cf transmission source.	N/A	INQ [Neutron count rate uncertainty should be documented in system test and all panel measurement results. Neutron background rate used to determine real or poor n/γ discrimination should be documented separately.]
	5.3.2	Gamma interference	Expert judgment	Contingent on the operator and on the manner in which the nuclear electronics are adjusted in situ to account for gamma-ray pileup pulses that exceed the lower-level discriminator setting on the Single Channel Analyzer (SCA). Low (~2%) if properly accounted for, or results could be unreliable if not properly accounted for.	N/A	Low to high [Same as previous. In addition, n/γ discrimination measurements should be documented in the measurement records.]
<b>5.4 Electronics</b>						
	5.4.1	EMI susceptibility	No information available	Instrumentation technical performance specifications not provided.	N/A	INQ [Parameter effect should be documented in test plan (with results) that evaluates performance over range of expected conditions.]
	5.4.2	RF pickup	No information available	Instrumentation technical performance specifications not provided	N/A	INQ [Same as previous]

Section	Report subsection	Physical influence parameter	Information used to support discussion	Comments regarding relative uncertainty	Primary reference source	Uncertainty range
	5.4.3	Amplifiers, discriminators, power supply, acquisition board	No information available	Instrumentation technical performance specifications not provided	N/A	INQ [Same as previous. In addition, the selection of these components should be described in the system technical basis design document, tested, evaluated, and documented, accordingly.]
	5.4.4	Signal processors	No information available	Instrumentation technical performance specifications not provided	N/A	INQ [Same as previous]
	5.4.5	Discriminators for pile-up rejection, wall effect	No information available	Instrumentation technical performance specifications not provided	N/A	INQ [Same as previous]
	5.4.6	Dead time	No information available	Instrumentation technical performance specifications not provided	N/A	INQ [Same as previous]
<b>5.5</b>	<b>Apparatus geometry</b>					
	5.5.1	Head misalignment	First-principle computation	Because the proximity between the source head, panel, and detector is close (< 6 in. [15.2 cm]), and it has been reported that BADGER sticks (or jambs) in some warped panels, the measurement geometry is likely not consistent throughout a single panel (see other parameters below)	Monte Carlo calculations conducted by authors in Appendix A	> 40% (on average areal density) [Logsheets should contain records for the difficulty in easily moving the heads up the rack. A look-up table should be prepared, based on experimental data, to determine the magnitude and direction of bias introduced at that measurement point.]
	5.5.2	Rack cell fit	No information available	Mitigated for with Section 5.5.1 and 5.5.3. Design element reflected in Section 5.5.5.	N/A	INQ [Same as previous]
	5.5.3	Compression springs, shims, vertical offsets	No information available	Uncertainty reflected in Section 5.5.1.	N/A	INQ [Mechanical stops, guidance, and shims should be described in the system technical basis document, and then tested to ensure the measurement is conducted in a stable geometry.]

Section	Report subsection	Physical influence parameter	Information used to support discussion	Comments regarding relative uncertainty	Primary reference source	Uncertainty range
	5.5.4	Effect of rack cell deformation: panel cladding bulges, collisions with assemblies	Expert judgment	Uncertainty similar to Section 5.5.1 across an axial segment due to (1) broad beam irradiation of point $^{252}\text{Cf}$ source across panel surface 2–3 in. (5–7.6 cm) from source; (2) detectors ~0.5 in. (1.3 cm) from panel; and (3) bulges reported with dimensions of ¼ in. (0.6 cm) or more. Neutron transmission measurements are very sensitive to these changes in measurement geometry.	N/A	[See Section 5.5.1 and 5.5.3]
	5.5.5	Determination of detector coverage of panel area	No information available	Design element to meet performance specification. A broad-beam point source projection across a panel surface 2–3 in. (5-7.6 cm) from source is subject to specific measurement controls placed on the uniformity of the irradiation. Uncertainty can be quite high, as opposed to a uniform, "pencil-beam" irradiating flux used in a laboratory-grade coupon-sample analysis (ex situ).	N/A	INQ [Design information not contained in open BADGER literature. This should be provided in the technical basis document, showing the trade-offs in spatial resolution, interference with “indirectly scattered” neutrons, etc.]
<b>5.6 Calibration</b>						
	5.6.1	Number, range, and precision of $^{10}\text{B}$ areal density of standard panels	No information available	Not known whether the BADGER calibration function extrapolates beyond the smallest $^{10}\text{B}$ areal density provided in the calibration panel. Since a logarithmic exponential function is fit to the calibration data, it is recommended that at least three calibration densities be run above the required minimum areal density, and two below.	N/A	INQ [The calibration report should include a certificate from the manufacturer of the various panels. The certificate should report the fabrication tolerance, with bias and precision listed separately.]
	5.6.2	Standard panel degradation	No information available	Low if specific administrative controls are in place to ensure that the standard panel does not suffer degradation. If necessary administrative controls are not in place, the bias in the BADGER measurement is directly proportional to the amount of loss in the standard panel.	N/A	INQ [Acceptable tolerances should be documented in a QC procedure/plan]

Section	Report subsection	Physical influence parameter	Information used to support discussion	Comments regarding relative uncertainty	Primary reference source	Uncertainty range
	5.6.3	Adjustment of calibration procedure for specific pool characteristics	No information available	Unknown effects of local pool characteristics on measurement uncertainty, relative to both the baseline calibration and to the site-specific calibration.	N/A	INQ [Site-specific adjustments to calibration and measurement protocols should be provided in measurement report. Estimate of uncertainty should be derived]
	5.6.4	Relevance of standard panel material to rack panel material, e.g. using a Boraflex calibration assembly to measure Carborundum or Boral <sup>®</sup> .	Expert judgment	Neutron channeling effects diminish as the thickness of the neutron absorber increases. During the calibration scan of panel segments of different thicknesses, the rate of change in areal density as a function of neutron transmission will be different for different materials.	References. 38 and 40	±30% (on areal density) [Any specific variability introduced between the standard panel and the reference panel should be described in the measurement report]
	5.6.5	Location and acclimatization of calibration cell in pool	No information available	Unknown. However, system response will likely vary with temperature.	N/A	INQ [Should be described in measurement reports]
	5.6.6	Choice of “zero-loss” reference panel and uncertainty of actual <sup>10</sup> B areal density	No information available	The reference panel, also referred to as zero-loss panel, is used as the y-intercept index to all other panels. Whether from a manufacturing tolerance on the reference panel or the misrepresentation of zero-loss, if the reference panel value is biased, all examined panel biases will be of the same sign and magnitude.	N/A	INQ [Should be described in measurement reports]

Section	Report subsection	Physical influence parameter	Information used to support discussion	Comments regarding relative uncertainty	Primary reference source	Uncertainty range
	5.6.7	Non-linearity of calibration curve, especially as it applies to flux-trap racks	No information available	Actual BADGER calibration data is not provided. Available reports use, for illustration purposes only, the exponential curve fit of detector count rate versus the known characteristic, $^{10}\text{B}$ areal density, from the calibration panel. The $^{10}\text{B}$ areal density range of calibration panels should extend beyond all likely panel densities, with at least three calibration densities above and two calibration densities below the minimum $^{10}\text{B}$ areal density credited in the rack. Sample exponential fits (and associated fit error) are shown in the text of Section 5.6.8.	N/A	INQ [A calibration methodology report should provide the results of all empirical models and include actual data to support the curve fit results and methodology that would allow one to calculate MSE]
	5.6.8	Uncertainties in calibration slope, especially as it applies to flux-trap racks	Expert judgment	The Watt-fission spectrum of neutrons emitted from the $^{252}\text{Cf}$ source is down-scattered by the time it reaches the first panel in a Region I (flux-trap) design. Neutrons that penetrate the first panel, with sufficient energy to do so, are subsequently down-scattered prior to reaching the face of the second panel. The down-scattered flux is of such low energy that the second panel is under-sampled and thereby overmoderated. Without knowing the degradation in the first panel, there is no way to estimate degradation (or areal density) in the second panel of a flux-trap design.	N/A	$\pm 50\%$ or more (on areal density) [Same as previous]
	5.6.9	Frequency of calibration during a BADGER campaign	No information available	The QC and recalibration plan used for ensuring measurement quality is unknown.	N/A	INQ [Requirements should be provided in the QC plan, which implements in part, the quality assurance requirements]
	5.6.10	Confirmatory analysis with destructive examination	No information available	Unknown in the literature how many confirmatory and validation measurements are conducted between the BADGER in situ measurements, and the collection of coupon samples, for subsequent laboratory analysis.	N/A	INQ [Confirmation and validation requirements and methods should be provided in the quality assurance plan]

Section	Report subsection	Physical influence parameter	Information used to support discussion	Comments regarding relative uncertainty	Primary reference source	Uncertainty range
	5.6.11	Panel-specific use and interpretation of unattenuated region data	No information available	Reports cited discuss a "drift" correction (see Reference 10), but it is unclear how this drift correction is conducted.	N/A	INQ [Same as 5.6.7]
	5.6.12	Algorithms to convert BADGER trace data into input for calibration curve	No information available	Details of the calibration curves used and how the contributing parameter uncertainties are propagated forward were not available for review, so no estimate on uncertainty can be made.	N/A	INQ [Same as 5.6.7]
<b>5.7 Data processing</b>						
	5.7.1	Reliance on operator experience to detect and characterize heterogeneous degradation	Expert judgment	Current experience is predominantly based on Boraflex and reliance on RACKLIFE as an aid to identify what is being observed. Until an equal experience base can be developed for recognizing the degradation features of neutron absorbers other than Boraflex, the uncertainty in scan interpretation will be high.	Reference 10	High enough to invalidate scans
	5.7.2	Applicability of Boraflex-based algorithms and experience to non-Boraflex material such as Boral <sup>®</sup> or Metamic, which experience different degradation mechanisms	Expert judgment	The formation of localized scallops and blisters in the localized geometry of the measurement will significantly impact the count rate of neutrons transmitted through the neutron absorber.	N/A	High

Section	Report subsection	Physical influence parameter	Information used to support discussion	Comments regarding relative uncertainty	Primary reference source	Uncertainty range
	5.7.3	Feedback procedure	No information available	Process control issue	N/A	INQ [Documented in operating and QC procedures primarily to identify pass/fail criteria of result]
<b>5.8 Statistical extrapolation and surveillance frequency</b>						
	5.8.1	Choice of test panels to survey	No information available	The statistical basis for selecting a subpopulation of panels to inspect by BADGER is not known. To some degree, RACKLIFE is used to estimate the most degraded panels, and then this estimate is used to estimate the nominal and worst case conditions for neutron absorber degradation.	N/A	INQ [Panel selection process should be documented in an inspection and test program plan type of report]
	5.8.2	Lack of duplicate scans of the same test panel	No information available	Unknown. However, duplicate scans provide a means to increase confidence in the estimated uncertainty range.	N/A	INQ [Requirements should be provided in the QC plan, which implements, in part, the quality assurance requirements to ensure that the system is reliable and stable (via duplicate measurements)]
	5.8.3	Application of results of selected panels to entire pool	No information available	Not an artifact of BADGER instrumentation; but a process issue.	N/A	INQ [Model validation report not contained in open BADGER literature]

<b>Section</b>	<b>Report subsection</b>	<b>Physical influence parameter</b>	<b>Information used to support discussion</b>	<b>Comments regarding relative uncertainty</b>	<b>Primary reference source</b>	<b>Uncertainty range</b>
	5.8.4	Frequency of BADGER campaigns, especially for panel materials where intermediate calculational methods such as RACKLIFE are not available	No information available	Unknown. Should start with high frequency until adequate experience base is developed to reduce frequency.	N/A	INQ [Interval frequency should be documented in an inspection and test program plan type of report]
	5.8.5	Application of final output to criticality analyses of record	No information available	N/A: Site specific	N/A	INQ [Model validation report not contained in open BADGER literature]
	5.8.6	Use of final output in abnormal or accident sequence criticality analyses	No information available	N/A: Site specific	N/A	INQ [Model validation report not contained in open BADGER literature]

This Page Intentionally Left Blank

## 7 CONCLUSION

This report documents sources of uncertainty in measurements of the Boron-10 Areal Density Gauge for Evaluating Racks (BADGER). The system was designed, assembled, and tested in the early-to-mid 1990s as a nondestructive scoping tool to evaluate neutron absorbers placed in spent fuel racks for confirmatory analyses of RACKLIFE predictions. As discussed in Section 2, available reports that were reviewed indicate use of a heuristic deployment strategy. The initial development and deployment effort of this tool was unable to benefit from some of the more recent advancements since 2001 in the areas of neutron detectors, signal-chain processing, and data acquisition systems for conducting in situ measurements that could reduce TMU. It is not known whether a systematic, parametric uncertainty analysis of the BADGER system has ever been performed. Hence, it is difficult to forecast what the net mean bias and precision truly is for any given deployment of the system. Estimates of uncertainty are provided in this report on the basis of many years of experience conducting neutron measurements and writing ANSI, ASTM, ISO, and IEC standards on the conduct of radiation measurements for NDA and NDT systems. Uncertainty terms were identified and discussed. Estimates for contribution to uncertainty were made to reflect potential magnitude.

Calculation of a TMU or the combined uncertainty of a measurement system requires a complete and thorough understanding of the interrelationships of the individual constituents. The BADGER estimated areal density values are determined through a series of constituent parameters through a functional relationship, which was not available for review. Consistent with Reference 17 and other good practice guides, when reporting a measurement result and its uncertainty, a list of components/factors that can affect the measurement results, such as that provided in Section 6, and a detailed description of how each component uncertainty was evaluated are necessary. The summary listing of constituent parameters provided in Table 6-1 is not all-inclusive, as important elements associated with BADGER design and implementation were unavailable for review, but it illustrates many of the necessary considerations that would need a thorough assessment and review for acceptance in the NDT professional community as a quantitative NDT tool. Because of limitations and constraints affiliated with obtaining test reports, procurement specifications, BADGER system technical specifications, and operating procedures (including those for QC), uncertainty of individual components listed in Table 6-1 could not be estimated with the exception of a limited few.

To develop detailed uncertainty estimates of a quantitative NDT device, the following need to be available for review: (1) a technical basis document describing in detail the neutron detectors, collimator assemblies, nuclear electronics, data acquisition systems, and algorithms; (2) an instrument qualification test plan to implement system specifications for range of use; and (3) appropriate electronics testing and labeling as having met specific instrument standards such as IEEE, CE, or UL. Additionally, a peer-reviewed document that the instrument will meet its intended purpose and application of use, up to and including the publication of a test standard, e.g., ASTM aids in developing the pedigree of the NDT device.

In the case of the BADGER system deployment, it is not clear if the systematic biases have been evaluated and corrected, as suggested in practice by ASTM C1592M-09 (Reference 16). As a result, a total propagated uncertainty analysis cannot be performed. The root MSE cannot be estimated, and summing the relative error terms is not appropriate. Monte Carlo radiation transport calculations documented in Appendix A show that the influence of individual parameters could be in excess of  $\pm 40$  percent on reported average areal densities. Thus, there is the notion that the total uncertainty could be much greater. When a more rigorous evaluation of the influence factors has been performed and made available, subsequent corrections to the algorithms made, and all deployment issues proven acceptable, a technically defensible estimate of TMU can be calculated and represented.

This Page Intentionally Left Blank

## 8 REFERENCES

1. U.S. Code of Federal Regulations, “Criticality Accident Requirements,” Part 50.68, Chapter I, Title 10, “Energy.”
2. U.S. Code of Federal Regulations, “Prevention of Criticality in Fuel Storage and Handling,” Part 50, General Design Criterion 62, Chapter I, Title 10, “Energy.”
3. U.S. Nuclear Regulatory Commission, “Gaps in Neutron-Absorbing Material in High-Density Spent Fuel Storage Racks,” NRC Information Notice 87-043, September 8, 1987, ADAMS Accession No. ML031130349.
4. U.S. Nuclear Regulatory Commission, “Degradation of Boraflex Neutron Absorber Coupons,” NRC Information Notice 93-070: September 10, 1993, ADAMS Accession No. ML031070107.
5. U.S. Nuclear Regulatory Commission, “Degradation of Boraflex Neutron Absorber in Spent Fuel Storage Racks,” NRC Information Notice 95-038, September 8, 1995, ADAMS Accession No. ML031060277.
6. U.S. Nuclear Regulatory Commission, “Degradation of Neutron-Absorbing Materials in the Spent Fuel Pool,” NRC Information Notice 2009-026, October 28, 2009, ADAMS Accession No. ML092440545.
7. U.S. Nuclear Regulatory Commission, “Boraflex Degradation in Spent Fuel Pool Storage Racks,” NRC Generic Letter 96-004, June 26, 1996, ADAMS Accession No. ML031110008.
8. Electric Power Research Institute (EPRI), “BADGER, A Probe for Nondestructive Testing of Residual Boron-10 Absorber Density in Spent Fuel Storage Racks: Development and Demonstration,” TR-107335, EPRI, Palo Alto, CA, October 1997.
9. EPRI, “Handbook of Neutron Absorber Materials for Spent Nuclear Fuel Transportation and Storage Applications – 2009 Edition,” 1019110, EPRI, Palo Alto, CA, November 2009.
10. U.S. Nuclear Regulatory Commission, “Boraflex, Racklife, and BADGER: Description and Uncertainties,” Technical Letter Report prepared by consultant Thomas C. Haley, September 6, 2012, ADAMS Accession No. ML12216A307. .
11. Sixth Inspection—EPRI Boraflex, Surveillance Assembly Technical Report #1003414, Electric Power Research Institute, Palo Alto, CA, July 2002.
12. ASTM International, C1671-2007, “Standard Practice for Qualification and Acceptance of Boron Based Metallic Neutron Absorbers for Nuclear Criticality Control for Dry Cask Storage Systems and Transportation Packaging,” West Conshohocken, PA.
13. EPRI, “The RACKLIFE Boraflex Rack Life Extension Computer Code: Theory and Numerics,” TR-107333, EPRI, Palo Alto, CA, July 1997.
14. EPRI, “The Boraflex Rack Life Extension Computer Code – RACKLIFE, Verification and Validation,” TR-109926, EPRI, Palo Alto, CA, March 1999.
15. Northeast Technology Co., “BADGER Test Campaign[s] at Turkey Point Unit 3, NETCO Results,” Kingston, NY: NET-165-01 (January 2001); NET-229-01 (June 2004); NET 279-01, (November 2007), ADAMS Accession No. ML101170072.
16. ASTM International, C1592M-2009, “Standard Guide for Making Quality Nondestructive Assay Measurements,” West Conshohocken, PA.

17. National Institute of Standards and Technology, "Guidelines for Evaluating and Expressing the Uncertainty of NIST Measurement Results," *United States Department of Commerce, Technology Administration, National Institute of Standards and Technology (NIST), Technical Note 1297*, 1994.
18. Northeast Technology Corp., "BADGER Test Campaign at Grand Gulf Nuclear Station," NET-287-01, Kingston, NY, October 2010, ADAMS Accession No. ML11112A099.
19. U.S. Nuclear Regulatory Commission, "Qualification, Calibration, and Error Estimation Methods for Nondestructive Assay," Regulatory Guide 5.53, Revision 1, ADAMS Accession No. ML003739240.
20. K. C. Smith, R. A. Stroud, K. L. Coop, and J. F. Bresson, "Total Measurement Uncertainty Assessment for Transuranic Waste Shipments to the Waste Isolation Pilot Plant," *Proceedings of the 6th Nondestructive Assay Waste Characterization Conference*, November 17–19, 1998, pp. 21–37, Salt Lake City, UT, 1998.
21. J. A. Chapman and S. Croft, "The Use of  $^{252}\text{Cf}$  for Calibrating Safeguards Monitors," *Proceedings of the 27th ESARDA Annual Meeting, symposium on Nuclear Material Management*, May 10–12, 2005, London, England, 2006.
22. U.S. Code of Federal Regulations, "Shippers – General Requirements for Shipments and Packagings," Part 173.435, Chapter I, Title 49, "Transportation."
23. Parrington, J.R., et al. "Nuclides and Isotopes, Chart of the Nuclides Fifteenth Edition," General Electric Company and KAPL Inc. San Jose, CA, 1996.
24. U.S. Energy Research and Development Administration, "BF<sub>3</sub> Gamma Tolerant Neutron Detector Tubes," Reactor Development Standards (RDT) Standard, RDT C 15-11T, Division of Reactor Research and Development, December 1975 (cancelled 1996).
25. S. Croft, and J. A. Chapman, "Practical Considerations for Selecting Cylindrical  $^3\text{He}$ -filled Proportional Detectors for Homeland Defense Applications," *Proceedings of the Institute of Nuclear Materials Management (INMM)*, July 2004.
26. O. W. Bilharz, "BF<sub>3</sub> Counter Background Study," *Institute of Radio Engineers (IRE) Trans. Nucl. Sci.* **9**(5), 32–47, November 1962.
27. G. F. Knoll, *Radiation Detection and Measurement*, Second Ed., John Wiley and Sons, Inc., New York, NY, 1989.
28. U.S. Nuclear Regulatory Commission, "Passive Nondestructive Assay of Nuclear Materials," NUREG/CR-5550, March 1991, ADAMS Accession No. ML091470585.
29. EPRI, "MCNP Validation of BADGER," GC-110539, EPRI, Palo Alto, CA, May 1998.
30. U.S. Department of Energy, "DOE Fundamentals Handbook, Instrumentation and Control, Volume 2 of 2," DOE-HDBK-1013/2-92, June 1992.
31. International Electrotechnical Commission, IEC 61000-4-3:2006, "Electromagnetic compatibility (EMC) – Part 4-3: Testing and measurement techniques–Radiated, radio-frequency, electromagnetic field immunity test," Ontario, Canada.
32. U.S. Nuclear Regulatory Commission, "Electromagnetic Compatibility Testing for Conducted Susceptibility Along Interconnecting Signal Lines," NUREG/CR-5609, August 2003, ADAMS Accession No. ML032960137.
33. E. Wong, "Spent Fuel Criticality: Neutron Absorbing Material Degradation Issues," U.S. NRC, 2010 Regulatory Information Conference, March 11, 2010.

34. Florida Power and Light Company, "Turkey Point Units 3 and 4 - License Amendment Request No. 204, Spent Fuel Pool Criticality Analysis Taking Credit for Boraflex," Dockets 50-250 and 251, February 25, 2010, ADAMS Accession No. ML100600789.
35. Northeast Technology Co., "BADGER Test Campaign at Turkey Point Unit 4," NET 346-01, Kingston, NY, June 2010, ADAMS Accession No. ML102250420.
36. American Society of Mechanical Engineers, ASME NQA-1-2008, "Quality Assurance Requirements for Nuclear Facility Applications," New York, NY.
37. NIST/SEMATECH, *e-Handbook of Statistical Methods*, 2010 (available from: <http://www.itl.nist.gov/div898/handbook/>).
38. EPRI, "Neutron Transmission Through Boral<sup>®</sup>: Impact of Channeling on Criticality," TR 1011819, EPRI, Palo Alto, CA, June 2005.
39. S. E. Turner, "Reactivity Effects of Streaming Between Discrete Boron Carbide Particles in Neutron Absorber Panels for Storage or Transport of Spent Nuclear Fuel," *Nucl. Sci. Eng.* **151**, 344–347 (2005).
40. U.S. Nuclear Regulatory Commission, "Application of ASTM Standard Practice C1671-07 when performing technical reviews of spent fuel storage and transportation packaging licensing actions," *Division of Spent Fuel Storage and Transportation, Interim Staff Guidance – 23*, January 18, 2011.
41. EPRI, "A Synopsis of the Technology Developed to Address the Boraflex Degradation Issue," TR 108761, EPRI, Palo Alto, CA, November 1997.
42. ASTM International, C1490-2004 (Reapproved 2010), "Standard Guide for the Selection, Training and Qualification of Nondestructive Assay (NDA) Personnel," West Conshohocken, PA.
43. Entergy, "Indian Point, Unit 2 License Amendment Request (LAR 01-010) for Spent Fuel Storage Pit Rack Criticality Analysis with Soluble Boron Credit," Docket No. 50-247, ADAMS Accession No. ML012680336.
44. Northeast Technology Co., "Criticality Analysis of the Peach Bottom Spent Fuel Racks for GNF 2 Fuel with Boraflex Panel Degradation Projected to May 2010," NET-264-02 NP, May 15, 2009, ADAMS Accession No. ML091740447.
45. IEEE, N323A-1997, "Radiation Protection Instrumentation Test and Calibration, Portable Survey Instruments" New York, NY.

This Page Intentionally Left Blank

## **APPENDIX A**

### **REPRESENTATIVE BADGER SCAN USING MAVRIC**

This appendix provides a representative BADGER test to demonstrate some of the impacts on measurement uncertainty. A surrogate BWR rack configuration was developed with the MAVRIC radiation transport sequence in SCALE (Reference A.1) to generate a representative calibration curve to observe the relative effects that minor changes, such as twist and offset misalignment, or calibration cell error can have on neutron transmission ratios and the effect on predicted areal density results. The MAVRIC model output results are presented in Appendix B for the different model configurations, and an example MAVRIC model input file is provided in Appendix C.

The surrogate BWR rack model is illustrated in Figure A.1. Water has been hidden in the drawing to facilitate visualization of cell components. Note that there are several variants of BWR spent fuel pool storage racks that could have been modeled, but the model for this report is provided to be representative of a typical BWR Region II storage rack and is not specific to an actual design. Each fuel storage rack cell is modeled as a square tube of steel that is 0.07 in. (0.18 cm) thick and has an inner dimension of 5.807 in. (14.75 cm.) A nominal generic  $^{10}\text{B}$  neutron absorber material was modeled having of a thickness of 0.09 in. (0.203 cm) and a nominal areal density of  $0.021 \text{ g } ^{10}\text{B}/\text{cm}^2$ . The  $^{10}\text{B}$  areal density was varied from 100 percent to 10 percent while maintaining a constant thickness, and thermal neutron counts were tallied for the four  $\text{BF}_3$  detectors. The  $\text{BF}_3$  detectors were represented as 96 percent enriched in  $^{10}\text{B}$ , and the  $^{252}\text{Cf}$  source was represented at strength of 1 mCi. For all transmission ratio values, the attenuated region count rates correspond to a scan where the neutron absorber panel at a given areal density is present, and all unattenuated region count rates correspond to a scan where the absorber panel was represented as water maintaining the same detector-to-source orientation. The illustrative calibration plots are shown in Figure A.2.

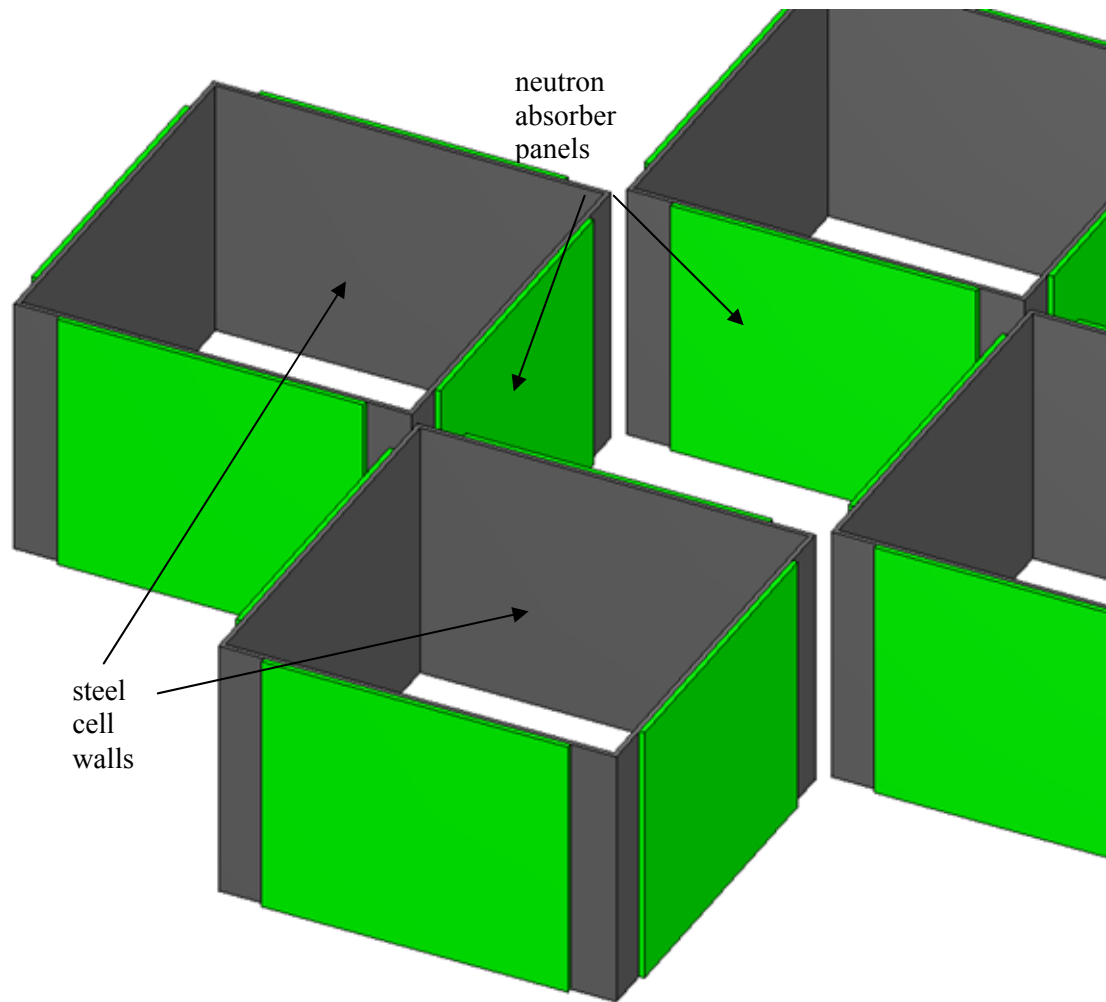


**Figure A.1. Cutaway view of representative Region II BWR storage rack model.**

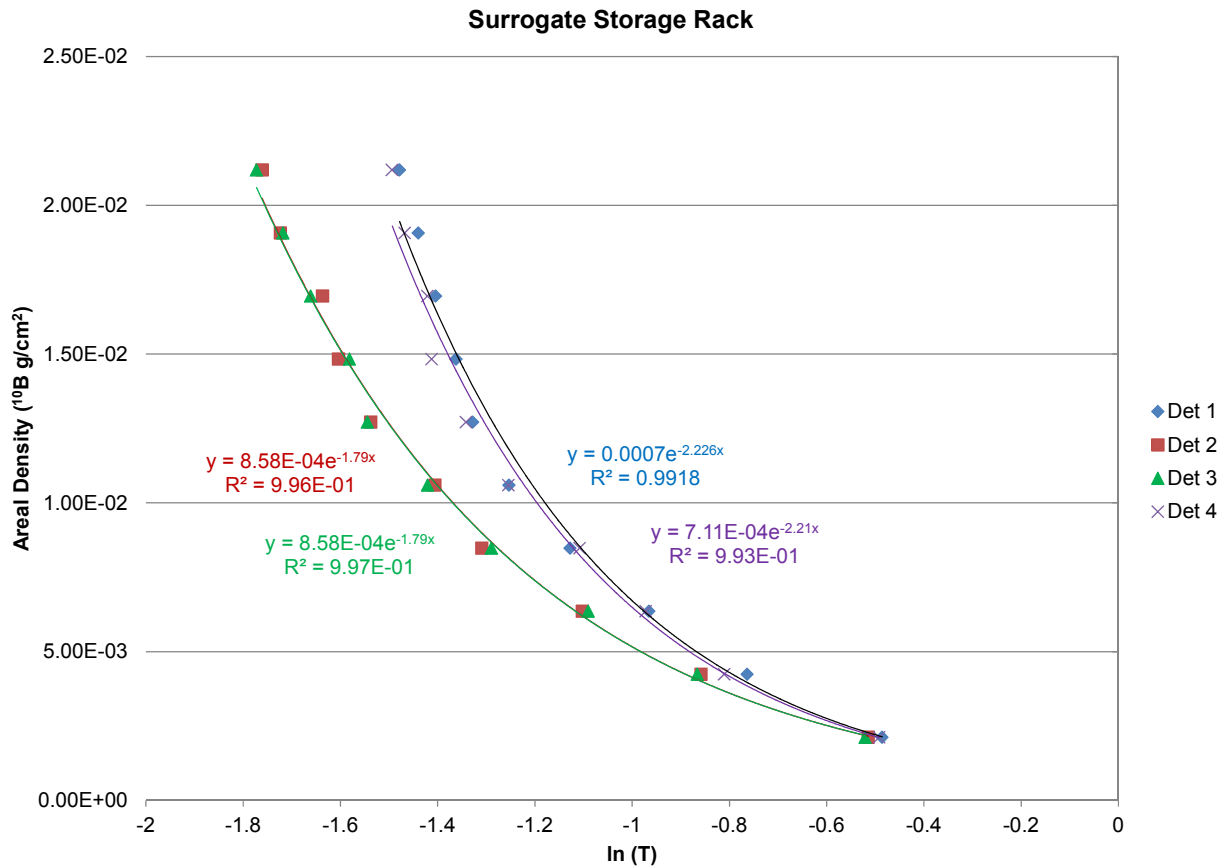


**Figure A.2. Areal density calibration curve for optimum source and detector head orientation positioning.**

Note: T = ratio of attenuated to unattenuated neutron counts

### Potential Uncertainty Due to Geometry Changes

Three types of geometric misalignment can affect neutron transmission test results: tilt, twist, and offset (see descriptions in Reference 8 and in Section 5.5.1). Each misalignment condition results in changes in the distance between the detectors and the source and has the potential to introduce water between the detector head and the rack wall being evaluated. To evaluate the relative magnitude of these effects, SCALE models were developed to simulate the effects of twist and offset misalignment.

Twist misalignment is when the probes are twisted instead of flush against the panel surface. Although different variants of twist misalignment can occur such as the source probe being twisted, the detector probe being twisted, or both probes being twisted, the SCALE models represented only the detector probe being twisted 1°, 2°, and 3°. An example of twist misalignment is shown in Figure A.3.

Offset misalignment can occur when the source and detector head are shifted. Spacer shims can be used to minimize the potential for this type of offset when the rack cell is significantly larger than the probe heads; however, there is still a clearance space that the heads could shift into. The offset represented in the SCALE model was 0.66-cm probe center-to-center distance, which represented the maximum offset

geometrically allowable for the representative storage rack configuration. An example of offset misalignment is shown in Figure A.5.

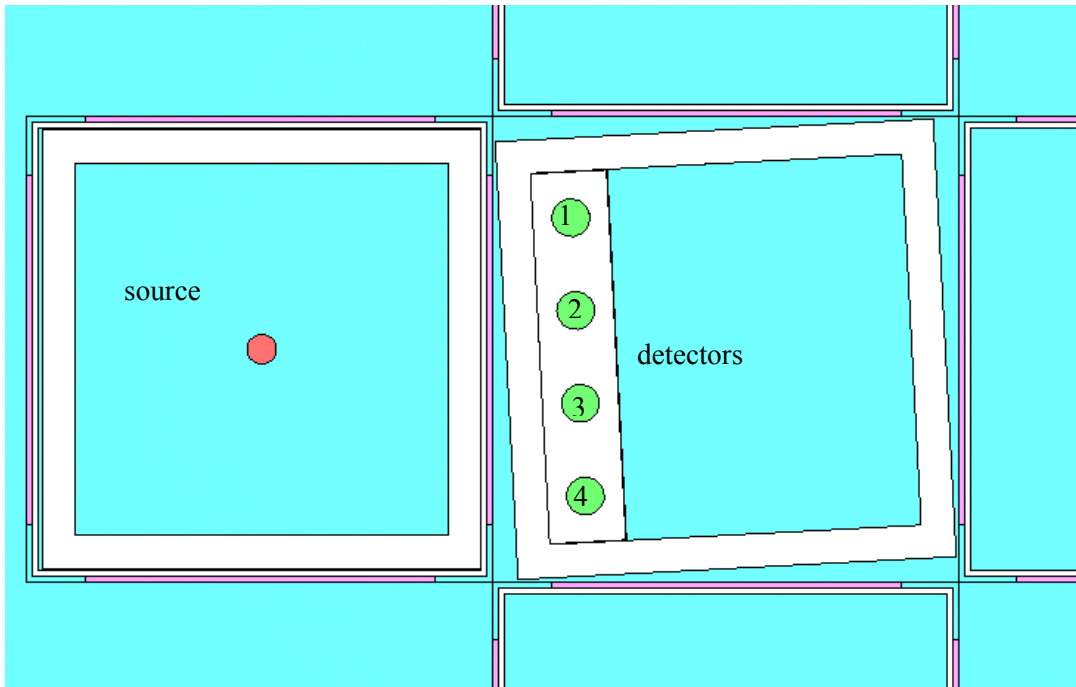


Figure A.3. Source and detector head positioning with 3° twist misalignment for detector head.

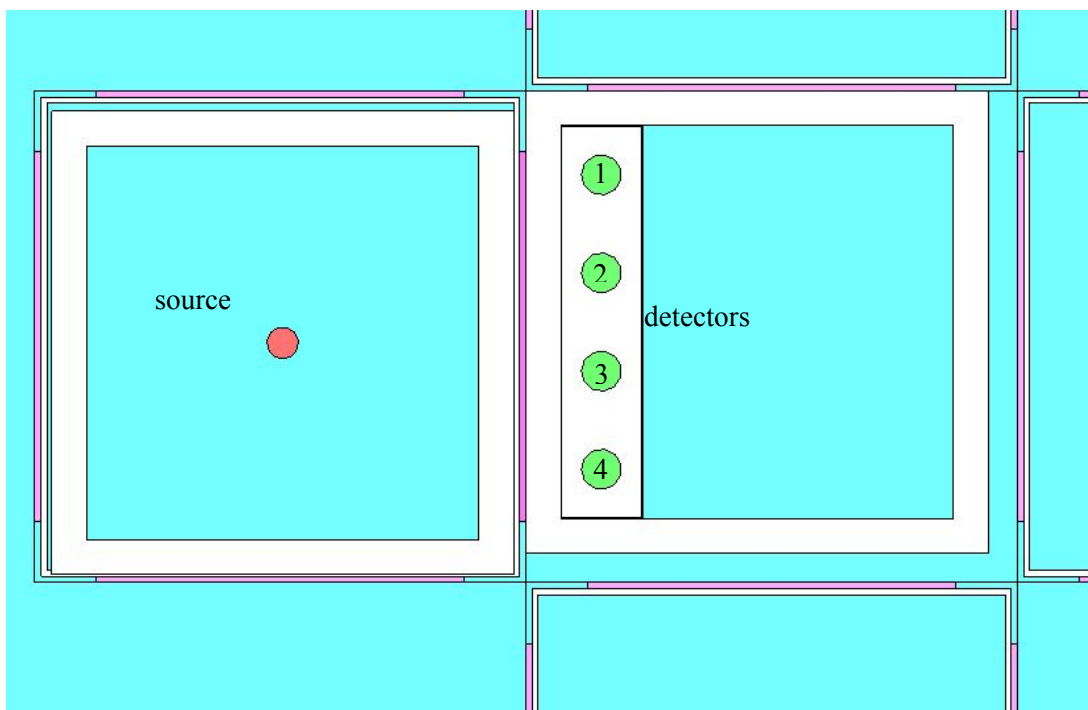
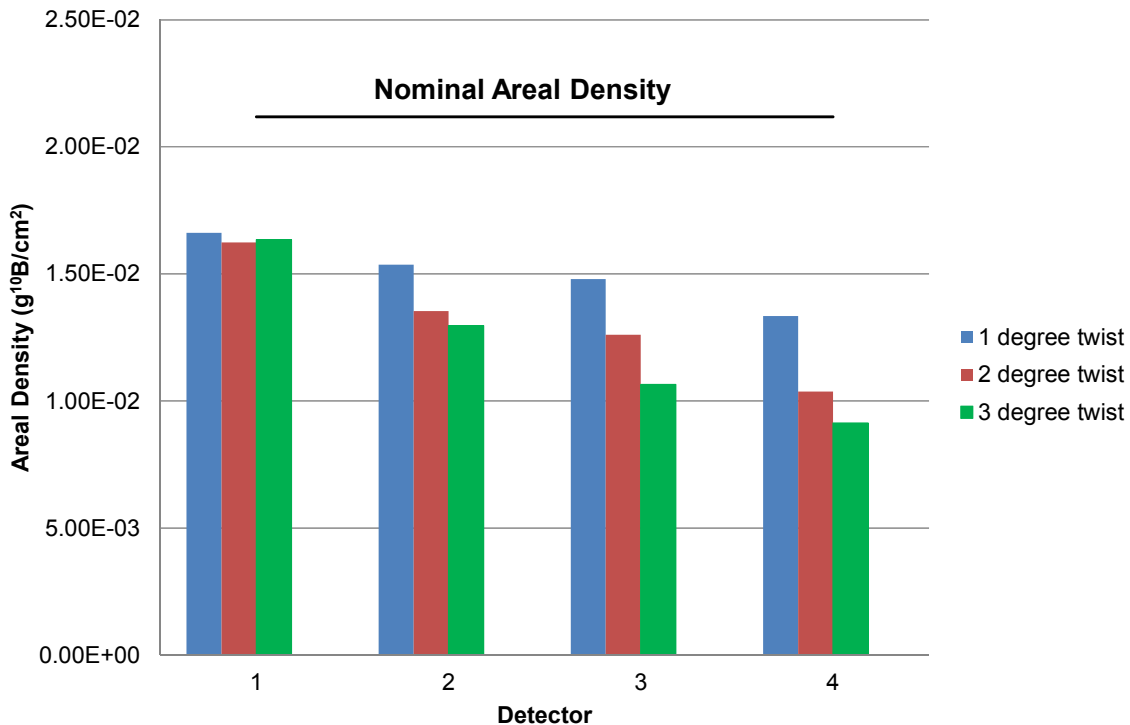


Figure A.4. Source and detector head positioning with a 0.66-cm probe center-to-center offset misalignment.

The effects of twist misalignment can be observed in Table A-1 and Figure A.5 for 1°, 2°, and 3° twist misalignments, and the effects of offset misalignment are presented in Table A-2 and illustrated in Figure A.6. The percent change from optimum is the relative difference between the misaligned counting geometry results and the optimum orientation counting geometry results. BADGER areal density scan results are typically reported as an average of the four detectors, therefore the four detector average results are presented as well. The results show how sensitive the measurements are to very small changes in the distance between the source and detectors. Note that the differences reported here are based on a calibration curve for the same identical panel. BADGER test implementation incorporates the transmission data normalized to a reference panel and a slope from a separate calibration curve, exacerbating the uncertainty.

**Table A-1. Relative change in areal density due to twist misalignment**

Rotation	Areal density (g <sup>10</sup> B/cm <sup>2</sup> )	Detector (% change from optimum)				Detector average
		1	2	3	4	
1°	0.0212	22%	27%	30%	37%	29%
	0.0148	9%	12%	20%	29%	18%
	0.0085	-1%	13%	19%	25%	14%
2°	0.0212	23%	36%	40%	51%	38%
	0.0148	16%	25%	31%	42%	28%
	0.0085	11%	23%	24%	35%	23%
3°	0.0212	23%	39%	50%	57%	42%
	0.0148	9%	30%	44%	51%	34%
	0.0085	16%	26%	32%	44%	29%



**Figure A.5. Change in recorded areal density due to twist misalignment.**

**Table A-2. Relative change in areal density due to offset misalignment**

Areal density (g <sup>10</sup> B/cm <sup>2</sup> )	Detector (% change from optimum)				Detector average
	1	2	3	4	
0.0212 (100%)	13%	5%	-6%	-30%	-5%
0.0148 (70%)	-1%	-13%	-17%	-44%	-19%
0.0085 (40%)	-9%	-10%	-16%	-38%	-18%

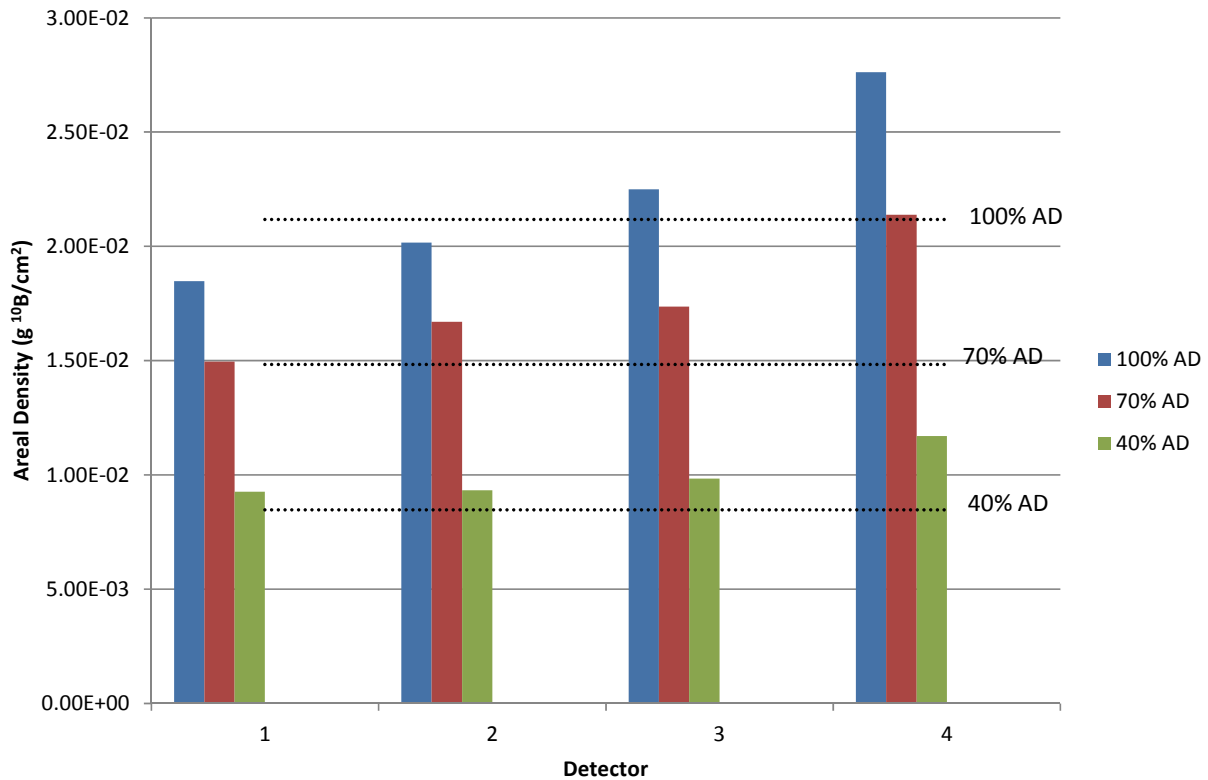


**Figure A.6. Change in recorded areal density due to offset misalignment.**

The results of the twist misalignment cases indicate that even though the detectors are moving away from the source which would effectively reduce the detector count rate in a vacuum, the addition of water between the detector head and the panel allows neutrons that were not absorbed in the neutron absorber to become more thermalized so that they can register in the detectors. This effect is combined with the decrease in unattenuated count rate (the denominator in the transmission ratio) with increasing distance between the source and detectors. This results in a shift of the equivalent calibration curve to the right in this example, indicating that all results are at lower areal densities. The curve shift would be to the left if the misalignment first occurred during development of the initial calibration curve (i.e., results would show higher areal densities than are actually present). The effect of twist misalignment is more pronounced at higher areal densities than at lower areal densities owing to the steepness of the slope, as illustrated in Figure A.2.

The effects of offset misalignment exhibit the competing effects of neutrons that did not traverse through the neutron absorber panel for the edge detector combined with changes in distance from the source. The negative values shown in Table A-2 indicate where a nonconservative areal density change is being interpreted as an increase in relation to the nominal calibration curve. The amount of possible offset will be dependent upon the rack cell size, and the maximum uncertainty can be determined during initial calibration by taking measurements of the reference panel while maximizing the allowable offset. Another method to detect offset could be careful observation of the unattenuated region count data, which would rely on keen observation by the operator and/or analyst.

## **A.1. REFERENCE**

- A.1. *SCALE: A Comprehensive Modeling and Simulation Suite for Nuclear Safety Analysis and Design*, ORNL/TM-2005/39, Version 6.1, Oak Ridge National Laboratory, Oak Ridge, Tennessee, June 2011. Available from Radiation Safety Information Computational Center at Oak Ridge National Laboratory as CCC-785.

# **APPENDIX B**

## **MAVRIC MODEL RESULTS**

This appendix lists the SCALE MAVRIC model count rate results for each detector that were modeled in this report. Table B-1 presents the optimum orientation configuration results, Table B-2 presents the twist misalignment results, and Table B-3 presents the offset misalignment results. Tally responses are in units of per cm<sup>3</sup> per second.

**Table B-1. MAVRIC-generated optimum orientation configuration results**

Panel areal density (g <sup>10</sup> B/cm <sup>2</sup> )	Detector							
	1		2		3		4	
	Tally Response	Relative uncertainty						
0.0212	13.664	0.018	13.606	0.017	13.622	0.017	13.565	0.018
0.0191	14.202	0.017	14.127	0.017	14.385	0.017	13.925	0.017
0.0169	14.716	0.017	15.403	0.016	15.227	0.016	14.587	0.017
0.0148	15.349	0.016	15.919	0.016	16.496	0.016	14.713	0.016
0.0127	15.886	0.016	17.009	0.015	17.117	0.015	15.795	0.016
0.0106	17.120	0.015	19.414	0.014	19.372	0.014	17.231	0.015
0.0085	19.406	0.015	21.375	0.013	22.083	0.013	19.950	0.014
0.0064	22.821	0.013	26.288	0.012	26.949	0.012	22.861	0.013
0.0042	27.934	0.012	33.549	0.011	33.729	0.011	26.863	0.012
0.0021	36.869	0.011	47.329	0.009	47.630	0.009	36.933	0.010
unattenuated region	59.920	0.009	79.154	0.008	80.154	0.007	60.398	0.009

**Table B-2. MAVRIC-generated twist misalignment configuration results**

Rotation	Panel areal density (g <sup>10</sup> B/cm <sup>2</sup> )	Detector							
		1		2		3		4	
		Tally Response	Relative uncertainty						
1°	0.0212	14.698	0.017	15.389	0.016	15.345	0.016	14.778	0.017
1°	0.0148	16.152	0.016	16.909	0.016	17.338	0.015	16.428	0.016
1°	0.0085	19.768	0.014	23.217	0.013	23.541	0.013	20.636	0.014
1°	unattenuated region	59.908	0.009	77.118	0.008	75.300	0.008	55.689	0.009
2°	0.0212	14.840	0.017	16.269	0.017	16.225	0.016	15.801	0.017
2°	0.0148	16.715	0.016	18.104	0.016	18.211	0.016	17.162	0.016
2°	0.0085	20.892	0.014	24.526	0.014	23.645	0.013	20.974	0.014
2°	unattenuated region	59.865	0.009	75.962	0.008	72.798	0.008	53.133	0.009
3°	0.0212	14.918	0.017	16.478	0.016	17.111	0.016	15.714	0.017
3°	0.0148	16.264	0.016	18.593	0.015	19.655	0.016	17.475	0.017
3°	0.0085	21.628	0.014	24.722	0.013	24.093	0.014	21.160	0.015
3°	unattenuated region	60.341	0.008	75.087	0.008	69.860	0.008	49.850	0.009

**Table B-3. MAVRIC generated offset misalignment configuration results**

Panel areal density (g <sup>10</sup> B/cm <sup>2</sup> )	Detector							
	1		2		3		4	
	Tally Response	Relative uncertainty						
0.0212	13.514	0.017	13.834	0.018	13.952	0.017	13.270	0.017
0.0148	14.895	0.014	15.405	0.013	16.126	0.013	14.907	0.014
0.0085	18.567	0.016	21.496	0.016	22.141	0.016	19.605	0.016
unattenuated region	58.831	0.009	82.173	0.007	86.743	0.007	69.553	0.008

## **APPENDIX C**

### **EXAMPLE MAVRIC CODE INPUT**

```

=====
' Basic MAVRIC Sequence items: title and SCALE Library
=====
=mavric
Example for 10-B(n,alpha)3-Li reaction rate calculation
v7-200n47g

-----
' Composition Block - standard SCALE input
-----
read composition
  paraffin      1 1 293  end
  polyethylene  2 1 293  end
  wtptype304ss  3 7.9  5
                                     14000 1
                                     24304 20
                                     25000 2
                                     26304 66.5
                                     28304 10.5
                                     1 293  end
b-10            4 0 1.05E-6 300 end
b-11            4 0 4.38E-8 300 end
f               4 0 3.28E-6 300 end
  h2o           5 1 300  end
  cf-252        6 1 300  end
'neutron absorber panel
wtptalb4c      7 2.677 4
                                     13027 75
                                     5010 3.894
                                     5011 15.672
                                     6000 5.434
                                     1 300  end
'detector head neutron shield
wtptalb4c      8 2.677 4
                                     13027 75
                                     5010 3.894
                                     5011 15.672
                                     6000 5.434
                                     1 300  end
al             9 1 300  end
  h2o         10 1 300  end
'test panel in rack
wtptalb4c     11 2.677 4
                                     13027 75
                                     5010 3.894
                                     5011 15.672
                                     6000 5.434
                                     1 300  end
end composition

-----
' Geometry Block - SCALE standard geometry package (SGGP)
-----
read geometry
  global unit 1
    com="global unit 1"
'east cell description
  cuboid 1  23.274  7.758  7.758  -7.758  40 -40
  cuboid 2  23.071  7.961  7.555  -7.555  40 -40
  cuboid 3  22.891  8.141  7.375  -7.375  40 -40
  cuboid 4  23.274  23.071  5.82  -5.82  40 -40
  cuboid 5  7.961  7.758  5.82  -5.82  40 -40

```

```

cuboid 6  21.336  9.696  7.758  7.555  40 -40
cuboid 7  21.336  9.696  -7.555  -7.758  40 -40

'west cell description
cuboid 11 -7.758 -23.274 7.758 -7.758  40 -40
cuboid 12 -7.961 -23.071 7.555 -7.555  40 -40
cuboid 13 -8.141 -22.891 7.375 -7.375  40 -40
cuboid 14 -7.758 -7.961 5.82 -5.82  40 -40
cuboid 15 -23.071 -23.274 5.82 -5.82  40 -40
cuboid 16 -9.696 -21.336 7.758 7.555  40 -40
cuboid 17 -9.696 -21.336 -7.555 -7.758  40 -40

'north cell description
cuboid 21 7.758 -7.758 23.274 7.758  40 -40
cuboid 22 7.555 -7.555 23.071 7.961  40 -40
cuboid 23 7.375 -7.375 22.891 8.141  40 -40
cuboid 24 7.758 7.555 21.336 9.696  40 -40
cuboid 25 -7.555 -7.758 21.336 9.696  40 -40
cuboid 26 5.82 -5.82 23.274 23.071  40 -40
cuboid 27 5.82 -5.82 7.961 7.758  40 -40

'south cell description
cuboid 31 7.758 -7.758 -7.758 -23.274  40 -40
cuboid 32 7.555 -7.555 -7.961 -23.071  40 -40
cuboid 33 7.375 -7.375 -8.141 -22.891  40 -40
cuboid 34 7.758 7.555 -9.696 -21.336  40 -40
cuboid 35 -7.555 -7.758 -9.696 -21.336  40 -40
cuboid 36 5.82 -5.82 -7.758 -7.961  40 -40
cuboid 37 5.82 -5.82 -23.071 -23.274  40 -40

cuboid 99 60 -60 60 -60 70 -70
hole 4 origin x=-15.4435 y=0 z=0
hole 2 origin x=-0.4555 y=0 z=0

media 5 1 1 -2 -4 -5 -6 -7
media 7 1 4
media 7 1 5
media 7 1 6
media 7 1 7
media 3 1 2 -3
media 5 1 3

media 5 1 11 -12 -14 -15 -16 -17
media 11 1 14
media 7 1 15
media 7 1 16
media 7 1 17
media 3 1 12 -13
media 5 1 13

media 5 1 21 -22 -24 -25 -26 -27
media 7 1 24
media 7 1 25
media 7 1 26
media 7 1 27
media 3 1 22 -23
media 5 1 23

media 5 1 31 -32 -34 -35 -36 -37
media 7 1 34
media 7 1 35
media 7 1 36
media 7 1 37

```

```

media 3 1 32 -33
media 5 1 33

media 10 1 99 -1 -11 -21 -31
boundary 99

unit 2
com="unit 2"
cuboid 3 7.3025 -7.3025 7.3025 -7.3025 7.3025 -7.3025
cuboid 4 6.1913 -6.1913 6.1913 -6.1913 6.1913 -6.1913
cuboid 5 -3.6313 -6.1913 6.1913 -6.1913 6.1913 -6.1913
cuboid 6 -3.6513 -6.1913 6.1713 -6.1713 6.1913 -6.1913

cylinder 31 0.635 2.54 -2.54 origin x=-4.9213 y=4.6434 z=0
cylinder 32 0.635 2.54 -2.54 origin x=-4.9213 y=1.5478 z=0
cylinder 33 0.635 2.54 -2.54 origin x=-4.9213 y=-1.5478 z=0
cylinder 34 0.635 2.54 -2.54 origin x=-4.9213 y=-4.6434 z=0

media 4 1 31 vol=6.4352
media 4 1 32 vol=6.4352
media 4 1 33 vol=6.4352
media 4 1 34 vol=6.4352

media 9 1 3 -4
media 5 1 4 -5
media 8 1 5 -6
media 9 1 6 -31 -32 -33 -34
boundary 3

unit 4
com="unit 4"
cuboid 3 7.3025 -7.3025 7.3025 -7.3025 7.3025 -7.3025
cuboid 4 6.1913 -6.1913 6.1913 -6.1913 6.1913 -6.1913
hole 5
media 9 1 3 -4
media 5 1 4
boundary 3

unit 5
com="unit 5"
sphere 1 0.5
media 6 1 1
boundary 1
end geometry

'-----
' Definitions Block
'-----
read definitions
response 5
title="the 10-B(n,alpha)3-Li macroscopic cross section"
mat=4 ZAID=5010 MT=107 macro
end response

distribution 1
title="Cf-252 neutrons, Watt spectrum a=1.025 MeV and b=2.926/MeV"
special="wattSpectrum"
parameters 1.025 2.926 end
end distribution
end definitions

'-----
' Sources Block

```

```

'-----
read sources
  src 1
    title="Cf-252 neutrons, Watt fission spectrum model, 1mCi"
    strength=37.0e6
    sphere 0.5  origin x=-15.4435 y=0.0 z=0.0
    neutrons
    eDistributionID=1
  end src
end sources

'-----
' Tallies Block
'-----
read tallies
  regionTally 1
    unit=2 region=1
    responseIDs 5 end
  end regionTally
  regionTally 2
    unit=2 region=2
    responseIDs 5 end
  end regionTally
  regionTally 3
    unit=2 region=3
    responseIDs 5 end
  end regionTally
  regionTally 4
    unit=2 region=4
    responseIDs 5 end
  end regionTally
end tallies

'-----
' Parameters Block
'-----
read parameters
  randomSeed=00003ecd7b4e3e8b
  perBatch=100000 batches=50
  noFissions
  noSecondaries
end parameters

end data
end

```

